**Sulfated zirconia deactivation during *n*-butane isomerization:
an *in situ* UV-vis-NIR spectroscopic study**

vorgelegt von
Diplôme d´Etudes Approfondies (D.E.A)
Carine CHAN THAW
aus Tamatave (Madagascar)

von der Fakultät II – Mathematik und Naturwissenschaften
der Technischen Universität Berlin
zur Erlangung des akademischen Grades
Doktorin der Naturwissenschaften
- Dr. rer. nat. -

genehmigte Dissertation

Promotionsausschuss:

Vorsitzender:	Prof. Dr. R. Schomäcker, TU Berlin
Berichter / Gutachter:	Prof. Dr. M. Lerch, TU Berlin
Berichter / Gutachter:	Prof. J. Sommer, ULP Strasbourg
Berichter / Gutachter:	Dr. J.Védrine, Université P.& M. Curie
Berichter / Gutachter:	Prof. E. Kemnitz, HU Berlin
Betreuer:	Dr. F. Garin, LMSPC Strasbourg
Betreuer:	Prof. Dr. R. Schlögl, FHI Berlin
Betreuerin:	Dr. F. Jentoft, University of Oklahoma
Betreuer:	Prof. G. Centi, University of Messina

Tag der wissenchaftlichen Aussprache: 20.11.2008

Berlin 2008
D 83

Thèse présentée pour obtenir le grade de
Docteur de l'Université Louis Pasteur
Strasbourg I

Discipline: Chimie – Catalyse hétérogène
par Carine CHAN THAW

**Sulfated zirconia deactivation during *n*-butane isomerization:
an *in situ* UV-vis-NIR spectroscopic study**

Soutenue publiquement le 20 Novembre 2008

Membres du jury:

Président de jury: Prof. Schomäcker, TU Berlin
Directeur de Thèse: Prof. M. Lerch, TU Berlin
Co-Directeur de Thèse: Dr. F. Garin, LMSPC Strasbourg
Rapporteur Interne: Prof. J. Sommer, ULP Strasbourg
Rapporteur Externe: Dr. J.Védrine, Université P.&M. Curie
Rapporteur Externe: Prof. E. Kemnitz, HU Berlin
Examinateur: Prof. R. Schlögl, FHI Berlin
Examinatrice: Dr. F. Jentoft, Université d'Oklahoma
Examinateur: Prof. G. Centi, Université de Messina

A mes Parents

Acknowledgements

Furthermore, I would like to thank my friends and family who have encouraged and supported me throughout my studies.

MERCI Papa et Maman de m'avoir donné le privilège d'étudier et de poursuivre mes études en Europe. Merci de m'avoir encouragée et soutenue en toutes circonstances.

Deaktivierung von sulfatiertem Zirkondioxid während der n-Butan Isomerisierung: Eine in situ UV-vis-NIR spektroskopische Untersuchung

vorgelegt von Carine Chan Thaw

Kurzzusammenfassung

Katalysatoren auf der Basis von sulfatiertem Zirkondioxid (SZ) desaktivieren, während der Isomeriesierung von kurzkettigen Alkanen, sehr schnell. Dieser schnellen Desaktivierung zu Reaktionsbeginn folgt eine zweite Phase mit verlangsamter Desaktivierung. Das Desaktivierungverhalten während der *n*-Butan-Isomerisierung über sulfatiertem Zirkonoxid (SZ) und mangandotiertem sulfatierten Zirkonoxid (MnSZ; 0,5 or 2,0 wt% Mn) wurden mit Hilfe der *in situ* UV-vis-NIR-Spektroskopie in diffuser Reflexion, d.h. simultane Analyse des Reaktiongases durch gaschromatographische Verfahren, untersucht.

Der derzeit akzeptierte Mechanismus für den Reaktionsstart ist eine oxidative Dehydrogenierung (ODH). SZ ist ein saurer Katalysator mit wenigen aktiven Oberflächenzentren, welche leicht durch Adsorption von Edukten/Reaktionsprodukten blockiert werden können. Diese Arbeit zeigt die Dualität des Einflusses von Wasser und Buten, der Reaktionsprodukte der ODH, ihren positiven und negativen Effekt auf die *n*-Butan-Isomerisierung. Ein optimaler Hydratisierungsgrad des SZ ist entscheidend für die Aktivität des Katalysators. Der Hydratisierungsgrad wird maßgeblich durch die Aktivierungsbedingungen (Gaszusammensetzung und Temperatur) bestimmt. Bei nicht Einhaltung des optimalen Hydratisierungsgrades kann Wasser (Absorptionband bei 1910 nm) die aktiven Zentren blockieren und somit die Aktivität des Katalysators herabsetzen. In der vorliegenden Arbeit kann gezeigt werden, dass die Bildung von Wasser in den ersten Stunden der Reaktion für die schnelle Desaktivierung zu Reaktionsbeginn verantwortlich ist.

Wie in der Literatur bereits beschrieben ist, wird Buten durch Protonierung an sauren Brønsted-Zentren, über Carbenium-Intermediate, in das entsprechende Alkoxid überführt. Die Skelettisomerisierung von *n*-Butan folgt einem bimolekularen Mechanismus und verläuft über die Alkylierung von Gasphasenolefinen mit *sec*-Butyl-Carbeniumionen. Die Gegenwart von größeren Mengen an Olefinen ist jedoch ein weiterer Grund für die Katalysatordeaktivierung. Die Zugabe von Propen zum Reaktionsgemisch führte zur Bildung von Polymeren. Die Zugabe von Sauerstoff zum Reaktionsgemisch führt zur Verbrennung von kohlenstoffhaltigen Ablagerungen auf der Katalysatoroberfläche und zur Bildung von Wasser, Kohlendioxid sowie Wärme, was vergleichbare Desaktivierungserscheinungen hervorruft. Die Freisetzung von Wärme fördert zusätzlich die Bildung von Polymeren. Oligomere konnten durch ihre Absorptionsbanden bei 370 und 450 nm auf der Katalysatoroberfläche nachgewiesen werden. Die vorliegende Arbeit zeigt, dass die Bildung oligomerer Spezies eine mögliche Ursache für den zweiten, langsameren Desaktivierungsvorgang ist. Die während der Reaktion gebildete monomere Allyl-Spezies (Absorption bei 295 nm) ist entgegen der Literatur nicht für die Desaktivierungsphänomene verantwortlich.

Keine der auf SZ gefundenen allylischen Spezies konnte auf MnSZ nachgewiesen werden. Jedoch desaktiviert MnSZ sehr schnell. Zwei Banden im UV-vis Bereich von Spektren der MnSZ-Katalysatoren werden beobachtet. Die fehlerhafte Zuordnung dieser Banden in der Literatur konnte durch Simulation der Spektren korrigiert werden. Die Absorption bei 580 nm ist auf Mn^{4+}, die bei 680 nm auf Mn^{3+} zurückzuführen.

Isomérisation du n-butane sur la zircone sulfatée: investigation in situ par spectroscopie UV-vis-NIR

par Carine Chan Thaw

Résumé court

Les phénomènes de désactivation des zircones sulfatées (ZS) dopées ou non au manganèse (MnZS; 0,5 et 2,0 % en masse) au cours de la réaction d'isomérisation du *n*-butane sont étudiés, à 323 ou 373 K, tout au long d´une réaction (mesures *in situ*) par spectroscopie à réflexion diffuse dans l´ultraviolet visible et proche infra rouge (UV-vis-NIR) et par l'analyse en ligne des gaz de réaction par chromatographie en phase gazeuse. Les catalyseurs « zircone sulfatée » se désactivent en deux étapes distinctes à 373 K : une phase initiale très rapide, et une seconde plus lente.

L´étape initiale de la réaction est toujours en discussion, mais plusieurs travaux scientifiques sont en faveur de la déshydrogénation oxydante (ODH). ZS contient très peu de sites actifs, et leur accès peut être bloqué quand certaines espèces y sont adsorbées.

Ce travail confirme le double caractère des produits de l´ODH : l´eau et le butène – leur effets positif et négatif sur l´isomérisation du *n*-butane. L´activité du catalyseur dépend du degré d´hydratation de ce dernier. Les conditions dans lesquelles (milieu gazeux et température) est activée la ZS sont d´une grande importance. De l´eau en excès, à la surface du catalyseur, peut bloquer l´accès des réactifs aux sites actifs ; diminuant ainsi l´activité de la ZS. Il est montré, dans ce travail, que l´eau formée lors des premières heures est responsable de la première étape de désactivation.

Comme reporté dans la littérature, le butène est un des produits de l´ODH. La protonation de ce butène par les sites actifs de Brønsted conduit à la formation des ions carbénium *sec*-butyle / groupes alkoxy adsorbés à la surface. Un mécanisme bimoléculaire faisant intervenir l´alkylation de l´ion carbénium *sec*-butyle avec une autre oléfine conduit à un réarrangement C-C. Les oléfines, en grande quantité, peuvent aussi être une des raisons de la désactivation du catalyseur. Nous avons montré que l´addition de propène au milieu réactionnel favorise la formation d´oligomères. Le même phénomène est aussi observé lorsque de l´oxygène est ajouté au système. Lors de la combustion, en présence d´oxygène, des espèces carbonées adsorbées à la surface du catalyseur, de l´eau, du dioxyde de carbone et de la chaleur sont produits. Cette chaleur peut favoriser la formation de polymères. Des oligomères absorbant à 370 et 450 nm ont été détectées à la surface de la ZS. Il est prouvé dans ce travail que qu´il existe une corrélation entre leur formation et la seconde étape de désactivation de la ZS. Ces espèces sont donc d'excellentes candidates pour expliquer la seconde phase de désactivation du catalyseur. Il est mis en évidence que les espèces monoénic allylique (absorbant à 295 nm) détectées à la surface de la ZS, au cours de la réaction d´isomérisation du *n*-butane, ne sont pas responsables de la désactivation du catalyseur, comme reporté dans la littérature, mais seulement des espèces spectatrices.

Ces espèces ne sont pas détectées dans les spectres UV-vis de la MnZS bien que ce catalyseur se désactive très vite. Les spectres UV-vis de la MnZS montrent deux bandes. Une attribution erronée de ces bandes dans la littérature a pu être corrigée grâce à des calculs. La bande d'absorption à 580 nm émane du Mn^{4+} et celle à 680 nm correspond à Mn^{3+}.

Sulfated zirconia deactivation during n-butane isomerization: an in situ UV-vis-NIR spectroscopic study

by Carine Chan Thaw

Abstract

The deactivation phenomena during *n*-butane isomerization on sulfated zirconia (SZ) and manganese-promoted sulfated zirconia (MnSZ, 0.5 or 2 wt% Mn) are investigated at 323 or 373 K by *in situ* UV-vis-NIR diffuse reflectance spectroscopy and on-line gas chromatography.
Sulfated zirconia (SZ) catalysts are found to deactivate in two steps at 373 K: a fast initial and a slow second phase.
The well accepted mechanism for the initiation step of the isomerization is the oxidative dehydrogenation (ODH). SZ is an acid catalyst with very few active sites. The access to these sites can be blocked when some species are adsorbed on them.
This work confirms the duality effect of the products of ODH: water and butene - their positive and negative effects on *n*-butane isomerization. An appropriate hydration level of SZ is important for the activity of the catalyst. Thus, the activation conditions (atmosphere and temperature) play a major role. However, excess water on the catalyst surface (band at 1910 nm in the NIR range) can block the access of the reactant to the active sites and thus diminishes the catalyst activity. In this work, it is shown that the water formed during the first few hours on stream is responsible for the first deactivation step.
As it has been reported in the literature, butene is another product of ODH and after its protonation by the Brønsted acid sites; sec-butyl carbenium ions stabilized by alkoxy groups are formed. The skeletal rearrangement can proceed through a bimolecular mechanism via an alkylation of the secondary butyl carbenium ion with another olefin. However, the presence of olefin in high quantities can be another reason for the deactivation of the catalyst. The addition of propene to the feed leads to the formation of oligomers. A similar effect on the deactivation of the catalyst is observed when oxygen is present in the system. The addition of oxygen to the feed leads to the combustion of carbonaceous deposits with the formation of water, carbon dioxide and heat. Moreover the heat can favour the formation of polymers. Oligomers were detected on the catalyst surface, with their absorption bands at 370 nm and 450 nm. The experiments showed that their formation corresponds to the second phase in SZ activity decline. These species are good candidates to explain the second step of SZ deactivation. Our study demonstrates that the monoenic allylic species (absorbing at 295 nm) detected on the catalyst during reaction, are only spectators, and not responsible for the deactivation phenomena, as reported in the literature.
These species were not detected in the UV-vis spectra of MnSZ in spite of its severe deactivation. However, two bands were observed in the visible range of MnSZ spectra. An erroneous assignment of these bands in the literature could be corrected with the help of calculations. The absorption band at 580 nm arises from Mn^{4+} and the one at 680 nm from Mn^{3+}.

Isomérisation du n-butane sur la zircone sulfatée: investigation in situ par spectroscopie UV-vis-NIR

Résumé long

L'isomérisation des *n*-alcanes à chaine courte est une réaction importante dans l'industrie pétrolière. En effet, grâce à leur indice d'octane élevé, les hydrocarbures branchés sont recherchés comme carburant, mais ils peuvent aussi servir de base à d'autres produits chimiques. En effet, ces hydrocarbures branchés servent à la production de composés tels que le méthyle *t*-butyle éther (MTBE). L'isomérisation de ces *n*-alcanes est donc une réaction très intéressante. La réaction cible de ce travail de thèse est la réaction d'isomérisation des *n*-alcanes et en particulier du *n*-butane :

$$n\text{-}C_4H_{10} \quad \rightleftharpoons \quad i\text{-}C_4H_{10}$$
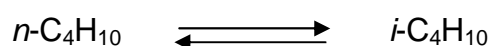
dont les données thermodynamiques dans les conditions standards (298 K et 101 kPa) sont les suivantes : enthalpie de réaction $\Delta_r H° = -7$ kJ mol^{-1}, entropie de réaction $\Delta_r S° = 15$ J K^{-1} mol^{-1}, et enthalpie libre $\Delta_r G° = -2.3$ kJ mol^{-1}. La formation d'isobutane est favorisée à basses températures (200 - 500 K). Un catalyseur actif dans cette gamme de température doit donc être trouvé.

En phase liquide, l'isomérisation des alcanes est catalysée par des acides forts tels que HF/SbF$_5$, RSO$_3$H/SbF$_5$ (R = C$_n$H$_{2n+1}$), CF$_3$SO$_3$H et HSO$_3$F.

Les catalyseurs utilisés en phase homogène, souffrent cependant de certains désagréments : le coté corrosif du catalyseur résulte en la formation d'eau usée acide et salée. Cette eau n'est ni facile à conserver ni à manipuler.

Ceci montre qu'il y a toujours des études scientifiques à réaliser pour trouver le catalyseur idéal, qui ne représente aucun danger (comme ceux cités plus haut) pour l'environnement.

Les catalyseurs à base d'alumine chlorée présentent à ce jour les meilleurs taux de conversion et de sélectivité en isomères. L'inconvénient de ce système catalytique est qu'il nécessite une chloration en continue et est sensible à des contaminants tels que l'eau, les oxydes de carbone et les oxygénés. Les zéolites comme catalyseurs peuvent être régénérées et sont peu sensibles aux contaminants décrits précédemment. Bien que les zéolites ne soient actives qu'à une température plus élevée que celle utilisée pour les catalyseurs à base d'alumine chlorée, le taux de

conversion maximum est limité par l'équilibre chimique non favorable. Les zéolites sont, de plus, moins sélectives que les catalyseurs à base d'alumine chlorée.

Les zircones sulfatées étant actives à une température inférieure à celle des zéolites l'équilibre chimique est plus favorable, par ailleurs elles peuvent être régénérées et ne nécessitent pas une chloration en continue.

En 1962, Holm et Bailey ont découvert que le platine-zircone-sulfatée était actif pour l'isomérisation de squelette d'hydrocarbures ; et ils ont déposé un brevet appartenant à Phillips Petroleum. En 1979 et 1980, il a été reporté que le *n*-butane peut s'isomériser, à température ambiante, avec comme catalyseur la zircone sulfatée (ZS). Comme il est extrêmement difficile d'isomériser le *n*-butane, cette découverte a amené de nombreux chercheurs à s'intéresser à cette nouvelle catégorie de matériaux.

La ZS est un catalyseur acide solide qui contient habituellement 5 à 6 % massique de SO_3. Idéalement, la ZS est composée de zircone ayant une structure nanocristalline quadratique et de sulfates à sa surface. L'activité catalytique peut être multipliée par 10 ou 100 en ajoutant une petite quantité de métaux de transition ou du manganèse qui a un effet positif sur l'activité de la ZS.

Dopée, ou pas, la ZS est active à basse température (e.g. 323 K). Malheureusement, elle se désactive, et cette désactivation peut être très rapide, dans le sens où elle a lieu dès les premières heures de la réaction. La désactivation d'un catalyseur peut s'expliquer d'une manière générale par la formation de composés de surface stables empêchant ainsi l'accès aux sites actifs. Ces composés, espèces stables de surface, peuvent être des composés (hydro)carbonés, mais aussi de l'eau, dans le cas des catalyseurs acides solides. Ces composés (hydro)carbonés et l'eau peuvent être soit des produits de réaction mais aussi provenir de certains contaminants que la phase gaz peut contenir. Des modifications structurales, morphologiques et chimiques seraient une cause plausible de la désactivation.

L'objectif de ce travail est de comprendre la ou les raisons pour lesquelles la ZS se désactive si vite au cours de la réaction d'isomérisation du *n*-butane. Afin de détecter non seulement de possibles modifications du catalyseur, mais aussi la présence d'espèces de surface, il est primordial d'étudier le catalyseur tout au long d'une réaction (mesures *in situ*). La spectroscopie à réflexion diffuse dans l'ultraviolet-visible et proche-infra-rouge (UV-vis-NIR) est une technique remarquable. En effet, il est possible d'identifier les modifications de la structure électronique du catalyseur en

étudiant les transferts de charges et les transitions *d-d*. Il est aussi possible d'observer les éventuelles formations d'espèces de surface comme des hydrocarbures saturés en analysant leur transition électronique et d'analyser la formation d'adsorbats tels que l'eau. Les modifications des groupements fonctionnels de surface peuvent être détectées par les modes de combinaisons des énergies vibrationnelles ou des transitions interdites qui se produisent. Les causes de la désactivation sont analysées en corrélant les données catalytiques et spectroscopiques.

Pour élucider si la désactivation observée est spécifique à un système catalytique ou est généralisable à ces matériaux, une comparaison a été faite entre les catalyseurs ZS non dopée ou dopée au manganèse.

La régénération du catalyseur a été réalisée par des traitements sous oxygène à haute température car nous supposons que la présence de dépôts (hydro)carbonés doit être brulée dans ces conditions.

Tout au long de ce travail, le catalyseur a été activé sous flux d'O_2 à 723 K. Les conditions de réactions ont été réalisées à 373 K sous flux continu d'un mélange gazeux à 5 kPa *n*-butane dilué dans du gaz inerte.

Selon les conditions expérimentales ci dessus, la ZS se désactive rapidement (60% de désactivation) dans les premières heures de la réaction; et elle continue plus lentement ce processus conduisant encore à 10 % de désactivation les 10 heures suivantes. Durant les premières heures (première phase de désactivation), l'eau est formée et est retenue à la surface. Ce qui est en accord avec la littérature. Après plusieurs heures, la concentration de l'eau en surface reste stable. On peut établir une corrélation entre la formation de l'eau et la rapide décroissance initiale de la vitesse d'isomérisation. L'empoisonnement des sites acides de Lewis lors de la production de l'eau est une explication possible, ce qui est confirmé par nos résultats. Nous avons clairement montré que l'eau se trouve être responsable de la désactivation rapide en début de réaction.

En plus de la formation de l'eau produite par déshydrogénation oxydante du réactif (ODH), d'autres espèces absorbant à 295, 370 et 450 nm, sont formées continuellement en fonction du temps (deuxième phase de la désactivation). Dans les publications, cette désactivation est attribuée à la présence de cations allyliques (absorbant à 295 nm). Leur formation peut être attribuée à la présence de certaines

impuretés (oléfines) dans le mélange réactionnel. Cependant, ce travail de thèse montre clairement que l'absence de ces espèces n'empêche en rien la désactivation à long terme de la ZS. Grâce à nos résultats expérimentaux, nous pouvons donc conclure que ces cations allyliques ne sont pas responsables de la désactivation du catalyseur, mais sont seulement des spectateurs. D'autres espèces insaturées, doivent donc expliquer cette désactivation à long terme de la ZS au cours de la réaction d'isomérisation. En effet, quand ces espèces poly-insaturées, absorbant à 370 et 450nm, sont formées et donc détectées, la ZS se désactive plus vite que si elles étaient absentes. La formation de ces espèces hautement conjuguées nécessite des réactions produisant de plus longues chaines carbonées (au moins sept atomes de carbone) suivies par une déshydrogénation. L'isomérisation du n-butane résulte en partie d'un mécanisme bimoleculaire. En effet, propane et pentanes sont détectés comme produits dérivés de réaction que des espèces C_8 doivent être formées par intermittence à la surface. Il est possible de favoriser la formation de ces espèces poly-insaturées lorsque des impuretés comme des alcènes ou oxygène sont présentes dans le mélange réactionnel. Les alcènes participent dans les réactions d'alkylation qu'il est possible d'envisager que les alcènes favorisent l'allongement des chaines carbonées. L'oxygène, comme réactif de la déshydrogénation oxydante, peut de façon directe contribuer à la formation d'espèces poly-insaturées. L'oxygène, indirectement, conduit à la combustion de dépôts carbonés à la surface du catalyseur. De la chaleur est ainsi produite et peut initier des réactions d'oligomérisation et de déshydrogénation. Lors d'une oxydation à température programmée, de l'eau et du CO_2 ont pu être détectés à 333 K. En nous basant sur nos résultats, nous arrivons à la conclusion que ces espèces poly-insaturées contrairement aux espèces mono-oléfiniques (qui sont rappelons le seulement des spectatrices) sont des poisons pour la ZS lors de l'isomérisation du n-butane.

Nous avons mis en évidence que l'eau et les espèces poly-insaturées sont responsables de la désactivation, en deux étapes, de la ZS. Il est cependant nécessaire de décrire aussi le rôle double de l'eau et des oléfines dans l'isomérisation du n-butane par la ZS pour comprendre sa désactivation.

Le rôle de l'eau est sujet à controverse car l'eau est un élément vital dans la phase d'initiation de l'isomérisation du n-butane. Malheureusement, une quantité excessive d'eau peut entraîner l'empoisonnement du catalyseur. Certains groupes scientifiques

proposent qu´un catalyseur actif doit contenir des sites actifs de Brønsted et de Lewis, dans un rapport 2 :1 respectivement. L´obtention de ce rapport n´est possible que si une certaine quantité d´eau est présente dans le catalyseur.

L´activité catalytique de la ZS non dopée dépend donc de la manière dont le catalyseur est activé et dans quelles conditions.

En plus de jouer un rôle important dans l´obtention d´une ZS active dans l´isomérisation du n-butane à basse température, l´eau est aussi un produit de réaction (par ODH). L´eau formée durant la phase d´initiation du mécanisme réactionnel s´adsorbe à la surface du catalyseur. L´accès aux sites actifs est ainsi bloqué. C´est la raison pour laquelle l´eau, élément majeur dans la phase d´initiation, se trouve être aussi un poison pour l´isomérisation du n-butane.

La ZS contient très peu de ces sites redox actifs (5 % de $S_2O_7^{2-}$) qui produisent l´acidité du catalyseur. Cette acidité permet de catalyser l´isomérisation du n-butane à basses températures.

L´étape initiale de cette réaction est donc la déshydrogénation oxydante du butane où le butène, l´eau et le SO_2 sont les produits de réaction. Le butène formé conduit aux ions carbénium secondaires avec les sites acides de Brønsted. Les ions carbénium sont stabilisés sous forme de groupes alkoxy, des intermédiaires de réaction. Cependant, ce groupe alkoxy peut aussi continuer à réagir et former par la suite d´autres produits qui bloqueront l´accès des sites actifs de la ZS ; conduisant ainsi à la désactivation du catalyseur. Introduire des oléfines, à haute concentration dans le système catalytique, induit à la formation d'autres espèces de surface telles que les oligomères. Les oligomères, détectées dans la partie UV-vis des spectres par les deux bandes à 370 et 450 nm, bloquent donc l´accès aux sites actifs, entraînant ainsi la désactivation de la ZS. Nous observons la même corrélation entre la désactivation du catalyseur et la formation d´espèces poly-insaturées quand la réaction d´isomérisation du n-butane a lieu en présence d´oxygène dans le mélange réactionnel. Dans ce dernier cas, les espèces intermédiaires, les groupes alkoxy, peuvent initier des réactions secondaires ; résultant ainsi à la formation de nouvelles espèces. Ces espèces peuvent causer la désactivation de la ZS.

Dans le cas où la ZS est dopée au manganèse (MnSZ), ce catalyseur se désactive également ; et cette désactivation est même plus rapide que celle observée dans le cas de la ZS. Au cours de la réaction d´isomérisation du n-C_4 sur la MnSZ, l´eau se

forme aussi lors des premières heures. A la différence de la ZS, aucune espèce insaturée n´est détectée dans la région UV-vis des spectres. De plus, le manganèse n´est pas réduit de manière significative, pour lui attribuer la désactivation de la MnSZ.

Nous devons cependant faire remarquer que les spectres UV-vis de la MnSZ sont différents de ceux de la ZS. En effet, les spectres de la MnSZ illustrent non seulement (i) le transfert de charge « ligand métal » dans la région 300 - 400 nm des spectres ; mais aussi (ii) les transitions *d-d* que nous observons par des bandes à 580 et 680 nm. La couleur de la MnSZ s´explique par ces transitions *d-d*. Il est trouvé que le milieu gazeux, dans lequel le catalyseur est activé, influence le degré d´oxydation du manganèse. Le nombre de bandes d'absorption dans les spectres UV-vis dépend du gaz utilisé pour activer le catalyseur. Dans un milieu inerte et oxydant, deux bandes sont observées. Dans un milieu réducteur, seule une bande d´absorption à 580 nm est observée dans les spectres. En opposition avec la littérature, ces bandes ne peuvent pas appartenir seulement appartenir au Mn^{3+}. Ces bandes doivent représenter deux différentes espèces du manganèse. En nous basant sur nos résultats expérimentaux, nous pouvons supposer que la bande à 580 nm est due au Mn^{4+} alors que la bande à 680 nm est due au Mn^{3+}.

Afin de confirmer ces hypothèses et en se basant sur les spectres expérimentaux de la MnSZ, nous avons demandé au Professeur Sophia Klokishner de réaliser des calculs théoriques afin d´interpréter nos résultats. Le catalyseur MnSZ a été activé sous flux d´hélium. Nous avons basé les calculs sur un modèle où les ions Mn^{3+} dans le réseau de la zircone induisent la création de lacunes d´oxygène afin de compenser la perte de charge. Ceci entraîne ainsi le déplacement η_1 et η_2 des atomes d´oxygène en direction de ces lacunes ; et la symétrie du complexe Mn^{3+} est supposée être trigonale. Enfin, pour ce modèle, nous avons négligé la contribution des transitions *d-d* des cations Zr^{3+}. Quand les ions Mn^{4+} se substituent aux ions Zr^{4+}, la position des 8 atomes d´oxygène (ligands) entourant le Mn^{4+} reste inchangée. C´est en se basant sur ce modèle et en utilisant un ensemble de paramètres pour illustrer les déplacements η_1 et η_2 des ions oxygène que nous pouvons exactement conclure que la bande d´absorption à 580 nm appartient au Mn^{4+} alors que celle à 680 nm appartient au Mn^{3+}. Selon la littérature, le Mn^{2+} devrait être présent dans ce

matériau. Il est cependant impossible d'observer les transitions *d-d* du Mn^{2+} car les transitions de spin sont interdites.

Au cours de la réaction d'isomérisation du *n*-butane à 373 K, le MnZS perd plus de 95 % de son activité catalytique après 16h de réaction; alors que le degré d'oxydation du manganèse est au plus réduit de 20%. La réduction du manganèse ne peut pas être la raison de la désactivation du MnZS. De plus, aucune des espèces détectées dans les spectres UV-vis de la ZS ne sont observées sur le MnSZ.

Sulfated zirconia deactivation during n-butane isomerization: an in situ UV-vis-NIR spectroscopic study

Long summary

One of the most important reactions in petroleum chemistry is the skeletal isomerization of short chain alkanes. Branched alkanes are desirable as fuels because of their high octane number. These isoproducts are also used in the production of gasoline components such as methyl *t*-butyl ether (MTBE), or as intermediates for more valuable hydrocarbons. The skeletal isomerization reaction is challenging. The target reaction of the present work is the isomerization of *n*-butane:

$$n\text{-}C_4H_{10} \rightleftharpoons i\text{-}C_4H_{10}$$
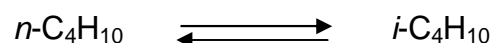
with the following thermodynamic data under standard conditions (298 K and 101 kPa): reaction enthalpy $\Delta_rH° = -7$ kJ mol^{-1}, reaction entropy $\Delta_rS° = 15$ J K^{-1} mol^{-1}, and Gibbs free energy $\Delta_rG° = -2.3$ kJ mol^{-1}. The isobutane formation requires a temperature range of 200 to 500 K. A catalyst active at this temperature should be found.

In liquid phase, alkane isomerizations are catalyzed by strong acids such as HF/SbF$_5$, RSO$_3$H/SbF$_5$ (R = C$_n$H$_{2n+1}$), CF$_3$SO$_3$H and HSO$_3$F. These homogeneous catalysts, however, suffer the following disadvantages: the acids are corrosive and cause handling and disposal problems.

The need for environmentally friendly production within the chemical industry is universally acknowledged, thus the use of heterogeneous catalysts (which have the potential to be recycled and avoid the aforementioned disadvantages) is an attractive alternative. Chlorided alumina based catalysts currently have the highest isomerization activity and yield available. However, they need a constant organic chloride co-feed, they cannot be regenerated and are sensitive to contaminants such as water, carbon oxides and oxygenates. Zeolitic isomerization catalysts are able to be regenerated and relatively contaminant tolerant. However, zeolitic catalysts are only active at much higher temperatures than chlorided alumina catalysts, thus the maximum conversion is limited by the unfavourable equilibrium position. Yields are also lower for the zeolitic catalysts than for the chlorided alumina catalysts as they are less selective. Sulfated zirconia based catalysts are active at lower temperatures than zeolitic catalysts (thus under more favourable equilibrium conditions); they can

be regenerated and do not require a chlorided co-feed or caustic scrubbing unlike the chlorided alumina catalyst.

In 1962, Holm and Bailey discovered that platinum-doped sulfated zirconia is active for skeletal isomerization and filed a patent assigned to Phillips Petroleum. In 1979 and 1980, it was claimed that sulfated zirconia (SZ) is active for the isomerization of n-butane at room temperature. Because butane is extremely difficult to isomerize, this discovery led to the current great interest in this class of materials.

SZ is a solid acid catalyst and typically contains 5–6 wt % SO_3. The desirable SZ consists of zirconia in a tetragonal nanocrystalline structure with sulfate on the surface. It has also been shown that it is possible to increase the catalytic activity by 1 or 2 orders of magnitude by adding small amounts of certain metal cations; e.g. manganese has a promoting effect on SZ catalysts.

Non-promoted and promoted SZ are active at low temperatures (e.g. 323 K), but suffer from deactivation, which can be very rapid, i.e. it occurs in the first few hours on stream. Catalyst deactivation is often due to formation of stable surface compounds, which block access to active sites. These stable surface species can be carbonaceous deposits or, in case of solid acid catalysts, water. They can be side products of the reaction or can arise from contaminants in the feed gases. Deactivation can also be caused by the structural, morphological or chemical transformation of the catalyst.

The aim of this work is to understand the reason(s) for the rapid deactivation of sulfated zirconia catalysts during alkane isomerization. In order to detect a change in the catalyst, or the presence of surface species, the sample needs to be investigated while the catalytic reaction is proceeding (in situ measurement). Diffuse reflectance ultraviolet-visible near-infra-red (UV-vis-NIR) spectroscopy is a powerful technique because (i) changes in the electronic structure of the catalyst can be identified through analysis of charge transfer or d-d transitions, (ii) formation of unsaturated hydrocarbon surface species can be followed via observation of their electronic transitions, and (iii) changes to surface functional groups or formation of adsorbates (water for example) can be detected through vibrational combination and overtone modes. The causes of deactivation are identified by correlating the catalytic and spectroscopic data.

To elucidate whether the observed deactivation behavior is specific for a particular catalyst, or valid for the entire class of SZ materials, unpromoted and manganese-promoted SZ catalysts are being compared.

Regeneration of the catalyst is attempted by oxidative treatment at high temperature, assuming the presence of carbonaceous deposits, which can be burnt.

In the course of this thesis, the catalyst was activated at 723 K in O_2. The reaction was conducted at 373 K in 5 kPa n-butane diluted in N_2.

For the unpromoted sulfated zirconia, the catalyst rapidly lost activity (60 % with a continuous flow of n-butane) within the first few hours on stream and then continued to deactivate slowly (10 %).

During the first few hours (first deactivation stage), water is formed and retained on the surface, consistent with literature reports. After a few hours, the water concentration on the surface is stable. A correlation can be drawn between the trend of water formation detected and the rapid decrease in the rate of isomerization. Poisoning of Lewis acid sites through the water produced is a possible explanation and most of the results are consistent with this observation.

Besides the water formation by oxidative dehydrogenation (ODH), other species (absorbing at 295, 370 and 450 nm) are observed. The band at 295 nm is frequently observed while the bands at 370 and 450 nm are occasionally formed. These species are continuously formed with time on stream and are considered to be candidates for causing the long-term deactivation. It was previously reported in the literature that the deactivation of the catalyst is to be due to formation of monoenic allylic species absorbing at a band position of 295 nm. In this work, it was found that their formation is linked to the presence of some impurities (alkenes) in the feed. However, the present work clearly shows that the absence of these species does not prevent the catalyst from longer term deactivation. It is thus concluded that the monoenic allylic species are only spectators in the loss of activity of the catalyst. Other species thus must be responsible for the long term deactivation of SZ during the reaction. Indeed, when the polyunsaturated species absorbing at 370 and 450 nm are detected during n-butane isomerization, SZ deactivates faster than without these species. The formation of these highly conjugated species requires reactions producing longer chains (at least seven carbon atoms) followed by dehydrogenation. The skeletal isomerization of n-butane occurs at least in part through a bimolecular

mechanism as propane and pentanes are detected as byproducts, and hence C_8 species must be formed intermittently on the surface. The presence of alkenes or oxygen impurities in the feed was found to promote the formation of the polyunsaturated species. Alkenes are partners in alkylation reactions and it is thus conceivable that they promote further chain growth. Oxygen can directly engage in the formation of polyunsaturated species as a reactant in oxidative dehydrogenation, and indirectly through combustion, the heat of which can initiate oligomerization and dehydrogenation reactions. Evidence for the latter assumption arises from a temperature programmed oxidation experiment, in which H_2O and CO_2 could be detected at 333 K. Based on all the results, it can be concluded that polyunsaturated species are most likely the poison for the catalyst during *n*-butane isomerization, rather than the monoenic allylic species which are only spectators.

Rather than showing that water and polyunsaturated species are two distinct reasons for SZ deactivation; this work also describes the dual role of water and olefins for *n*-butane isomerization on sulfated zirconia which has to be considered for understanding SZ deactivation.

The role of water is debated, as water (i) is a vital component in the initiation part of the *n*-butane isomerization, but (ii) can act as a poison when it is in excess. Some groups explained that an active catalyst should contain a ratio of Brønsted to Lewis acid sites, 2:1 respectively. This ratio could be achieved in the presence of a certain amount of water. The activity of unpromoted sulfated zirconia catalyst depends thus on the way in which the catalyst is activated and under which conditions. Besides being an important component for an active catalyst in the *n*-butane isomerization on SZ at low temperature, water is also a product of alkane activation via ODH. The water formed during the initiation step of *n*-butane isomerization adsorbs on the surface of the catalyst. The access to the active sites can thus be blocked. For this reason, water which is a vital component in the initiation step was revealed to act as poison during the skeletal isomerization.

Sulfated zirconia which, according to the literature, contains few redox active sites ($S_2O_7^{2-}$) provides the acidity to catalyze the *n*-butane isomerization at low temperatures. This reaction is initiated by the oxidative dehydrogenation of *n*-butane to butene, water and SO_2. The formed butene forms *sec*-carbenium ions with Brønsted acid sites and isomerizes via carbenium ions that are stabilized in the form of alkoxy group intermediates. However, the alkoxy group can also react further to

form side products blocking the access to the active sites of SZ; and leading to the deactivation of the catalyst. Introducing higher concentrations of olefin in the reaction chamber induced the formation of additional surface species, including oligomers. The oligomers detected in the UV-vis range of the spectra at 370 and 450 nm blocked the access to the active sites and deactivated sulfated zirconia catalyst. Similar correlation between the catalyst deactivation and the formation of highly conjugated species was observed in the case of O_2 addition to the feed. In this case again, the intermediate species, alkoxy groups, can undergo side reactions and produce species which can also cause the deactivation of the catalyst.

Manganese promoted sulfated zirconia (MnSZ), deactivates even faster than SZ. Based on the NIR spectra, the same observation of the water formation during the first few hours on stream can be drawn for the manganese-promoted and unpromoted-sulfated zirconia.

The UV-vis spectra of the manganese promoted sulfated zirconia are different from the spectra of unpromoted SZ. The spectra are different because (i) ligand to metal charge transfer occurs in the wavelength range 300 - 400 nm and (ii) manganese *d-d* transitions are observed at band positions 580 and 680 nm. The latter justifies that MnSZ is a colored catalyst. The activation atmosphere was found to influence the oxidation state of manganese. The number of absorption bands in the UV-vis range of the spectra of MnSZ depends on the activation atmosphere. In inert or oxidizing atmosphere, two bands were observed. In reducing atmosphere, one absorption band at 580 nm is observed in the spectra. In contrast to the literature, these bands cannot belong to only one species, Mn^{3+}. These bands must represent two different species. Based on the experimental results it can be assumed that the band at 580 nm belongs to Mn^{4+}, while the band at 680 nm is due to Mn^{3+}.

To verify the assignments of these bands, calculations were performed and interpreted by Prof. Sophia Klokishner based on the obtained spectroscopic data of MnSZ activated with He (the course of this work). Furthermore, the calculations were based on a model where Mn^{3+} ions in the zirconia lattice induce the generation of oxygen vacancies for charge compensation leading to the displacements η_1 and η_2 of the oxygen atoms towards the oxygen vacancies; and the symmetry of the Mn^{3+} complex is assumed to be trigonal. Moreover, the *d-d* transitions of Zr^{3+} were excluded for our calculations. When Mn^{4+} ions substitute Zr^{+4} ions, the position of 8 oxygen ligands surrounding the Mn^{4+} is assumed not to be changed. Based on this

model and using two sets of parameters for the O^{2-} displacements, it is clearly shown that the absorption band at 580 nm belongs to Mn^{4+} and the one at 680 nm to Mn^{3+}. Mn^{2+} should be also present in these materials according to the literature, however, the *d-d* transitions of the Mn^{2+} ions are not observable because they are spin forbidden.

During the *n*-butane isomerization at 373 K, SZ loses more than 95 % of its activity within 16 hours while the manganese is not reduced by more than 20 % of its initial oxidation state. Manganese reduction is thus not responsible for the deactivation of manganese-promoted sulfated zirconia. Furthermore, none of the unsaturated species, formed in the case of unpromoted sulfated zirconia, are detected in the UV-vis range of the spectra during reaction over manganese promoted sulfated zirconia.

_____

Abbreviations

SHZ	Sulfated hydrous zirconia
SZ	Sulfated zirconia
MnSZ	Manganese sulfated zirconia
PtSZ	Platinum sulfated zirconia
RuSZ	Ruthenium sulfated zirconia
t	tetragonal
m	monoclinic
wt.%	weight percent
vol.%	volume percent
UV-vis-NIR	Ultraviolet-visible-near infra red
DRS	Diffuse Reflectance Spectroscopy
DRA	Diffuse Reflectance Attachment
KM	Kubelka Munk function
TOS	Time on stream
R %	Reflectance
T	Temperature
GC	Gas chromatography
FID	Flame ionisation detector
TCD	Thermal conductivity detector
RF	Response factor
GC-MS	Gas chromatography-mass spectrometer
XANES	X-ray absorption near edge structure
ODH	Oxidative Dehydrogenation

Table of contents

_____

1.1. Introduction

Skeletal isomerization of linear short chain alkanes is an important reaction in petroleum chemistry. Because of their high octane numbers, branched alkanes improve the combustion properties and are desirable as fuels. Alternatively, they can be further converted to other chemicals. Isobutane, which has a research octane number of 100.4[1], is not added directly to gasoline but used for the production of alkylate or – after dehydrogenation – for the synthesis of ethers like methyl t-butyl ether (MTBE) [2]. The isomerization of the reactant molecule of interest in this thesis, n-butane, has the following thermodynamic data under standard conditions (298 K and 101 kPa): reaction enthalpy $\Delta_rH° = -7$ kJ mol^{-1}, reaction entropy $\Delta_rS° = 15$ J K^{-1} mol^{-1}, and Gibbs free energy $\Delta_rG° = -2.3$ kJ mol^{-1}.

Isomerization of n-butane:

$$n\text{-C}_4\text{H}_{10} \rightleftharpoons i\text{-C}_4\text{H}_{10}$$
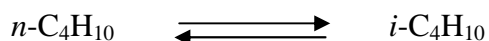
Low temperatures (200 – 500 K) are desirable for n-butane isomerisation, as the equilibrium is shifted towards the desired product (branched alkane). This required low temperature can be seen in Figure 1 - 1 which represents the equilibrium composition for butane as function of temperature[3].
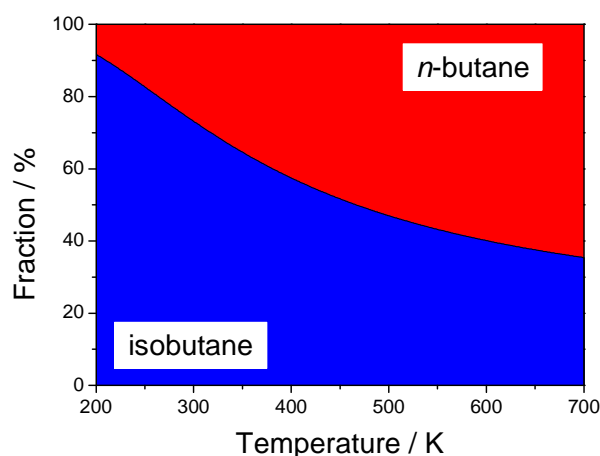
Figure 1 - 1: Equilibrium composition for n-butane/isobutane isomerization as a function of temperature (the temperature dependence of the reaction enthalpy was neglected).

The alkane isomerization is also catalyzed in liquid phase by using strong acids such as HF/SbF$_5$, RSO$_3$H/SbF$_5$ (R = C$_n$H$_{2n+1}$), CF$_3$SO$_3$H and HSO$_3$F[4]. However, these acids are not as friendly as they cause corrosion, handling and disposal problems; separation of the catalyst from the product is also a source of problems. Environmentally friendly heterogeneous catalysts are thus subject of attention. For several years the alkane isomerization reaction has been industrially performed using platinum on chlorided alumina[1,5] (393-453 K) or zeolites (533 K) in presence of H$_2$ in the feed to achieve stable catalytic operation. However, for the former catalysts, a continuous supply of chlorinated compounds is needed and for the zeolite-based catalyst, which is environmentally friendly, a higher temperature is required[6]. Hence, there is an ongoing search for better catalysts. In 1962, Holm

and Bailey[7] discovered that platinum-doped sulfated zirconia is active for skeletal isomerization and filed a patent assigned to Phillips Petroleum. It was only in 1979 and 1980, when Hino and Arata[8,9] claimed sulfated zirconia (SZ) is active for the isomerization of *n*-butane at room temperature, that the catalyst drew more attention. Because butane is extremely difficult to isomerize, this discovery led to the current great interest in this class of materials.

As the role of platinum and hydrogen is not clear in the stabilization process, SZ was selected for this thesis as an example to identify the reasons for deactivation in absence of platinum and hydrogen in the feed. The suspected reasons for deactivation are several, but hydrocarbon deposits[10,11,12] and water[13] adsorbed on the surface have been most frequently proposed.

1.2. Sulfated zirconia deactivation

Isobutane formation is favored at low temperature as shown in Figure 1 - 1 at which SZ is an active catalyst. SZ can be promoted with different transition metal cations[14] and this leads to an increase in the catalytic activity of the catalyst by 1 or 2 orders of magnitude[15]. Lange *et al.*[14] reported that the effect of promotion on the maximum activity follows the trend

Mn > Fe>> Co>> Ni> Zn.

However these catalysts suffer from deactivation as shown in Figure 1 - 2.
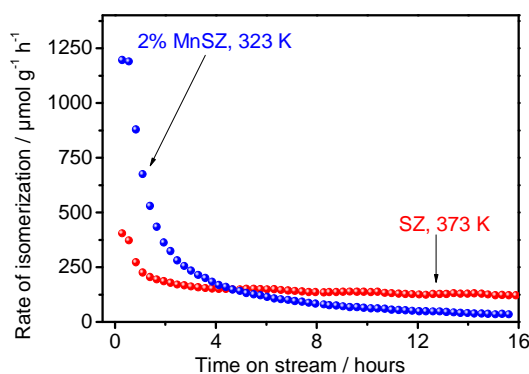
Figure 1 - 2: Typical reaction profile of SZ and MnSZ. Reaction conditions: both catalysts were activated under O_2 at 723 K for 30 minutes. Reaction under 5 kPa *n*-butane diluted in N_2 at 373 K for SZ and 323 K for MnSZ.

Several reasons have been proposed to explain this loss in activity: (i) carbonaceous deposits[10,11,12,13], (ii) surface poisoning by water[6,13,16,17,18], (iii) reduction of the sulfate group[19] and H_2S formation[20], (iv) change in the surface phase of zirconia from tetragonal to monoclinic[21] and (v) reduction[22] of Zr^{4+} to Zr^{3+} but so far this is only speculation as no proof has been found for this reduction. For promoted SZ, Millet *et al.*[23] explained the deactivation by the reduction of the Fe promoter in the Fe-containing SZ. However,

Yamamoto *et al.*[24] refuted the idea that Fe has been reduced by *n*-butane as no changes in the Fe valence was observed. For the Mn promoted SZ under *n*-butane exposure, no direct correlation has been found between the deactivation and the catalytic performance.

_____

1.2.1. Carbonaceous deposits

The alkane isomerization on the solid acid catalyst SZ was first believed to proceed via carbocation-like intermediates[25], in analogy to the isomerization of alkanes in liquid superacids. Many authors[26,27,28] classified SZ as superacid on the base of their investigations using Hammett indicators. The carbenium ion is the final product[29] of a protolytic activation of a C-H bond via formation of a carbonium ion with a pentacoordinated carbon atom, which releases H_2. However, this mechanism is subject for controversy in the case of SZ which is proved not to be a superacid[30,31] but a strong acid. Investigation into the acid sites was carried out by using probe molecules such as pyridine and CO and most of the time these studies were combined with IR; and it resulted that the acidity of the sulfated zirconia is linked to either its Brønsted or Lewis acid sites.

The carbenium ion has been proposed to be formed by (i) activation via direct hydride abstraction by Lewis acid sites[32,33], (ii) protonation on Brønsted acid[34] sites of alkenes impurities that the feed might contain and (iii) oxidative dehydrogenation[35] of the alkane implying that the alkenes are generated during the reaction but not provided by the feed (Figure 1 - 3). The alkenes can then be dehydrogenated because of the strong acidity of the catalyst that the formation of oligomers, polymers and aromatics compounds can be imagined. They are adsorbed on the catalyst surface and are blocking the active sites; resulting thus in the decrease of the catalytic activity.

Up to now, the skeletal rearrangement of alkanes is still under debate. Different reports proposed this rearrangement can proceed through a unimolecular (intramolecular or monomolecular) or / and a bimolecular (intermolecular) mechanism. Garin *et al.*[36] performed some experiments on sulfated zirconia and platinum promoted sulfated zirconia with $^{13}C_1$-butane and $^{13}C_2$-methyl-2-propane. The isotope distribution in the products shows an intramolecular rearrangement. In contrast, Adeeva *et al.*[37] showed, using double ^{13}C-labelled *n*-C_4 ($^{13}CH_3$-$^{12}CH_2$-$^{12}CH_2$-$^{13}CH_3$) on sulfated zirconia and by studying the reaction products (reaction at 403 K) with a mass spectrometer, that this reactant isomerizes via a bimolecular mechanism, in which a C_8 intermediate is involved.
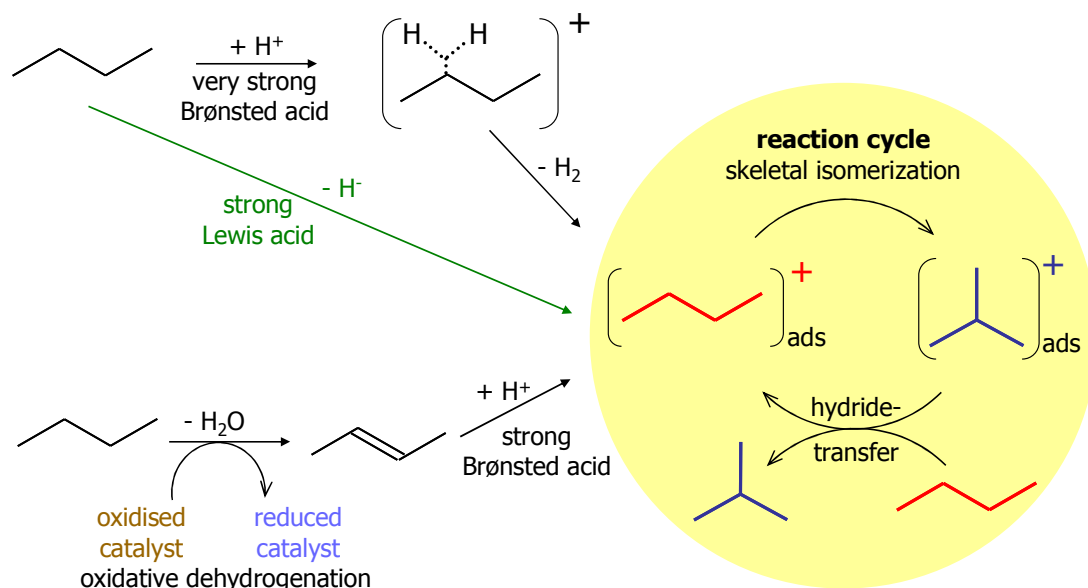
Figure 1 - 3: Mechanism of *n*-butane isomerization with three proposed possibilities for the initiation step

Chen *et al.*[10] first reported the deactivation of the SZ under *n*-butane (9 kPa) isomerization at 523 K as a result of hydrocarbon deposits on the surface. Their UV-vis spectra obtained at the end of the reaction show an intense band at 292 nm that they ascribed to allylic species. Spielbauer *et al.*[11] performed a similar reaction (8.5 kPa *n*-C_4 in He) on SZ in a temperature range of 393 - 473 K. After the reaction, using UV-vis diffuse reflectance spectroscopy measurement, they obtained three bands at 306, 366 and 400 nm. They assigned the first band position to allylic cations; the one at 366 and 400 nm are ascribed to polyenylic cations and aromatic compounds. Based on a D_2O-exchanged solid acid H-USY and isobutane at 373 K study, Sommer *et al.*[38] observed a band at 292 nm that they ascribed to cyclopentenyl cations, and later after several cycles, they also observed the formation of polyenylic and aromatic ions. Up to now, only one paper[12] reported the formation of surface deposits during *in situ* UV-vis diffuse reflectance spectroscopy (DRS) of the *n*-butane isomerization on sulfated zirconia, and they are consistent with the previous authors which impute the deactivation of the SZ to the formation of allylic species. The assignment of the species observed after *n*-butane isomerization on SZ, are for the most part based on investigations of propene adsorption on zeolitic materials. Three bands in the range 290-330, 350-380 and 430-460 nm are developed and assigned to mono-, di- and trienylic carbenium ions[39,40,41,42].

However, the correlations between the information obtained by the spectroscopic data and the activity of the catalyst during the reaction are limited.

_____

Besides the hydrocarbon deposits on the surface of the catalyst, which is one of the most reported reasons for deactivation, water adsorbed on the surface of the catalyst is also reported to be responsible for the deactivation[13,16,17,18,43].

1.2.2. Water

The role of water is debated, as water (i) is a vital component in the initiation part of the *n*-butane isomerization, but (ii) can act as a poison when it is in excess. Several reports were published to explain the role of water in alkane isomerization on SZ at low temperature. Several groups support the idea that the carbenium ion is formed through butane oxidative dehydrogenation[22,43,44,45,46] (ODH). The *n*-butane ODH (Figure 1 - 3) produces water and butenes. Besides being a product of the reaction[47], water is also initially present in the catalyst which is hydrophilic, and is also reported to be a possible poison for the active sites[13]. Thus, the activation atmosphere (He or N_2, O_2, H_2) and temperature[22,48] are important parameters for the degree of surface hydration of the catalyst[20,49] and for the catalyst activity respectively.

For instance, Gonzalez *et al.*[16] claimed that a water concentration of 75 $\mu mol\ g^{-1}$ is optimal while Song and Kydd[48] reported a best catalytic performance on SZ at 200 $\mu mol\ g^{-1}$. A decrease in the water content of the activated catalyst results in a decrease of Brønsted acidity and an increase in Lewis acidity. Song[50] explained that an active catalyst should contain a ratio Brønsted to Lewis acid sites 2:1. This ratio could be achieved in presence of water. The reaction of *n*-butane isomerization on sulfated zirconia is thus dependent on the level of hydration of the catalyst.

Wen[51], Dumesic[16,17,18] and Song[52] reported the positive effect of water on the initiation part of the reaction. Dumesic *et al.*[16,17] showed the importance of the water content by varying the temperature of calcination; and by adding successively a certain amount of water (74 $\mu mol\ g^{-1}$ H_2O) until a maximum catalytic activity (5256 $\mu mol\ g^{-1}h^{-1}$ isobutane) was reached during *n*-butane isomerization (10 kPa at 423 K).

However, Dumesic[16,17,18] and Song and Kydd[52] also claimed the negative effect of adding too much water on the catalyst: a small amount of water has a promotional effect on the catalytic activity of the SZ (75 $\mu mol\ g^{-1}$ of water to obtain the maximum activity), but at higher amounts the water acts as a poison of the catalyst. Comelli *et al*[13]. speculated, without showing any data corroborating this assumption, that the partial transformation of Lewis into Brønsted acidity in the presence of water can explain the deactivation of sulfated zirconia. In 2004, the activity response of the SZ catalyst to feed containing water during a pilot plant test

_____

was described in an abstract by UOP LLC[53]. The addition of 30 wt-ppm water results in a significant performance loss at 436 K. However; this performance loss can be minimized by simply raising the reactor temperature (450 K) and finally, when the dry feed is re-introduced, the performance is fully recovered. Li *et al.*[43] reported an in-situ IR investigation of *n*-butane isomerization on SZ at 373 K. Formation of water is observed with the increase in intensity of the band at 1600 cm^{-1} with time on stream, which is ascribed to water deformation. Additionally the IR band at 3580 cm^{-1}, corresponding to the OH stretching vibration of water, also increased in intensity. The water was formed only during the induction period and once the steady state had been reached, the rate of accumulation of water was significantly slower. These authors concluded, based on their data, that *n*-butane isomerization was initiated by ODH. Klose *et al.*[45] also reported adsorbed water on the catalyst surface during the induction period of the *n*-butane isomerization on SZ; and this water is potentially a product of oxidative dehydrogenation.

Up to now in the literature, there is not a direct correlation between the actual water content and the catalytic performance of SZ.

1.2.3. Reduction of sulfate

The reduction of sulfate takes place during the initiation through ODH. Once the carbenium ion is generated, an infinite number of skeletal isomerization cycles is possible. The reduction of sulfate cannot be thus the reason of deactivation.

The ODH pathway was recently supported by Li *et al.*[43] . They could detect the three products of oxidative dehydrogenation during reaction of *n*-butane isomerization, which are butene (from *n*-butane temperature programmed reaction spectroscopy); formation of water (by *in situ* IR spectroscopy) and reduction of sulfate (by thermally desorbing the various sulfur species). At high reaction temperature, 523 K, during the *n*-butane isomerization on SZ, Ng and Hovart[54] detected hydrogen sulfide in the reactor product gas by bubbling the gas through a solution of $Cd(O_2CCH3)_2$ and analyzing via GC-MS. This hydrogen sulfide results from a sulfate loss which then reduces the acidity of the catalyst (Brønsted sites) during the initiation step. However, Klose *et al.*[45] investigated the deactivated manganese promoted sulfated zirconia, MnSZ, after exposure to 5 kPa *n*-butane at 323 K. After regeneration in N_2 of the deactivated MnSZ, they did not find any evidence of sulfur loss; meaning here that the reason of deactivation can not be sulfur loss.

_____

1.2.4. Phase change

Zirconia is a polymorphous material: monoclinic, tetragonal and cubic. The monoclinic phase which is stable at room temperature transforms into the tetragonal phase at 1443 K. The tetragonal phase can then be transformed into the cubic phase at 2643 K.[55] The tetragonal and cubic phases can be stabilised at room temperature by the addition of various dopants (including sulfate)[56] and also crystallite size effects (by < 30 nm sized crystals)[57-60]. Metastable cubic and tetragonal sulfated zirconia are active isomerization catalysts, whereas monoclinic sulfated zirconia has been reported to be inactive,[61] or 4-5 times less active than tetragonal zirconia[62]. Morterra et al.[28] reported that the sulfated cubic (yttria-stabilized) zirconia is even more active than the tetragonal zirconia. The desirable SZ consists of zirconia in a tetragonal nanocrystalline structure[56,59], with sulfate on the surface. Phase changes of zirconia can lead to the deactivation of the catalyst.

Li et al.[21] claimed that the SZ deactivation is due to a surface phase change from tetragonal to monoclinic. They established a correlation between the deactivation of SZ catalysts after *n*-butane isomerization at 453 K with the zirconia phase change observed by recording UV Raman spectra.

1.2.5. Reduction of Zr^{4+}

The reacting hydrocarbons can act as reducer. It can be assumed that they reduced Zr^{4+} to Zr^{3+}. However it is difficult[63] to reduce Zr^{4+} to Zr^{3+}.

1.2.6. Reduction of promoter

The faster deactivation and the drastic loss in the catalytic activity of manganese promoted sulfated zirconia than the one observed with the non promoted catalyst, is not understood. It is accepted that butane is activated through ODH to give water and butenes together with the reduction of the catalyst. Millet et al[23]. suggested the deactivation of the Fe promoted SZ is due to the reduction of the promoter; results refuted by Yamamoto[24]. Data for the changes in the promoter valence as a consequence of a potential ODH are controversial.

The role of activation atmosphere was observed by Song and Kydd[52]. The activation atmosphere, He or air, did not affect the activity of the unpromoted SZ; while activation in air resulted in a higher activity of the iron manganese promoted sulfated zirconia than activation in He. Wan et al.[64] believe that the activation of the Fe-Mn promoted sulfated zirconia at high temperature in air generates a rather labile but reactive oxy species. These resulting oxy species could then play a role in providing an initial oxidative dehydrogenation of *n*-butane to

_____

butene at room temperature (303 K). Jentoft *et al.*[65] reported that during *ex situ* experiments (1% *n*-butane in N_2 at 338 K) with Mn-promoted SZ samples activated in dry nitrogen at 723 K, Mn was reduced. The same authors[66] reported the results of an *in situ* XANES study of Mn in promoted SZ catalysts. Here it was found that Mn in 2 wt% MnSZ catalysts does not act as a stoichiometric redox-active initiator in *e.g.,* an oxidative dehydrogenation reaction. Furthermore, they showed that a higher valence directly prior to reaction correlates with a higher maximum conversion. It was also shown that the average valence of Mn depends on the presence of sulfate in the catalyst.

Manganese is not reduced during the reaction of isomerization but manganese promoted sulfated zirconia deactivates. Other reasons must thus exist to explain the deactivation of this promoted catalyst.

1.3. Scientific aims and strategy

SZ deactivates within few hours on stream, and this loss in activity is reported to be mainly due to unsaturated species deposited on the catalyst surface. Additionally, water adsorbed on the surface of the catalyst is also reported to act as a poison in this reaction.

This work has the objective to contribute to the understanding of the deactivation process by studying the carbonaceous deposits and water formation during the reaction of *n*-butane isomerization on SZ. For this purpose, manganese promoted and non promoted sulfated zirconia were prepared and characterized following a procedure validated by a previous PhD dissertation from the group[67].

1.3.1. Selection of samples

SZ is an attractive catalyst for *n*-butane isomerization at low temperatures. The maximum rate of isobutane can be improved by promoting SZ with manganese. As the manganese-promoted and unpromoted sulfated zirconia, MnSZ and SZ, deactivate; their activity can be stabilized by adding some modifiers to SZ, Pt and Ru-like, and hydrogen to the feed.

1.3.2. Selection of reactants

For the present work, *n*-butane which is in gas phase was studied as it is easy to handle; but the mechanism is complicated to study. The mechanisms for the longer chain hydrocarbons *n*-hexane and *n*-heptane are better understood. These hydrocarbons were thus chosen to study the deactivation kinetic.

_____

1.3.3. Selection of methods

Understanding how the activity and selectivity of the catalyst in a catalytic reaction depend on its structural and electronic properties is one of the major goals in catalysis research. This can be achieved by studying catalytic materials by *in situ* spectroscopy in combination with gas chromatography (GC).

Spectroscopy in the ultraviolet (UV), visible (vis) and near-infrared (NIR) region of the electromagnetic spectrum is often called electronic spectroscopy because electrons are transferred from low energy (**H**ighest **O**ccupied **M**olecular **O**rbital –HOMO) to high energy (**L**owest **U**noccupied **M**olecular **O**rbital-LUMO) when the material is irradiated by light. This electron transfer occurs in (i) transition metal ion complexes (*d-d* transitions and ligand to metal or metal to ligand charge transfer transitions), and (ii) inorganic or organic molecules (mainly n $\rightarrow$ π* and π $\rightarrow$ π* transitions). This electron transfer in the UV-vis range is responsible for the colour of matter. In the NIR range it is additionally possible to study the vibrational transitions of species. Thus, UV-vis spectroscopy is a method used for several applications.

Solutions and gases are investigated by transmission spectroscopy, which is quite difficult with powders and solids, due to problems with light scattering phenomena. Because transmission can be low with powders and the surface of the powders is matt (dull, scattering surfaces); the reflected light is studied. The diffuse reflected light can be collected by the so-called Diffuse Reflectance Spectroscopy technique.

UV–vis–NIR spectra contain information on the catalyst itself via the electronic and vibrational transitions of the species present: oxidation state and coordination can be obtained from *d-d* and charge transfer transitions; dispersion of supported oxidic or metallic species can be estimated; and the band gap of semiconductors can be determined. The nature of functional surface groups can be deduced from overtone and combination modes of their vibrations. Also, surface adsorbates – probes, reactants, products, intermediates, side products – can be detected; if they contain chromophoric group or vibrational pattern with pronounced overtone and combination modes. Unsaturated species, which contain carbon-carbon double bonds, can be highly conjugated so that aromatics compounds can be formed. Several research groups adsorbed propene on a zeolite and reported the formation of allylic species[42], polyenylic cations and aromatic compounds[41] to explain the deactivation of the catalyst. Moreover, water, which can be detected in the NIR range by its vibrations, is also reported to be a reason for the deactivation of the catalyst as proposed by Comelli *et al.*[13].

As we are interested in the deactivation process during *n*-butane isomerization on SZ by possible formation of unsaturated species or water, UV-vis NIR spectroscopy is the appropriate method.

It is known that some of the surface species on the catalyst are very reactive and can be easily transformed when are exposed to air. Therefore, they have to be studied in situ; so in situ UV-vis-NIR spectroscopy is applied in the present work.

In addition to the spectroscopy, the catalytic performance of the catalyst was investigated by analyzing the effluent gas via online GC. This method was used to detect the reaction products and to study their formation with time on stream.

A direct correlation can thus be drawn between the surface changes and the activity of the catalyst.

1.3.4. Prevention of deactivation and stabilization: an exploratory study

The activity of SZ can be stabilized by adding a modifier, platinum, to the catalyst. The presence of hydrogen in the feed with a Pt promoted SZ (PtSZ) catalyst is essential to maintain the catalytic activity[68]. Besides platinum, ruthenium is alternatively used, because, different from platinum which can isomerize *n*-alkanes[69,70], it will not contribute to the product formation as it does not catalyze alkane isomerization (it has hydrocracking properties). Moreover, for economical reasons, Ru being cheaper than Pt, it is interesting to investigate also RuSZ in the short alkane isomerization. Furthermore, Hino and Arata[71,72] claimed that ruthenium promoted sulfated zirconia (RuSZ) is a highly active superacid catalyst for the isomerization of butane to isobutane with He as carrier gas. In our case, RuSZ deactivates so the kinetics of the deactivation is investigated.

[1] P.J. Kuchar, R.D. Gillespie, C.D. Gosling, W.C. Martin, M.J. Cleveland, P.J. Bullen, *Hydrocarbon Eng.* 1999, March, 50-57

[2] G. Pahlke, H. Leonhard, M. Tappe, *Erdöl, Erdgas, Kohle* 116, 2000, 10, 498-504

[3] D'Ans Lax, *Taschenbuch für Chemiker und Physiker*, Band II Organische Verbindungen, 4. Auflage, Springer-Verlag, Berlin, 1983

[4] G. A. Olah, G. K. Surya Prakash and J. Sommer, *Superacids*, John Wiley & Sons, New York, 1985, pp. 254-259

[5] C. Gosling, R. Rosin, P. Bullen, T. Shimizu and T. Imai, *Petroleum Technology Quarterly*, Winter 97/98, 55-59

[6] G. C. Anderson, R. R. Rosin, M. A. Stine and M. J. Hunter, *2004 NPRA Annual Meeting*, San Antonio, TX, USA, March 21–23, 2004, paper AM-04-46.

[7] V.C.F. Holm, G.C. Bailey, *US Patent 3*, 032, 599 (1962)

[8] M. Hino, S. Kobayayashi, K. Arata, *J. Am. Chem. Soc.* 101 ,1979, 6439-6441

[9] M. Hino, K. Arata, *J. Chem. Soc., Chem. Commun.* 1980, 851-852

[10] F.R. Chen, G. Coudurier, J. Joly, J.C Védrine, *J. Catal.*, 143 (1993), 616

[11] D. Spielbauer, G.A.H. Mekhemer, E. Bosch, H. Knözinger, *Catal. Lett.* 36 (1996) 59

[12] R. Ahmad, J. Melsheimer, F.C. Jentoft, R. Schlögl, *J. Catal.* 218 (2), 2003, 365-374

[13] R.A. Comelli, C.R. Vera, J.M. Parera, *J. Catal.* 151, 1995, 96-101

[14] F.C. Lange, T.-K. Cheung and B.C. Gates, *Catal. Lett.*, 1996, 41, 95-99

[15] C.Y. Hsu, C.R. Heimbuch, C.T. Armes, B.C. Gates, *J. Chem. Soc. Chem. Commun.*, 1992, 1645.

[16] M.R. Gonzalez, J.M. Kobe, K.B. Fogash, J.A. Dumesic, *J. Catal.* 160,1996, 290-298

[17] G. Yaluris, R. B. Larson, J.M. Kobe, M.R. Gonzalez, K.B. Fogash, J.A. Dumesic, *J. Catal.* 158, 1996, 336-342

[18] J.M. Kobe, M.R. Gonzalez, K.B. Fogash, J.A. Dumesic, *J. Catal.* 164, 1996, 459-466

[19] G. Resofszki, M. Muhler, S. Sprenger, U. Wild, Z. Paal, *Appl. Catal. A: General* 240, 2003,71-81

[20] B. Li, R.D. Gonzalez, *Catal. Today* 46(1), 1998, 55-67

[21] C. Li, P.C. Stair, Catal. Lett. 36, 1996, 119-123

[22] C.R. Vera, C.L. Pieck, K. Shimizu, C.A. Querini, J.M. Parera, *J. Catal.* 187(1), 1999, 39-49

[23] J.M.M.Millet, M. Signoretto, P. Bonville, *Catal. Lett.* 64(2-4), 2000, 135-140

[24] T. Yamamoto, T. Tanaka, S. Takenaka, S. Yoshida, T. Onari, Y. Takahashi, T. Kosaka, S. Hasegawa, M. Kudo, *J. Phys. Chem. B* 103(13), 1999, 2385-2393

[25] J. Sommer, R. Jost and M. Hachoumy, *Catal. Today*, 38, 1997, 309-319

[26] M. Hino, S. Kobayashi and K. Arata, *J. Am. Chem. Soc.*, 1979, 101**,** 6439-6441

[27] K. Tanabe, H. Hattori, T. Yamaguchi, *Crit. Rev. Surf. Chem.* 1, 1, 1990, 1-25

[28] C. Morterra, G. Cerrato, F. Pinna, M. Signoretto, *J. Phys. Chem.* 98, 1994, 12373-12381

[29] T. K. Cheung and B. C. Gates, *Chem. Commun.*, 1996, 1937-1938

[30] V. Adeeva, J.W. de Haan, J. Jänchen, G.D. Lei, V. Schünemann, L.J.M. van de Ven, W.M.H. Sachtler, R.A. van Santen*, J. Catal.* 151, 1995, 364-372

[31] L.M. Kustov, V.B. Kazansky, F. Figueras, D. Tichit, J. Catal. 150, 1994, 143-149

[32] M. Marczewski, *J. Chem. Soc., Faraday Trans.,* 82, 1986, 1687-1701

[33] M. Marczewski, *Bull. Soc. Chim. Fr.*, 1986, 750-755

[34] J. E. Tabora and R. J. Davis, *J. Am. Chem. Soc.,* 118**,** 1996, 12240-12241

[35] A. Ghenciu and D. Fărcaşiu, *Chem. Commun.*, 1996, 169-170

[36] F. Garin, L. Seyfried, P. Girard, G. Maire, A. Abdusamad and J. Sommer, *J. Catal.* 151 (1995) 26

[37] V. Adeeva, G.D. Lei, , W.M.H. Sachtler, *Catal. Lett.* 33 (1995) 135

[38] J. Sommer, A. Sassi, M. Hachoumy, R. Jost, A. Karlsson and P. Ahlberg, *J.Catal.* 171, 1997, 391-397

[39] I. Kiricsi, G. Tasi, H. Förster, P. Fejes, *J. Mol. Structure*, 218, 1990, 369-374

[40] . Chiappetta, S. Bodoardo, F. Geobaldo, F. Fajula, E. Garrone, *Res. Chem. Intermed.* 25, 1999, 111

[41] I. Kiricsi and H. Förster, *J. Chem. Soc. Faraday Trans. I* , 84, 1988, 491- 499

[42] A.V. Demidov, A. A. Davydov, *Materials Chem. Phys.* 39, 1994, 13-20

[43] X. Li, K. Nagaoka, L. J. Simon, R. Olindo, J. A. Lercher, A. Hofmann and J. Sauer, *J. Am. Chem. Soc.*, 2005, 127, 16159-16166

[44] Z. Hong, K.B. Fogash, R.M. Watwe, B. Kim, B.I. Masqueda-Jiménez, M.A. Natal-Santiago, J.M. Hill and J. A. Dumesic, *J. Catal.* 178, 1998, 489-498

[45] B.S. Klose, F.C. Jentoft, R. Schlögl, *J. Catal.* 233, 2005, 68-80

[46] B.S. Klose, F.C. Jentoft, P. Joshi, A. Trunschke, R. Schlögl, I. R. Subbotina, V.B. Kazansky, *Catal. Today* 116, 2006, 121-131

[47] B. Klose, F.C. Jentoft, R. Schlögl, I.R. Subbotina, V.B. Kazansky, *Langmuir* 21 (23), 2005, 10564-72

[48] S. X. Song, R.A. Kydd, J. Chem. Soc., *Faraday Trans.*, 94, 1998, 9, 1333-1338

[49] C. Morterra, G. Cerrato, F. Pinna, M. Signoretto, G. Strukul, *J. Catal.* 149(1), 1994, 181-188

[50] S. X. Song, R.A. Kydd, *J. Chem. Soc., Faraday Trans.*, 94, 1998, 9, 1333-1338

[51] M.Y. Wen, I. Wender, J. W. Tierney, *Energy Fuels*, 1990, 4, 372

[52] S.X. Song, R.A. Kydd, *Catal. Lett.* 51, 1998, 95

[53] G. C. Anderson, R. R. Rosin, M. A. Stine and M. J. Hunter, *2004 NPRA Annual Meeting*, San Antonio, TX, USA, March 21–23, 2004, *paper AM-04-46*.

[54] F.T.T. Ng and N. Horvat, *Appl. Catal. A: General* 123, 1995, L197-L203

[55] J. Luo and R. Stevens, *J. Am. Ceram. Soc.*, 1999, 82, 1922-1924.

[56] M. A. Ecormier, K. Wilson and A. F. Lee, *J. Catal.,* 2003, 215, 57-65.

[57] R. C. Garvie and M. F. Goss, *J. Mater. Sci.*, 1986, 21, 1253-1257.

[58] R. C. Garvie, *J. Phys. Chem.*, 1965, 69, 1238-1243.

[59] R. C. Garvie, *J. Phys. Chem.*, 1978, 82, 218-224.

[60] A. Christensen and E. A. Carter, *Phys. Rev. B*, 1998, 58, 8050-8064.

[61] C. Morterra, G. Poncelet, F. Pinna and M. Signoretto, *J. Catal.*, 1995, 157, 109-123.

[62] W. Stichert, F. Schüth, S. Kuba and H. Knözinger, *J. Catal.*, 2001, 198, 277-285.

[63] A. Girginov, T.Z. Tzvetkoff, M. Bojinov, *J. Appl. Electrochemistry 43*, 1995, 993-1003

[64] K.T. Wan, C.B. Khouw, M.E. Davis, *J. Catal.* 1996, 158, 311-326

[65] R.E. Jentoft, A. Hahn, F.C. Jentoft and T. Ressler*, J. Synchrotron Radiat.*, 2001, 8, 563-565

[66] R.E. Jentoft, A.H.P. Hahn, F.C. Jentoft, T. Ressler, *Phys. Chem. Chem. Phys.*, 2005, 7, 2830-2838

[67] B. S. Klose, *PhD dissertation*, 2005

[68] F. Garin, D. Andriamasinoro, A. Abdusamad and J. Sommer, *J. Catal.* 131,1991, 199

[69] F.G. Gault, V. Amir-Ebrahimi, F. Garin, P. Parayre and F. Weisang, *Bull. Soc. Chim. Belg.* 88,1979, 475

[70] F.G. Gault, Adv. Catal. 30, 1981, 1

[71] M. Hino and K. Arata, *React. Kinet. Catal. Lett*. 66,1999, 2, 331-336

[72] M. Hino and K. Arata, *React. Kinet. Catal. Lett*. 71, 2000,1, 71-76

2.1. Synthesis of Sulfated Zirconia Catalysts

2.1.1. Characteristics and drying procedure

Different routes of preparation of the sulfated zirconia are reported in the literature[1] and they can be generalized as follows: (i) Precipitation via hydrolysis of zirconium salt solutions followed by sulfation. Ex. $ZrOCl_2$ or $ZrO(NO_3)_2$; (ii) sol-gel synthesis from organic precursors and (iii) thermal decomposition of zirconium sulfate. SZ, obtained by calcination after sulfation, is a solid acid catalyst and typically contains 5–6 wt % SO_3, sulfate which increases the Lewis acid sites, thus the activity of the SZ. Many models - the tridentate[2] and bidentate[3] monosulfate, and the tetradentate pyrosulfate[4] - have been proposed for the sulfate structure. Thus, the target in the preparation route of the catalyst is to obtain a tetragonal ZrO_2 which is metastable and stabilized at room temperature by addition of sulfate.

A commercially available starting material (precursor), sulfated hydrous zirconia (MEL Chemicals XZO 682/01), served as the raw material. This material has a particle size of $15\,\mu m$, contains water and, according to the manufacturer, has the approximate stoichiometry $ZrO_2 * 2.5\ H_2O$ (ZrO_2 content 70-80 wt %). This sulfated hydrous zirconia ("SHZ") contains $(NH_4)_2SO_4$ equal to a SO_3 content of 5-6 wt% on ZrO_2. For further use, a portion of 20 g of the precursor was dried (drying oven) at 383 K for 21 h and cooled to room temperature in a desiccator. During this drying procedure, the material lost 17-18 % of its weight.

2.1.2. Preparation of Mn-promoted sulfated hydrous zirconia

Dried SHZ was used and $Mn(NO_3)_2$ was employed as the promoter source. For the addition of the promoter, 0.5 and 2.0 wt% Mn, the incipient wetness method was chosen, as described elsewhere[5,6]. Mn (II) nitrate was dissolved in just as much water as necessary to wet the required amount of support. This solution was then added drop-wise under vigorous stirring to the dried precursor. The resulting powder was dried at room temperature before the calcination procedure.

2.1.3. Calcination of non-promoted and promoted sulfated hydrous zirconia

The sulfated hydrous zirconia or the Mn-promoted sulfated hydrous zirconia was loaded in a quartz boat with a volume of 17.1 mL and 2 mm thick walls. The boat was completely filled with about 20-25 g of precursor and was placed into a 29 mm I.D. quartz tube, which in turn was placed into a tubular furnace (Heraeus RO 4/25).

The un-promoted starting material was calcined for 3 h at 823 K while the promoted sample was calcined at 923 K (3 K/min ramp) in a flow of 200 mL/min synthetic air to obtain sulfated zirconia (SZ) or manganese-promoted sulfated zirconia (MnSZ).

2.1.4. Preparation of Pt/Ru-promoted sulfated zirconia (PtSZ and RuSZ)

The incipient wetness method was used to add 0.5 wt % Pt[7] or Ru to calcined SZ. H_2PtCl_6. 6 H_2O and $RuCl_3$ were used as promoter sources. Each promoter source, in a powder form, was diluted to obtain an aqueous solution of 2 wt% Pt or Ru. Only the required amount of metal was added drop-wise to the dried and calcined SZ under gentle stirring before the calcination and reduction treatment.

2.1.5. Calcination and reduction of the Pt- and Ru-promoted sulfated zirconia

PtSZ or RuSZ were obtained by a calcination for 3 hours at 573 (5 K/min ramp) in a flow of synthetic air, then cooled to room temperature under helium, before being heated in hydrogen at 573 K for 3 hours. The total flow of each atmosphere was 40 mL/min. The catalyst was loaded in a Pyrex tube of 34 cm length and 28.4 mm inner diameter. The tube was then placed in a tubular furnace.

2.2. Characterization

2.2.1. X-ray diffraction (XRD)

The X-ray diffraction (XRD) measurements were performed on a STOE STADI P transmission diffractometer equipped with a primary focusing Ge (111) monochromator (Cu $K\alpha_1$ radiation, $\lambda = 1.542$ Å) and position sensitive detector.

Scattered monochromatic X-rays are diffracted according to Bragg's law:

$$n\lambda = 2d \sin\theta$$

where n is the order of reflection (usually assumed 1), λ is the wavelength of Cu $K\alpha_1$ radiation, d is the lattice spacing, and θ Bragg's angle at which diffraction occurs.

From the diffractograms shown in Figure 2 - 1, it can be seen that the catalysts contain mainly the tetragonal phase (SZ has about 2 wt% m-ZrO_2 and MnSZ with 2 wt% Mn loading has less than 1 wt% m-ZrO_2, values determined by Rietveld fit), which corresponds to the desired phase[8] and is required for the reaction of isomerization.

_____
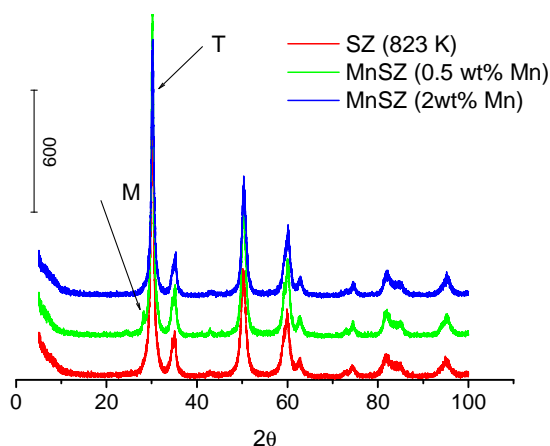
Figure 2 - 1 : X-ray diffractograms of promoted and unpromoted SZ

It is known from the literature that besides promoting the activity by 1 to 2 orders of magnitude, Mn stabilizes[5] the tetragonal phase (t-ZrO_2) of the ZrO_2. Only the 0.5 wt% Mn loading leads to a small amount of monoclinic phase (c.a. 5 wt%, green diffractogram) which means that the loading of Mn was not high enough to completely stabilize the tetragonal phase of ZrO_2.

2.2.2. Surface area by nitrogen adsorption

Porosity and surface area influence the properties and performance of catalysts strongly.

The Brunauer-Emmett-Teller (B.E.T) equation is the most commonly used analysis of adsorption data to determine catalyst surface areas. BET surface areas were measured after an outgasing procedure in vacuo at 523 K for 3 h, using a Quantachrome Autosorb apparatus and a multipoint method.

Catalysts	T_{calc} (K)	Surface area (m^2 g^{-1})
SZ	823	150
0.5 MnSZ	923	103
2.0 MnSZ	923	101
0.5 PtSZ	823 and 573	131
0.5 RuSZ	823 and 573	134

Table 2 - 1 : Specific surface area of promoted and unpromoted SZ. 0.5 PtSZ and 0.5 RuSZ were calcined twice and heated in a hydrogen flow

The surface areas values in Table 2 - 1 are consistent with the values found by Klose[9]. The Mn-promoted sulfated zirconia has a lower surface area than the non-promoted SZ because of the higher calcination temperature[10].

2.2.3. Sulfate content by ICP-AES

ICP-AES stands for Inductively Coupled Plasma – Atomic Emission Spectrometry. ICP-AES is a type of emission spectroscopy that uses plasma to produce excited atoms that emit electromagnetic radiation at a wavelength characteristic of a particular element. The intensity of this emission is indicative of the concentration of the element within the sample.

In our case this technique gives the sulfur, S, content that can be converted to sulfur trioxide SO_3 content (wt%). The order of magnitude of the sulfate content usually corresponds to several wt% SO_3 in the final catalyst. The most common calcination temperature ranges from 823 to 923 K. The typical sulfur content of SZ is in a range of 0.8 – 3 wt%[10] to obtain an active material. In this study, as Table 2 - 2 shows, the necessary SO_3 content is achieved. These values show the loss of SO_3 after calcination (before calcination the SO_3 content is about 5-6 wt%) and after n-butane isomerization.

Catalysts		Composition of the Catalysts - Content in %				
		S	SO_3	Mn	Pt	C
SZ	fresh	1.53	3.82	-	-	-
	After reaction	< 0.20	< 0.5	-	-	< 0.30
MnSZ (0.5 wt% Mn)	fresh	1.81	4.52	0.48	-	-
	After reaction	1.70	4.25	0.48	-	< 0.30
MnSZ 2 wt% Mn	fresh	1.92	4.80	1.85	-	-
	After reaction	1.86	4.65	1.83	-	< 0.30
PtSZ (0.5 wt% Pt)	fresh	1.46	3.65	-	0.59	-
	After reaction	2.57*	6.42*	-	0.60	No data

Table 2 - 2 : Composition of different catalysts before and after 18 h on stream n-butane isomerization (5 kPa) in N_2 at 373 K. The values with * are not understood.

2.3. Conclusions

The synthesized catalysts were characterized and the results obtained are consistent with the literature[9]. The diffractograms prove that the SZ catalysts are metastable as they consist mainly of the tetragonal zirconia phase. For many years it was believed that the tetragonal phase is necessary for the catalytic activity of the sulfated zirconia in n-butane isomerization[8], more recent work revealed that monoclinic and cubic SZ can also be active in this reaction[11].

_____

The surface areas are consistent with those obtained so far in the group[9], and the sulfate contents are in the optimal range for a good catalytic performance of SZ[10].

[1] F.C. Jentoft, *Oxo-Anion Modified Oxides*, in *Handbook of Heterogeneous Catalysis*, ed. G. Ertl, H. Knözinger, F. Schüth and J. Weitkamp, Wiley-VCh, 2nd edn., in press.

[2] C. Morterra, G. Cerrato and V. Bolis, *Catal. Today*, 1993, 17, 505-515

[3] K. Arata and M. Hino, *Mater. Chem. Phys.*, 1990, 26**,** 213-237

[4] A. Hofmann and J. Sauer, *J. Phys. Chem. B*, 2004, 108, 14652-14662

[5] *C. Y. Hsu, C.R. Heimbuch, C.T. Armes, B.C. Gates, J- Chem. Soc.,Chem. Commun. , 1992, 1645-1646*

[6] F.C. Lange, T.-K. Cheung and B.C. Gates, *Catal. Lett.,* 41, 1996, 95-99

[7] S. Vijay, E.E. Wolf, *Appl. Catal.A: General* 264, 2004, 117-124

[8] C. Morterra, G. Cerrato, F. Pinna, M. Signoretto, *J. Catal.*, 157 (1), 1995, 109-123

[9] B. S. Klose, *PhD dissertation*, 2005

[10] X. Song and A. Sayari, *Catal. Rev., Sci-Eng.*, 38 (3), 1996, 329-412

[11] W. Stichert, F. Schüth, S. Kuba, H. Knözinger, J. Catal. 2001, 198 (2), 277-287

3.1. Motivation

Unless special measures are taken, sulfated zirconia deactivates during *n*-butane isomerization. Of the many reasons claimed for the deactivation, the formation of surface deposits ("coke") is most commonly reported and the nature of the coke (allylic cations) was investigated by Chen *et al*[1]. after the end of the reaction with UV-vis spectroscopy. A second speculated reason of deactivation is the formation of adsorbates, namely water[2], which is detected by NIR spectroscopy. However, there are few experiments in the literature[3,4] that connect the reaction profile consisting of induction period, maximum conversion and deactivation of the catalyst to spectroscopic data obtained in situ. To overcome this lack of correlation, and investigate the deactivation of the catalyst, chromatograms and spectroscopic data are recorded simultaneously during *n*-butane isomerization on non-promoted and promoted sulfated zirconia.

3.2. System requirements and apparatus

The reaction of interest is the isomerization of *n*-butane at low temperatures (323 and 373 K) after activation of the catalyst at 723 K. The reactor should then be able to operate in the range temperature from 303 to 723 K to allow *in situ* activation. As the activation and reaction atmospheres can vary, a gas delivery system, with activation and reaction parts, is required. The spectroscopic data are recorded with a Perkin Elmer spectrometer, Lambda 950. The analysis of products of reaction, on line, requires a gas chromatograph (GC), which can separate and detect the different hydrocarbons (short alkanes and alkenes) and their isomers.

3.2.1. Experimental set-up

Figure 3 - 1 shows a scheme of the whole set-up which consists of a gas dosing system, an *in situ* cell combined with a spectrometer and an instrument to analyze the gas product. Most of the tubing is made from stainless steel (Dockweiler, 1/8" × 0.56 mm) apart for the tubing carrying the product of reaction to the on line GC analysis, which is a copper line (Dockweiler, 1/8" × 0.71 mm). The lines carrying the gases first to the reactor and then to the GC are heated at 313 K to prevent condensation of some of the compounds. For activation and for reaction, nitrogen, helium, oxygen and hydrogen (all 99.999% purity) are provided by Westfalen. The feed which is composed of 5 vol% *n*-butane (99.95% purity from Messer Griesheim, Westfalen or Air Liquide) in nitrogen, helium or hydrogen, was either pre-mixed industrially or self-mixed in the laboratory. The large variety of gas providers is explained by

19

the different contracts that the Max Planck Society established in the course of this thesis. Seven three-way valves (Parker) allow the choice between the different activation and reaction atmospheres, whereas two four-way valves (VICI, Valco Instruments) allow the activation of the catalysts while the feed stream is analyzed by the GC. To remove particulate matter, all gases flow through filters (Swagelok, 7 μ m) before they reach the mass flow controllers (Bronkhorst, $\Delta p = 2 bars$). Six check-valves (5-10 PSI) prevent any backflow of the gases. In the tubing connecting the *in situ* cell and the GC, a filter (2 μ m) and for some experiments a check-valve (Swagelok, 1 PSI) are placed to prevent the presence of any particles in the analyzing system and backflow of gas to the *in situ* cell.
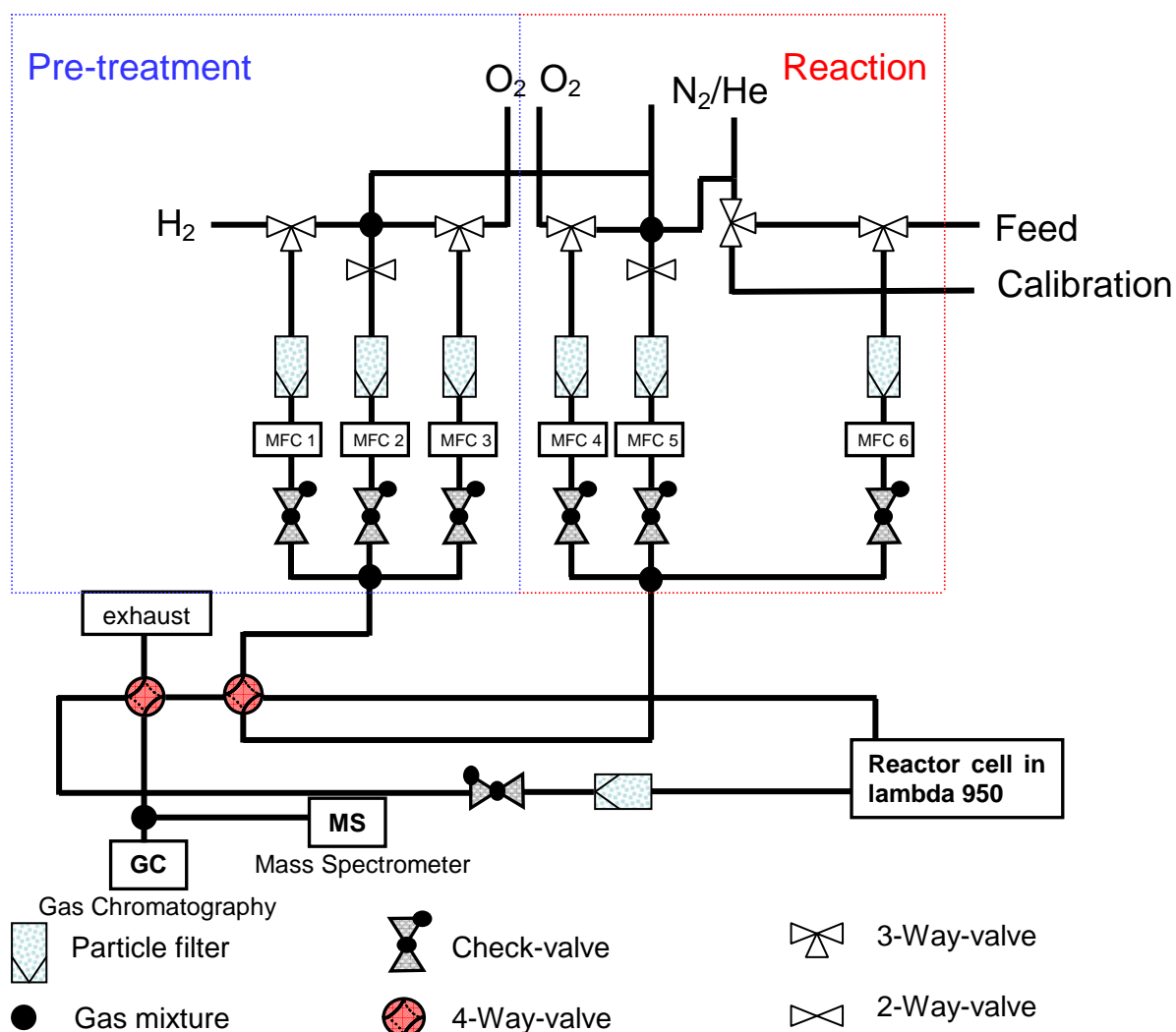
Figure 3 - 1: Scheme of the experimental set-up

3.2.2. In situ Diffuse Reflectance Spectroscopy (DRS)

3.2.2.1. The spectrometer

In situ diffuse reflectance UV–vis–NIR spectroscopy was performed using a PerkinElmer Lambda 950[5] spectrometer equipped with a Harrick Praying Mantis™ DRP-P72 accessory and HVC-VUV reaction chamber (Figure 3 -2). The main components of the Lambda 950 are the light sources, the double monochromator and the detectors. The excited D_2 molecules from the deuterium lamp are dissociated into excited D atoms; which emit strongly in the UV (200-400 nm). The tungsten-halogen lamp emits strongly between 320 and 2500 nm (the visible and NIR ranges). Two sets of holographic gratings can be differentiated: 1440 lines/nm for the UV-vis and 360 lines/nm for the NIR. A photomultiplier is used for detection of the radiation in the UV-vis range (200 - 860 nm) and a PbS detector is used in the NIR range (860- 2500 nm).
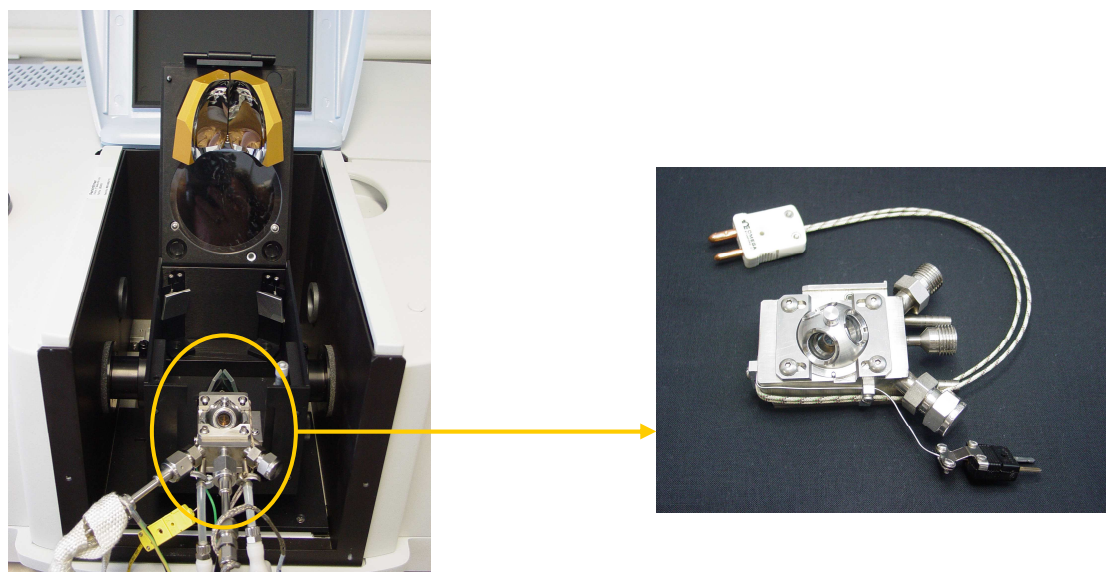
Figure 3 -2 : Photo of the spectrometer Lambda 950 (sample compartment) including the diffuse reflectance attachment (Praying Mantis[TM]) and the reaction chamber (on the right).

3.2.2.2. Diffuse reflectance attachment

The optical configuration of the Harrick Praying Mantis[TM] diffuse reflectance attachment[6] (DRA) is shown in Figure 3 - 3. The DRA incorporates two 6:1 90° off-axis ellipsoidal mirrors (M3 and M4), which are arranged with a common focal point S. Mirrors M1 and M2 transfer the spectrometer beam to the first of these mirrors, M3. This ellipsoid mirror focuses the beam

on the sample while the ellipsoid M4 collects the diffusely reflected radiation from the sample. This radiation is then directed by mirrors M5 and M6 towards the detector.
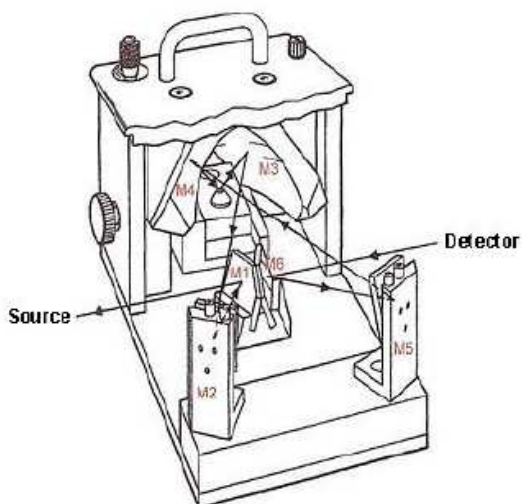
Figure 3 - 3 : Optical configuration of the DRA

3.2.2.5. The reaction chamber

In addition to the DRA, the equipment incorporates a reaction chamber[7] (HVC-VUV) constructed of chemically resistant 316 stainless steel, which can be heated up to 873 K.

This reaction chamber (Figure 3 - 4) features (i) a sample holder that is part of a temperature-controlled sample stage, (ii) a removable dome and (iii) three gas ports for flowing gas through the sample. The sample is loaded on a wire mesh in the sample holder. Thus the gas can flow through the sample and the reactor can be assimilated to a fixed-bed reactor.

The sample stage incorporates a cartridge heater and K-type thermocouple. Furthermore, the stage is thermally isolated from the outer chamber. The reaction chamber includes two quartz windows and a glass observation window. These windows are mounted in the removable stainless steel dome using o-ring

Figure 3 - 4: reaction chamber (HVC-VUV)

_____

seals. A water-cooling jacket is provided to control the temperature (set at 313 K for this work) of the outer chamber and windows during high temperature operation.

3.2.2.6. The temperature controller

As described earlier, the catalysts are activated at 723 K and the reaction takes place at 323 or 373 K. A temperature controller is then necessary to increase and decrease the temperature with a defined rate. As there is a difference between the temperatures recorded by the K-type thermocouple placed on the bottom of the reaction chamber and the actual temperature on the surface of the catalyst, some corrections (Table 3 - 1) were applied to achieve the desired temperature. These set temperatures were obtained by introducing a thermocouple from one of the exhaust gas ports through the sample, SZ, which was loaded in the sample holder; and then the thermocouple was slightly bent to reach the surface of the catalyst. The values measured by the additional thermocouple were compared to the values obtained by the K-type thermocouple placed on the bottom of the reaction chamber. Some literature reported the correction applied to achieve the corresponding target temperature.

Target temperature (K)	Set temperature (K)
323	323
373	423
423	473
473	523
523	573
573*	673-698*
673*	843-853*
723	823

Table 3 - 1: Corrections applied to the set temperature (sample cup) to reach the target temperature (sample surface) for the activation or the reaction processes. The values highlighted in yellow are taken from Gao *et al*.[8]

By using a Harrick DRS cell (HVC-DR2) with a DRA, Gao *et al*.[8] studied the oxidation of propane over zirconia-supported vanadium oxide catalysts. They reported a difference between the temperature of the sample cup, made of Cu, and the temperature recorded at the surface of the sample powder. They explained this variation in temperature by the fact that the sample cup has an excellent thermal conductivity but a small heat capacity; thus the sample cup heats up faster than the sample that it contains. When the V_2O_5 content (%) or the gas

mixture was changed, the set temperature to reach the target temperature of 573 K, which is varying between 673 and 698 K, had to be adapted; for a sample surface temperature of 673 K a temperature of 843-853 K at the sample cup was necessary. However, in our case the values applied to the set temperature to reach the target temperature are not similar to the one obtained by Gao *et al.* as shown in Table 3 - 1.

3.3. Data acquisition and spectra analysis

3.3.1. Product analysis by gas chromatography

For a better understanding of the changes occurring during the reaction of isomerization, the catalytic performance is correlated with spectroscopic data. For this purpose, the effluent gas from the *in situ* cell is analyzed on-line by GC. A Varian 3800 GC was equipped with a Chrompack capillary column (PLOT Fused Silica type), has a length of 27.5 m and an inside diameter of 0.32 mm. The components injected onto the column are separated and thus detected as they exit the GC column. The thermal-conductivity (TCD) and mainly the flame-ionization (FID) detectors were used for the present work.

3.3.1.1. Diffusion limitations

This part of the work has the aim to evaluate film diffusion limitations during the reaction of *n*-butane isomerization on SZ at 373 K.

The residence time of the hydrocarbons on the catalyst could not be kept constant by varying the amount of the catalyst; thus the flow was varying from 20 to 80 mL min^{-1} and all conversions to isobutane (%) were corrected to the one obtained at 40 mL min^{-1}. Figure 3 - 5 shows at low flow film diffusion; thus the choice of the flow at 40 mL min^{-1}.
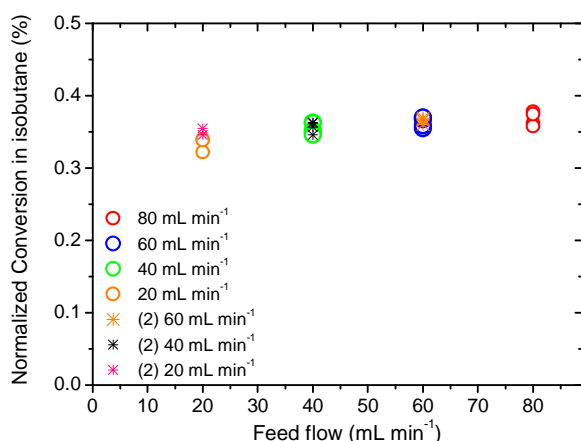
Figure 3 - 5: Variation of conversion to i-C$_4$ vs. the feed flow. (2) stands for the reproducibility at one flow. SZ was activated in O$_2$ at 723 K for 30 minutes. Reaction conditions: 5 kPa *n*-butane in nitrogen on SZ at 373 K.

3.3.1.2. GC calibration

During the reaction of *n*-butane isomerization on SZ at 373 K, the main product of reaction is isobutane. The side products are propane, iso-pentane and pentane. The column used for this work is able to separate light alkanes C_1 to C_6 and light alkenes. To identify the products of reaction, calibration using standard mixtures is carried out. The gas mixtures N17 (Concentration in Vol % of 100 ppm for each component) and N18 (1000 ppm) are used for the light alkanes (Figure 3 -6 left); and these mixtures consist of CH_4, C_2H_6, C_3H_8, i-C_4H_{10}, n-C_4H_{10}, C_5H_{12} and C_6H_{14} and N_2. The standard gas mixtures N19 (100 ppm) and N20 (1000 ppm) are used to determine the alkenes retention time under the method used to heat the column (start for 5 minutes at 373 K, followed by a ramp of 20 K min^{-1} to reach 478 K which is held for 5 minutes). The alkenes (Figure 3 -6 right) standard gas mixture consists of C_2H_4, C_2H_2, C_3H_6, i-C_4H_8, *cis*-C_4H_8 and *trans*-C_4H_8 and N_2. The method used for heating the column for the reaction of interest was optimized to separate the isobutane to the *n*-butane and does not separate C_2H_4 from C_2H_2, and the C_4 olefin isomers as well which have with this method similar retention time values to the *n*-butane; a longer waiting time at 373 K would have helped to differentiate the retention times of C_2H_4 and C_2H_2. Thus the butenes can not be separated from the iso and *n*-butane. The most recent response factors ($RF = \dfrac{Concentration\ in\ ppm}{Peak\ area}$) of each component with helium as carrier gas are gathered in the following table (Table 3 - 2).
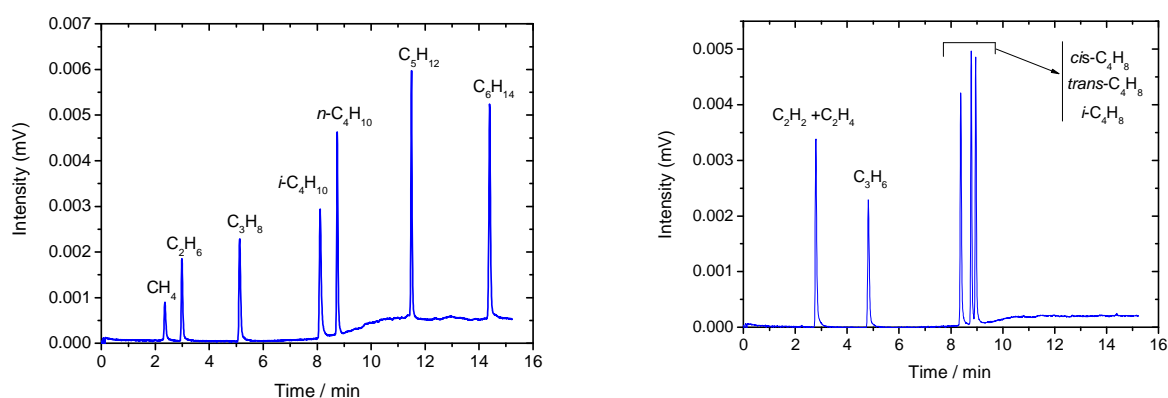
Figure 3 -6 : Chromatogram of the gas mixture N17 (100 ppm) on the left and the gas mixture N19 (100 ppm) on the right

Components	Concentration (ppm)	Retention time (min)	Response Factor (ppm mV^{-1} min^{-1})
CH_4	100	2.35	0.02893
	1000		0.02882
C_2H_6	100	2.98	0.01436
	1000		0.01461
C_3H_8	100	5.13	0.00983
	1000		0.00982
i-C_4H_{10}	100	8.11	0.00701
	1000		0.00674
n-C_4H_{10}	100	8.75	0.00681
	1000		0.00697
C_5H_{12}	100	11.5	0.0055
	1000		0.00573
C_6H_{14}	100	14.4	0.00457
	1000		0.00511

Table 3 - 2: Last response factors calculated from the alkanes standard mixtures N17 (Concentration in Vol % of 100 ppm for each component) and N18 (1000 ppm) from Air Liquide

Components	Concentration (ppm)	Retention time (min)	Response Factor (ppm mV^{-1} min^{-1})
C_2H_2	100	2.79	0.00824
C_2H_4	1000		0.00782
C_3H_6	100	4.82	0.00955
	1000		0.00967
i-C_4H_8	100	8.38	0.00736
cis-C_4H_8	1000		0.00732
$trans$-C_4H_8	100	8.78	0.00686
	1000		0.00680
	100	8.95	0.00655
	1000		0.00682

Table 3 - 3 : Response factors calculated from the alkenes standard mixtures N19 (Concentration in Vol % of 100 ppm for each component) and N20 (1000 ppm) from Air Liquide.

The response factors are reevaluated several times and it should be mentioned that the carrier gas changed from He (28-04-2005) to N_2 (17-05-2006 to 12-10-2007) and later to He (02-04-2008) again. With the change in the carrier gas from N_2 to He, the flow can fluctuate thus the response factor values as well, as shown in Table 3 - 4 with isobutane as reference.

Date	*iso*-butane	*n*-butane
28-04-2005	0.0054 (He)	0.0051
17-05-2006	0.0033	0.0031
18-05-2006	0.0033	0.0030
08-08-2007	0.0037	0.0028
02-04-2008	0.0070 (He)	0.0068

Table 3 - 4: Response factors within months, years with the standard gas mixture N17 (100 ppm) from Air Liquide

3.3.1.3. Bypass measurements

During this work, different starting gases were used to obtain the feed of 5 % *n*-butane in N_2 or He. All the gases fulfilled the required specification (*n*-butane purity of 99.95 %) and were at the time, the best purities available on the market.

The bypass measurements of the different gas-mixtures are investigated (Figure 3 - 7). In one of the gas-mixtures, the chromatograms of the bypass measurements show the presence of propane in the feed. Propane, less reactive than butane, is also a product of reaction, so propane cannot thus have a decisive influence in the catalytic performance of SZ.

The bypass measurement of the gas-mixture from Linde contains an unidentified species at retention time 9.8 min. The peak area of this species needs to be verified during the reaction so that it can be stated if these species react on the catalyst.

The olefins (*i*-butene, *cis*-butene and *trans*-butene) have a retention time very close to the main reactant *n*-butane. It could not be completely excluded that the different gas-mixtures were exempt of few ppm of olefins.

Additionally, it was impossible to discriminate some ppm of oxygen in the feed as nitrogen was used as carrier gas for most of this thesis. When helium was used as carrier gas no oxygen had been detected by TCD. Nevertheless, it was impossible to exclude some traces of oxygen in any of the gas mixtures.

In conclusion, chromatography with FID and the method used to separate to compounds revealed the presence of propane and unidentified compounds in some gas-mixtures; and did not discriminate the presence of olefins ad oxygen in the feed composition.
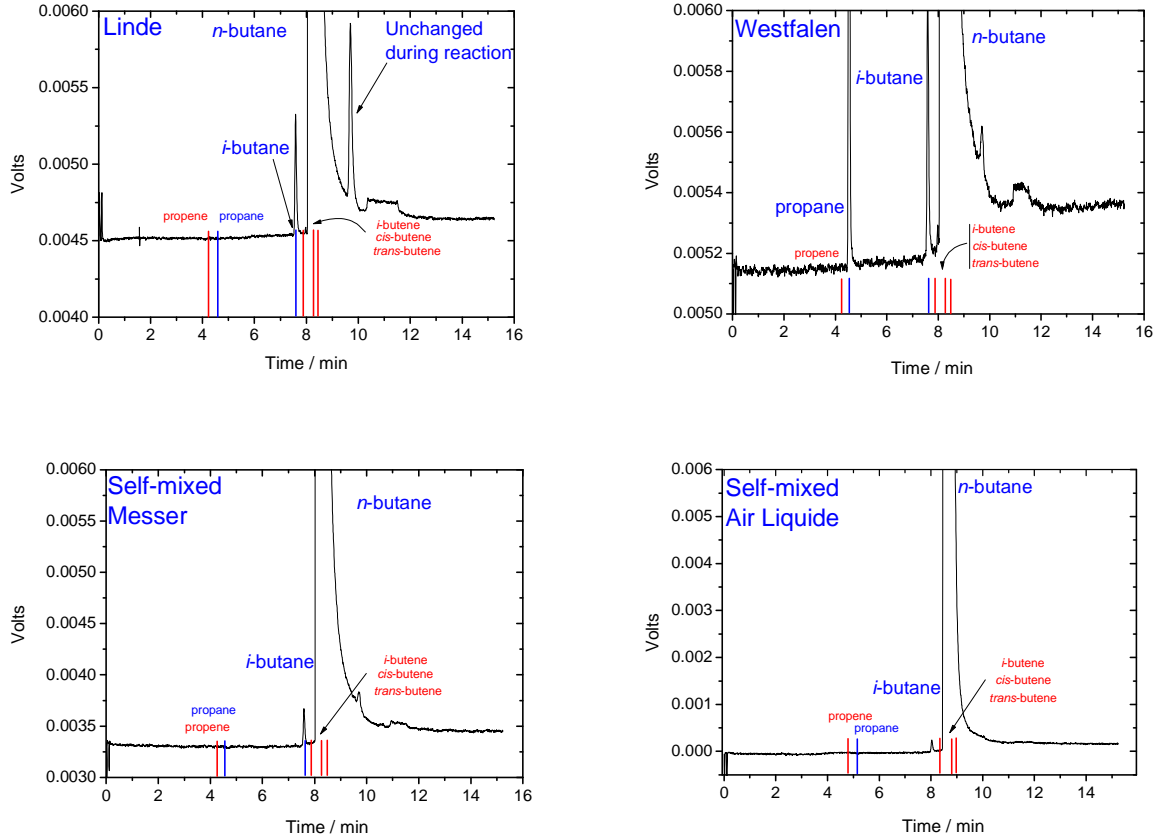
Figure 3 - 7: Chromatograms of bypass measurements of 5 kPa *n*-butane in N₂ with a total flow of 40 mL/min. The alkanes and their positions are in blue, while the alkenes and their corresponding positions are in red

3.3.1.4. Rate of isomerization

The rate of isomerization in $\mu mol\ g^{-1}\ h^{-1}$ for 5 % *n*-butane feed was obtained from the following equation showing the different modifications applied to obtain the working unit:

$$\text{Rate in } \mu mol\ g^{-1}\ h^{-1} = \frac{Flow_{feed}}{V_{mol}} \times 1000 \times C_{i-C_4} \times \frac{1}{m_{cat}} \times 60$$
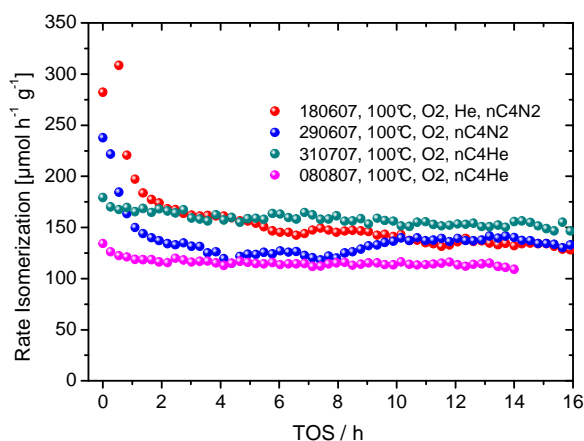
Figure 3 -8 : Reproducibility of the catalytic activity of an activated sulfated zirconia in O₂, under 5 kPa *n*-butane self-mixed and diluted in He or nitrogen at 373 K.

where Flow in the velocity of the feed is in $mL \min^{-1}$, V_{mol} the molar volume of a ideal gas at 293 K corresponding to 24 L mol^{-1}, C_{i-C_4} the concentration in ppm of produced isobutane, and m_{cat} the mass of the catalyst in g. The numbers 1000 and 60 correspond to the conversion L to mL and mol to μmol ; and to the conversion minutes to hours respectively.

Several experiments of isomerization with a self-mixed feed have a rate of about 150 $\mu mol\ h^{-1}\ g^{-1}$ The catalytic activity of SZ, in the course of this work shows thus a relevant reproducibility as shown in Figure 3 -8.

3.3.2. The spectrometer settings

The spectroscopic data are recorded by using a UV WinLab 5-2 Software which guides the user through methods development and the analysis of results. The method, including the settings used for all the experiments, is shown in Table 3 - 5.

Section	Parameter	Settings
D_2 lamp		On
Tungsten lamp		On
Method Settings	Scan from Scan to Data Interval	2500 nm 250 nm 1 nm
Lamps change	D_2 lamp to tungsten lamp	319.20 nm
Monochromator	Change point	860.80 nm
Cycles	Number of cycles Cycle time	25-120 As fast as possible
Common Beam Mask (CBM)	Source Value	Fixed 90 %
Slits	UV-vis mode NIR mode UV-vis width NIR width	Fixed Servo (slit adjusts according to the wavelength) 2.50 nm 2 nm
Data Settings	UV-vis Gain NIR Gain UV-vis Response NIR Response	Auto 3 0.20 s 0.20 s
Beam Selection		Sample Beam Front
Common Beam Depolarizer (CBD)		Enable
Attenuators	Reference beam attenuator Sample beam attenuator	10 % 100 %
Detector Settings	Mode Detector change point	% R 860.80 nm

Table 3 - 5: Spectrometer settings used for each experiment

3.3.3. Reference measurement (Background correction)

For the experiments a defined atmosphere is required and the sample is placed in a cell. Therefore, a correction not only for the optical components of the spectrometer, but also for reflection and absorption on the windows becomes necessary. The diffuse reflectance of a sample of interest is always measured relative to a white standard. Several references exist and to cover the whole studied spectroscopic range ($BaSO_4$ for example does not cover the NIR range). Spectralon® (Labsphere), a polytetrafluoroethylene-based standard (PTFE), was chosen. The reference measurement, called "autozero" (also called background correction) for the UV WinLab 5-2 software provided with the spectrometer, is performed with the Spectralon® standard in the sample position (covered by the removable dome).

_____

3.3.4. Spectra representation and conversion

During the experiment, the spectra are recorded in reflectance. As the sample is loaded in a cell of 3.15 mm height (and 6.2 mm diameter), the catalyst can be considered as "infinitely thick"- all light is either reflected or absorbed, no light is transmitted- and that the reflection is related to an apparent absorption (K) and an apparent scattering coefficient (S) via the Kubelka Munk (KM) equation. The Kubelka–Munk function (dimensionless) is the counterpart in reflection spectroscopy of what the absorbance function represents in transmission spectroscopy.

$$\frac{K}{S} = \frac{(1-\rho_\infty)^2}{2\rho_\infty} = F(\rho_\infty)$$

Where ρ_∞ is the reflectance at infinite sample thickness and $F(\rho_\infty)$ is the Kubelka-Munk or remission function. $F(\rho_\infty)$ gives the correct values when considering boundary cases:

For a non-absorbing sample, i.e. $K \rightarrow 0$, all light should be reflected, and indeed $\rho_\infty \rightarrow 1$. For a non-scattering sample, i.e. $S \rightarrow 0$, no light should be reflected, and indeed $\rho_\infty \rightarrow 0$.

If the absorption coefficient K is small and S does not vary with c, the Kubelka-Munk function becomes proportional to the concentration:

$$F(\rho_\infty) = \frac{K}{S} \propto \frac{\kappa c}{S}$$

$F(\rho_\infty)$ will be written F(R) in the experimental part.

Because of this proportionality between the KM function and the concentration c, it is of great interest for this work to convert the data recorded in reflectance to the KM function. The conversion into the KM function is only possible when the data in reflectance do not exceed 100%. Spectralon® is by far the best white standard for the energy range used in the experiments; however, some artefacts can arise during the activation or reaction procedure of an experiment, and the reflectance may exceed 100 % (Figure 3 -9, top left). These artefacts can be explained by the white standard, Spectralon®, which is used several times and may lose reflectance; or due to some changes of some parts of the spectrometer during the experiment. To record one spectrum, some changes occur to the spectrometer such as (i) lamp switch from the deuterium lamp in the UV regime to the tungsten halogen lamp for the vis-NIR range at 309 nm; (ii) monochromator change from UV-vis to NIR gratings at 860 nm; (iii) detector change from photomultiplier to PbS detector, and (iv) filter change (usually several throughout the whole wavelength range). The position of the specimen, particularly the height, in the optical accessory can vary from the background correction to the sample

_____

measurement, as the cell has to be removed from the DRA. Thus, a change in the beam path can produce y-offsets of sections of the spectrum, generating steps or spikes at wavelengths where optical elements are switched. In order to convert the data into the KM function, the reflectance data are normalized (Figure 3 -9, top right). The normalization factor varies from 1.1 to 1.45 in order to adjust the maximum values in reflectance (mainly in the NIR range) to around 100 %.

Spectra in reflectance before normalization

Spectra in reflectance after normalization

Spectra in Kubelka Munk function for the band at 1406 nm

Spectra in Kubelka Munk function for the band at 1916 nm
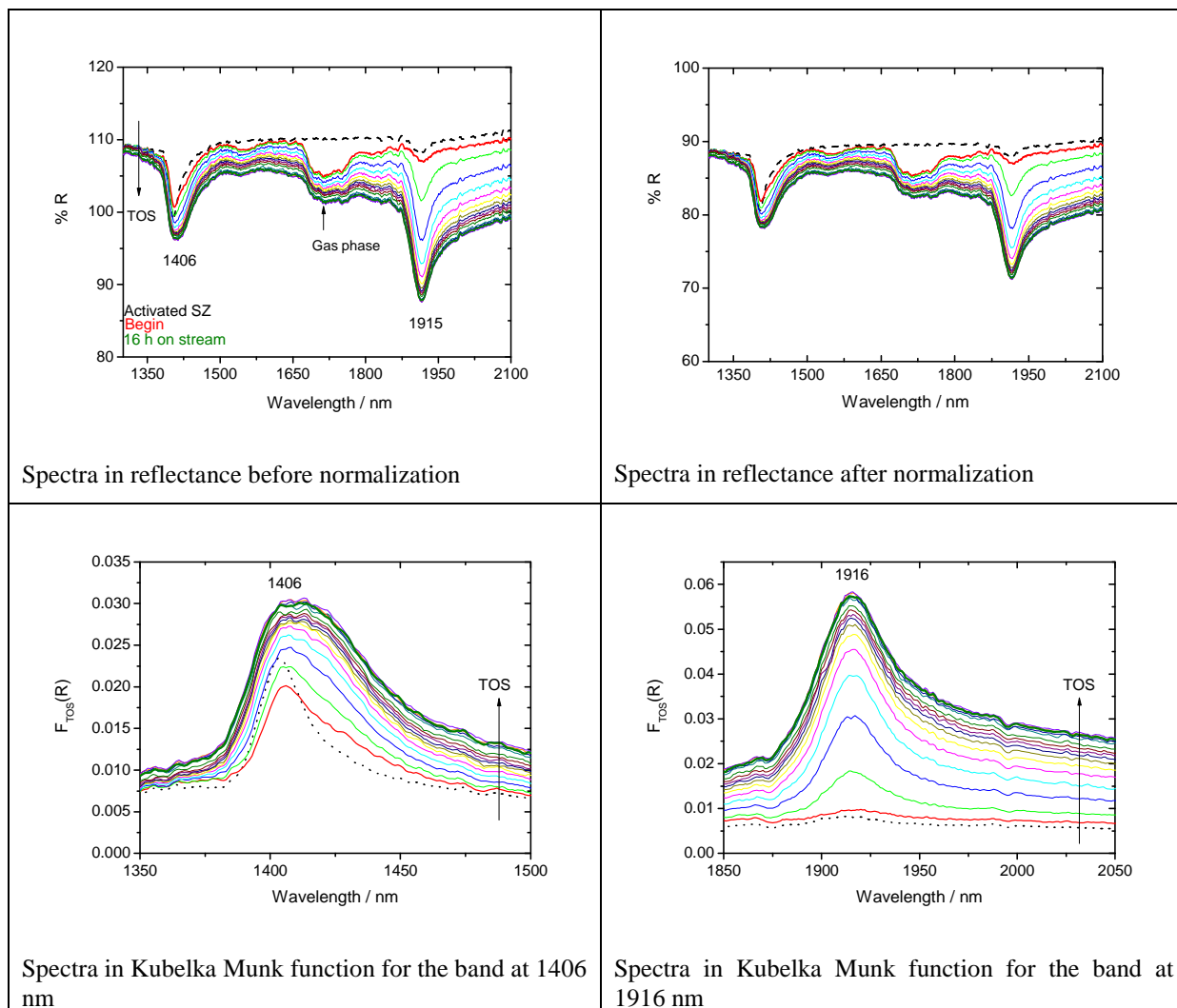
Figure 3 -9 : The two plots on the bottom represent the conversion in Kubelka Munk function. Except for the spectrum corresponding to the activated SZ (dotted line), all spectra are difference spectra obtained through the subtraction of the spectrum of the activated catalyst. Reaction conditions: SZ was activated at 723 K in O_2 for 30 min and cooled down to reaction temperature in O_2. 5 kPa *n*-butane in N_2 on SZ at 323 K.

Figure 3 - 10 shows the spectra of activated SZ in O_2 which correspond to the catalytic activities in Figure 3 -8. Apart from the spectrum in magenta which was not normalized as the reflectance data did not exceed 100 %, the three other spectra were normalized. Thus the three

normalized spectra overlap while the non-normalized is shifted from the others. An overlapping of the spectra is thus possible when the spectra are normalized.
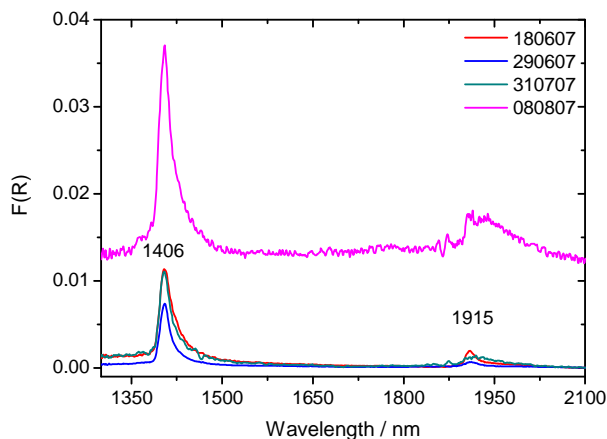
Figure 3 - 10: Spectra reproducibility of activated SZ in O_2. These spectra correspond to the catalytic activities plotted in Figure 3 -8. The spectrum in magenta represents the Kubelka Munk data of a non-normalized reflectance data as the initial reflectance was not exceeding 100 %.

During the reaction of isomerization, new species can be formed and a deep investigation of the evolution of these species is recommended. For a better understanding of what occurs on the surface of the catalyst after the contact to the feed, the spectrum of the activated catalyst (spectrum recorded at the reaction temperature, after activation in oxygen) is drawn in a dotted line whereas the spectra corresponding to the reaction part are in full line in the plots. Moreover, the development of the species on the surface can be correlated with time on stream by plotting the maximum of the bands intensity of each spectrum in the KM function vs. time on stream. The evolution of species at different band positions, 295, 1406 and 1916 nm is then drawn together with the activity of the catalyst vs. time on stream (Figure 3 -11).
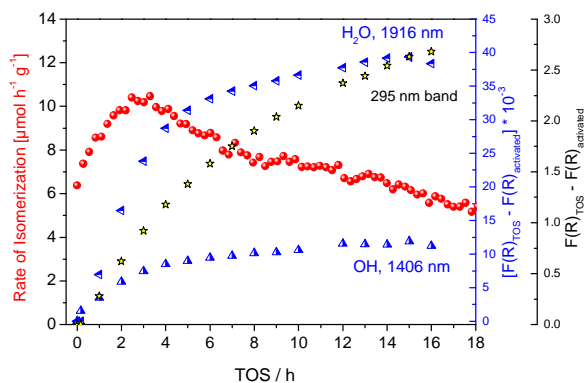
Figure 3 -11 : Catalytic activity versus time on stream. The general trend of the formation of each species at different wavelength is plotted also in the same plot. Conditions: Activation at 723 K in O_2 for 30 minutes. Reaction under 5 kPa *n*-butane in N_2 on SZ at 323 K.

3.4. Conclusions

In order to correlate the deactivation of the catalyst during *n*-butane isomerization on sulfated zirconia to the spectroscopic data, a combination of a gas delivery system, a spectrometer

equipped with a diffuse reflectance attachment, a reaction chamber with a temperature controller and a gas chromatograph is compulsory.

The set temperature corresponding to the temperature of the sample cup was necessary to make sure that the temperature on the sample surface is the one necessary for the experiment. Because of the artefacts described previously, a few of the spectra recorded in reflectance were normalized to allow the conversion into the Kubelka Munk function.

[1] F.R. Chen, G. Coudurier, J-F. Joly, J.C. Vedrine, *J. Catal.*, 143, 1993, 616-626

[2] R.A. Comelli, C.R. Vera, J.M. Parera, *J. Catal.* 151, 1995, 96-101

[3] R. Ahmad, J. Melsheimer, F.C. Jentoft, R. Schlögl, *J. Catal.*, 2003, 218 (2), 365-374

[4] R. Ahmad, *Doctorial Thesis*, Freien Universität, 2003

[5] www. las.perkinelmer.com

[6] http://www.harricksci.com/accessories/H_prayingmantis.pdf

[7] http://www.harricksci.com/accessories/H_prayingmantischamber.pdf

[8] X. Gao, J-M. Jehng and I. E. Wachs, *J. Catal.*, 209, 2002, 43-50

4. 1. Motivation

Sulfated zirconia (SZ) can be used for the isomerisation of *n*-butane at low temperature, after being activated under inert or oxidizing atmosphere[1,2].

The role of activation temperature and atmosphere is of importance in the performance of this catalyst in the reaction of interest. Song and Kydd[3] reported how vital water is in the activity of SZ. By activating the catalyst in oxidizing atmosphere at various temperatures in the range 423 – 773 K, they optimized the water content to 200 $\mu mol\ g^{-1}$ for the most active catalyst. They are thus in agreement with Dumesic *et al.*[4,5] who also claimed that minor amounts of water promote the catalyst activity and excess of water diminishes it. Song and Kydd disagree with Morterra *et al.*[6], Keogh *et al.*[7] and Comelli *et al.*[8] who mentioned a poisoning effect of water on SZ catalyst. The role of the activation atmosphere was investigated by Song and Kydd[9].

A reducing activation atmosphere is required when SZ is modified with Pt. Pt modified SZ needs to be pre-reduced at a temperature that does not exceed 573 K to avoid the reduction of SO_4^{2-} into S^0 or H_2S and to obtain an active catalyst. A poisoning effect of sulfur species for Pt was described by Wang *et al.*[10] and Menon *et al.*[11].

In addition to the role played by the sulfate content, the zirconia phase and the water content on the performance of SZ in the *n*-butane isomerization. The activity of the catalyst can be increased by promoting SZ with different transition metal cations[12]. Lange *et al.*[12] reported that the effect of promotion on the maximum activity follows the trend

Mn > Fe>> Co>> Ni> Zn. The promoters increase the activity, but they do not increase the measurable acidity of the catalyst[13,14,15]. The activation atmosphere, He or air, did not affect the activity of the unpromoted SZ; while activation in air resulted in a higher activity of the iron- and manganese-promoted sulfated zirconia than activation in He. Wan *et al.*[16] believe that the activation of the Fe-Mn promoted sulfated zirconia at high temperature in air generates a rather labile, but reactive, iron oxy species. These resulting iron oxy species could then take part in the oxidative dehydrogenation of *n*-butane to butene which is the initial step for the isobutane formation. Oxidative dehydrogenation is assumed to be one of the initiatial steps in *n*-butane isomerization[17,18,19,20].

Manganese promoted sulfated zirconia also suffers from deactivation. This fast and drastic loss in the catalytic activity in the presence of manganese is not understood. Jentoft *et al*[21]. reported that during *ex situ* X-ray absorption near edge spectroscopy (XANES) experiments (1% *n*-butane in N_2 at 338 K), Mn, which is in the majority incorporated in the ZrO_2 lattice[22],

36

was reduced after activation (in dry nitrogen at 723 K) of Mn-promoted SZ samples. The same authors[23] reported the results of an *in situ* XANES study of Mn in promoted SZ catalysts. Here it was found that Mn in 2 wt% MnSZ catalysts does not act as a stoichiometric redox-active initiator in *e.g.,* an oxidative dehydrogenation reaction. Furthermore, they showed that a higher valence directly prior to reaction correlates with a higher maximum conversion. It was also shown that the average valence of Mn depends on the presence of sulfate in the catalyst.

This chapter aims to interpret the spectra of manganese- promoted and unpromoted sulfated zirconia catalysts before and after activation in different atmospheres. The effect of the activation atmosphere on the water content on the catalyst surface and the electronic state of manganese are investigated.

4. 2. Catalyst behaviour during activation

4.2.1. Sulfated zirconia

4.2.1.1. Oxidizing atmosphere

Non-promoted sulfated zirconia was activated for 30 min at 723 K in 40 mL/min of O_2 and with a ramp of 5 K/min. The catalyst was cooled to the reaction temperature, 323 or 373 K, under O_2 flow (Figure 4 - 1) or He flow (Figure 4 - 2); or cooled under O_2 flow followed by a purge in inert gas (Figure 4 - 3) before starting the reaction of isomerization.
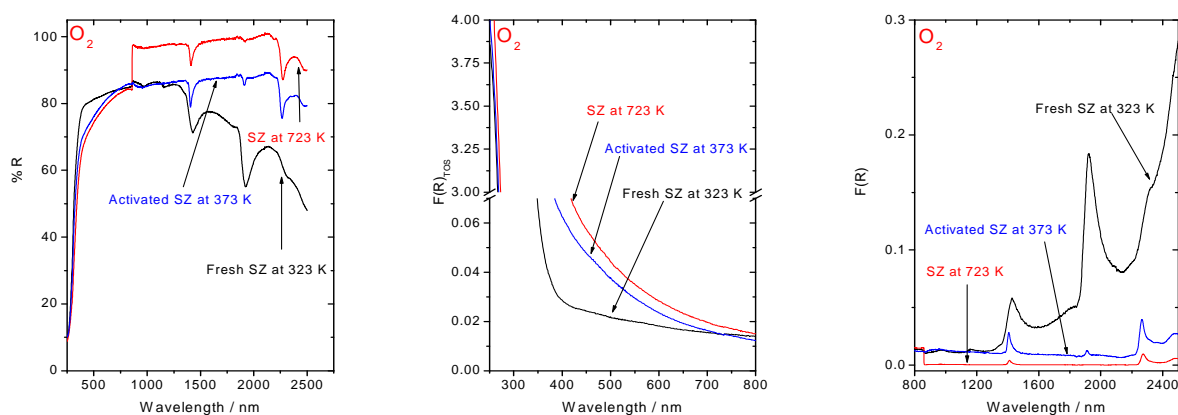

Figure 4 - 1: SZ activated in 40 mL/min O_2 at 723 K for 30 min with 5 K/min ramp. The spectra of the fresh SZ at 323 K (black), at 723 K (blue) and after cooling in O_2 at 373 K are shown in reflectance (left) and in the Kubelka Munk function (UV-vis region in the middle and NIR region on the right)
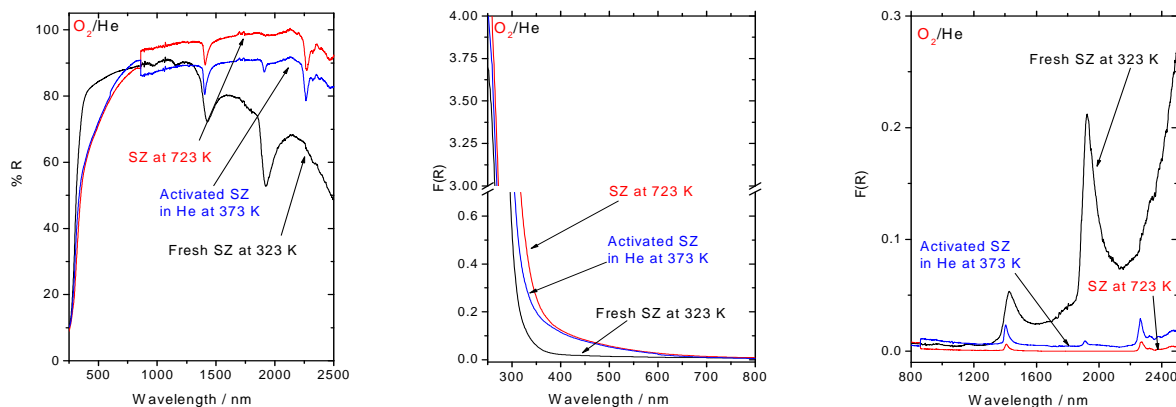
Figure 4 - 2: SZ activated in 40 mL/min O_2 at 723 K for 30 min with 5 K/min ramp. SZ is cooled to reaction temperature under He flow. The spectra of the fresh SZ at 323 K (black), at 723 K (blue) and after cooling in O_2 at 373 K are shown in reflectance (left) and in the Kubelka Munk function (UV-vis region in the middle and NIR region on the right)

The activation under O_2 alone, or followed by a helium purge at high activation temperature or at reaction temperature resulted in more than a 95 % loss[24] of the water (band at 1915 nm) adsorbed initially on the catalyst. The band at 1405 nm is ascribed to an overtone of OH stretching vibrations. Moreover, it should be specified that water started desorbing only at 473 K (spectra not shown).

The high absorption in the UV range is not the band gap of zirconia which is at 240 nm (5.07 eV).
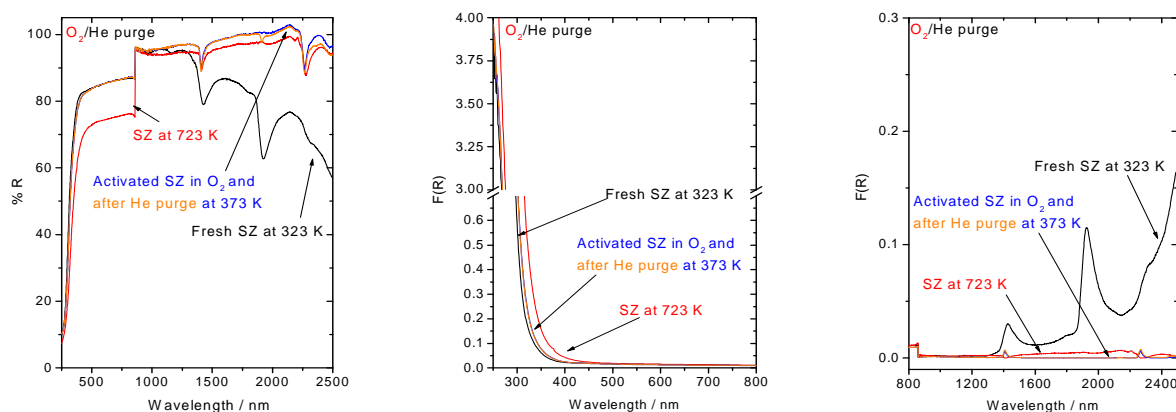
 Figure 4 - 3: SZ activated in 40 mL/min O_2 at 723 K for 30 min with 5 K/min ramp. SZ is cooled to reaction temperature under O_2 flow and then purged under He for 40 min before starting the reaction. The spectra of the fresh SZ at 323 K (black), at 723 K (blue) and after cooling in O_2 at 373 K are shown in reflectance (left) and in the Kubelka Munk function (UV-vis region in the middle and NIR region on the right)

The gases, O_2, He, N_2 and H_2, used for this work have a purity of 99.995%. The inert gases were dried by using oxy- and hydrosorb cartridges (Alphagas - purifier O_2-free and H_2O-free

from Air Liquide) before entering the corresponding mass flow controller. However, it was not possible to achieve a completely water-free environment as shown in Figure 4 - 4. During the purge in He, a small amount of water was adsorbed on the surface of the catalyst.
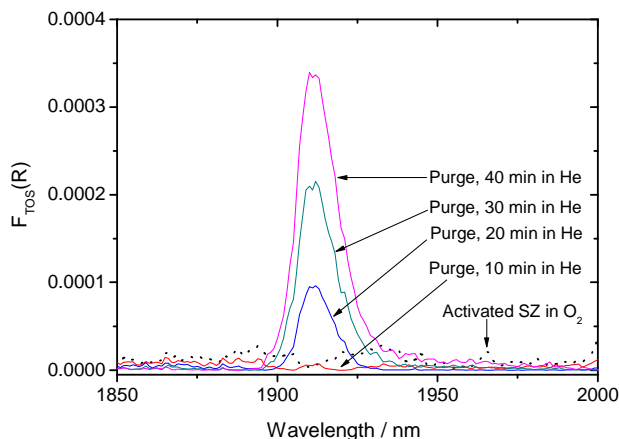
Figure 4 - 4: Evolution of surface water concentration under the He purge. Additional plot to Figure 4 - 3.

These results show that water that was accumulated on the surface of the catalyst during storage is removed. Indeed, during storage, SZ, which is highly hydrophilic, was assumed to reach equilibrium in the water content. A catalyst active in *n*-butane isomerization will be obtained if this water is partially removed, as described by Song and Kydd[3].

4.2.1.2. Reducing atmosphere

Activation of SZ under H_2 flow required lower temperature to avoid the reduction of sulfate[10] to S^{2-}, known as a poison for the catalyst. Thus, SZ was activated at 523 K for 120 minutes before it was cooled to the reaction temperature.
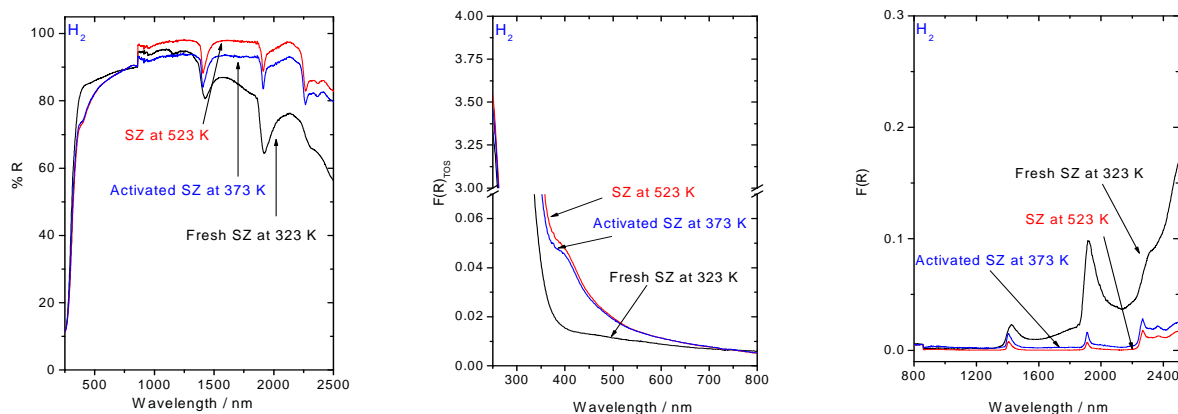
Figure 4 - 5: SZ activated in 40 mL/min H_2 at 523 K for 120 min with 5 K/min ramp. The spectra of the fresh SZ at 323 K (black), at 523 K (blue) and after cooling in H_2 at 373 K are shown in reflectance (left) and in the Kubelka Munk function (UV-vis region in the middle and NIR region on the right)

Figure 4 - 5 shows that during the activation under reductive atmosphere a band at 400 nm was appearing in the UV-vis region (Figure 4 - 5 in the middle).

Foster *et al.*[25] performed some plane wave density functional theory calculations of oxygen vacancies and interstitial oxygen atoms in monoclinic zirconia. They showed a singly charged oxygen vacancy V^+ at an energy level of 3.33 eV corresponding to 380 nm.

The NIR region showed a higher intensity of the band of water at 1915 nm, implying that the activation temperature was not enough to remove more than 95 % of water, as was the case under O_2 atmosphere. This high concentration of water on the surface could play a role in the activity of SZ for *n*-butane isomerization at 373 K (Section 5.1.4.3).

4.2.2. Manganese promoted sulfated zirconia

4.2.2.1. Oxidizing atmosphere

Manganese-promoted sulfated zirconia was activated under O_2 flow from 323 K to 723 K (final temperature kept for 30 minutes, ramp 5 K/min) and cooled under O_2 to the reaction temperature. Three absorption bands were observed at positions 300-400, 580 and 680 nm (Figure 4 - 6 middle). Furthermore, fewer OH groups (1405 nm) than on SZ were observed because of the higher calcination temperature[15].
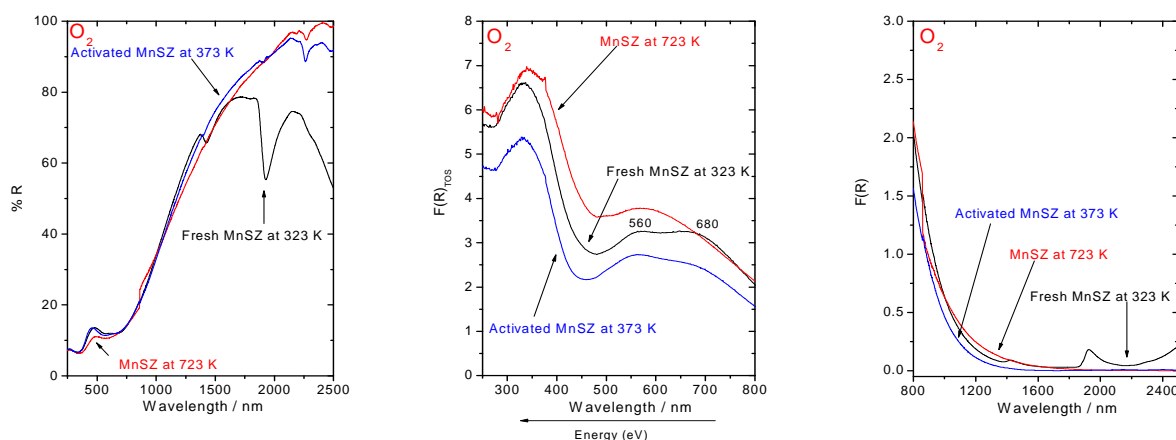

Figure 4 - 6: MnSZ (0.5 wt% Mn) activated in 40 mL/min O_2 at 723 K for 30 min with 5 K/min ramp. The spectra of the fresh MnSZ at 323 K (black), at 723 K (red) and after cooling in O_2 at 373 K are shown in reflectance (left) and in the Kubelka Munk function (UV-vis region the middle and NIR region on the right).

With increasing temperature, the intensity of the band at 580 nm increased without changing position. The band at 680 nm decreased during the heating phase; and increased again during the cooling to 373 K. However, like the band at 580 nm, the band at 680 nm did not change position, only the intensity of the band varied. Such temperature behaviour is characteristic of *d-d* transitions (decrease in the intensity and no change in the band position with temperature increase[26]). These observations allow the assumption that the band at 580 nm and at 680 nm

arise from *d-d* transitions: at the same time, the band in the range 300-400 nm increased in intensity and shifted to lower energies. This band in the UV range originates from ligand-metal charge transfer (an electron from the ligand O^{2-} was transferred to the metal Mn^{n+}, where n can be 2, 3 or 4).

The fact that the intensity of the band at 680 nm decreased at higher temperature and further increased at lower temperatures is due to a change in the oxidation state of the manganese cation. With increasing temperature, the manganese cation at 680 nm is oxidized to the cation responsible for the band at 580 nm; resulting thus a shift of the charge transfer to lower energies. The bands at 580 and 680 nm were ascribed in the literature[27,28] to *d-d* transitions of Mn^{3+}.

4.2.2.2. Inert atmosphere

The activation in inert atmosphere at 723 K for 30 minutes, with increasing temperature, led to a decrease in the intensity of the band in the range of 300-400 nm with a shift to higher energies (Figure 4 - 7).
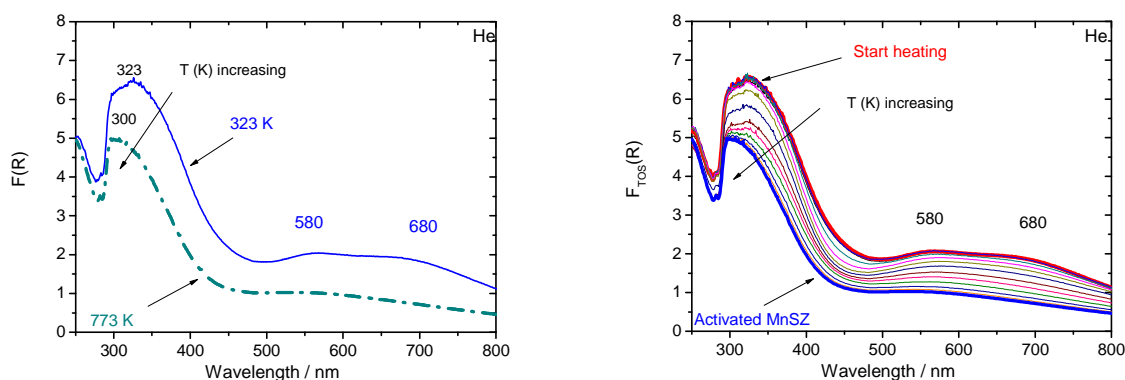
Figure 4 - 7: Activation of manganese (2 wt%) promoted sulfated zirconia under 20 mL/min He. In full line the fresh catalyst at 323 K and in dash-dot line the catalyst at 723 K. On the left only the spectra before and after activation are shown. On the right, the evolution of the spectra with increasing temperature is shown.

In the temperature range 323 - 373 K, the band in the visible part of the spectra showed two specific maxima at 580 and 680 nm. With increasing temperature, the intensities of these maxima decreased, but not concurrently. Indeed, the changes (namely, the decrease in intensity) of the maximum at 580 nm were large, but less drastic than the changes occurring with the band at 680 nm (almost no band observed at high temperature). The different temperature behaviour of these bands led to the assumption that these two bands belonged to different species. The spectra in the UV range (300 - 400 nm) underwent changes as well, as

shown in Figure 4 - 7. With increasing temperature, the intensity of this maximum decreased, and simultaneously its position shifted to higher energies. It can be seen that at T = 323 K (blue line) the maximum was observed at 323 nm, while at 723 K (dotted line) the maximum occurred at 300 nm.

4.2.2.3. Reducing atmosphere

Similar conditions to the one used for SZ were applied to the activation of Mn promoted sulfated zirconia. After activation in H_2, like with SZ, the catalyst contained more water adsorbed than the catalyst after activation in O_2. Only the band at 580 nm was observed in the visible range; meaning here that only one type of Mn^{n+} existed in the catalyst. No changes were observed in the intensity of this band; and this could be explained by the reductive atmosphere (Figure 4 - 8). The band at 680 nm is already weak on a fresh manganese-promoted sulfated zirconia (0.5 wt% Mn); the effect of the manganese content can be an explanation for the absence of the species responsible for this band.
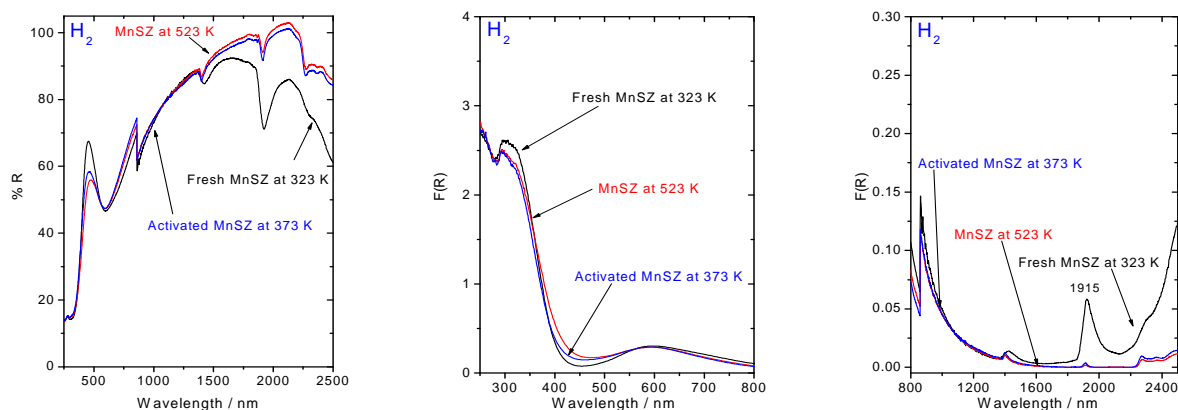
Figure 4 - 8: MnSZ (0.5 wt% Mn) activated in 40 mL/min H_2 at 523 K for 120 min with 5 K/min ramp. The spectra of the fresh MnSZ at 323 K (black), at 723 K (blue) and after cooling in H_2 at 373 K are shown in reflectance (left) and in the Kubelka Munk function (UV-vis region in the middle and NIR region on the right).

From the beginning of the activation, the Mn was at the lowest oxidation state and could not be reduced further (Mn^{2+} was excluded because its *d-d* transitions are spin forbidden). Moreover, the intensity of the charge transfer in the UV range decreased without any shift to lower or higher energy. The results confirmed that the charge transfer occured always with the same manganese cation.

The assignments of the bands at 580 and 680 nm in the literature[27,28] are not satisfying. Indeed, these bands were both ascribed to Mn^{3+}, but the spectra obtained during heating in

oxidizing, inert and reducing atmosphere show that the two bands do not change concomitantly and thus originate mostly from two different species. To have a better understanding of which manganese cations were observed in the visible range; theoretical calculations were performed and interpreted by Prof. Sophia Klokishner based on the spectroscopic data of MnSZ activated under He obtained in the course of this work.

4. 3. Interpretation of UV-vis spectra of Mn-promoted sulfated zirconia

The activation of the MnSZ (2 wt% Mn) took place in inert atmosphere (He) and the following calculations were based on the activation described in 4.2.2.2.

The spectroscopic data of the MnSZ show bands at 580 and 680 nm in the UV-vis range. Kijlstra et al.[27] ascribed these bands to the d-d transition of Mn^{2+} or Mn^{3+} with the precision that the d-d transition of Mn^{2+} are spin forbidden and are by consequence very weak. Lopez et al.[28] ascribed these additional bands observed in the Mn spectra to Mn^{3+} d-d transitions.

Some observations can be made on the interaction responsible for the shape of the d-d bands:
(i) the optical d-d bands are very broad and the width of these bands of the order of 10^3 - 6×10^3 cm^{-1}; (ii) the d-d bands in a crystal field are considerably broader than the lines in the atomic spectra; (iii) the interaction of d electrons with the crystal field or molecular vibrations are responsible for the width of the d-d bands.

4.3.1. Shape of the band arising from a d-d transitions

An octahedral metal complex ML_6 constitutes of a central ion and adjacent ligands.

The interaction of the d ion electrons with the ligand, whose position can vary, constitutes the electron vibrational interaction. This interaction represents the change in the energy of the cluster due to the displacements of the ligands.

The full symmetric vibration of the ML_6 complex, Q, can be written:

$$Q = \frac{1}{\sqrt{6}} (x_1 - x_4 + y_2 - y_5 + z_3 - z_6)$$

The electron vibrational interaction is defined by $H_{ev} = v(\vec{r}) Q$ where

$$v(\vec{r}) = \left(\frac{\partial V(\vec{r}, \vec{R})}{\partial R} \right)_{R=R_0} \quad \text{is the vibronic parameter,}$$
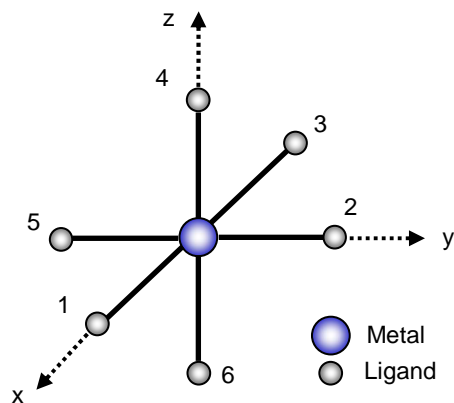
Figure 4 - 9: Octahedral Metal - ligand ML$_6$ complex

and $V = \sum\limits_{i=1}^{6} \dfrac{Z\,e^2}{\left|\overrightarrow{r} - \overrightarrow{R_i}\right|}$ is the energy of interaction between the electron of the metal ion and the ligand; Ze the charge of the ligand; e the electron charge; $\overrightarrow{r}$ the electron coordinate and $\overrightarrow{R_i}$ the position vector of the ligand L_i.

The Hamiltonian of the coupled electron-vibrational system can be written after two steps of adiabatic approximation: (i) the kinetic energy of the ligands is neglected because the ligands are heavy ions and (ii) the vibronic interaction is averaged over all possible positions of the electron.

$$U_i(Q) = E_i + v_i\,Q + \frac{\eta\,\omega}{2}\,Q^2$$

E_i is the energy of an electron in a static crystal field with the corresponding wave-function Ψ_i; v_i is the vibronic parameter for the state i; $v_i\,Q$ represents the averaged energies of the interaction of the electron with the vibration Q; $\dfrac{\eta\,w}{2}\,Q^2$ is the potential energy of vibrations.
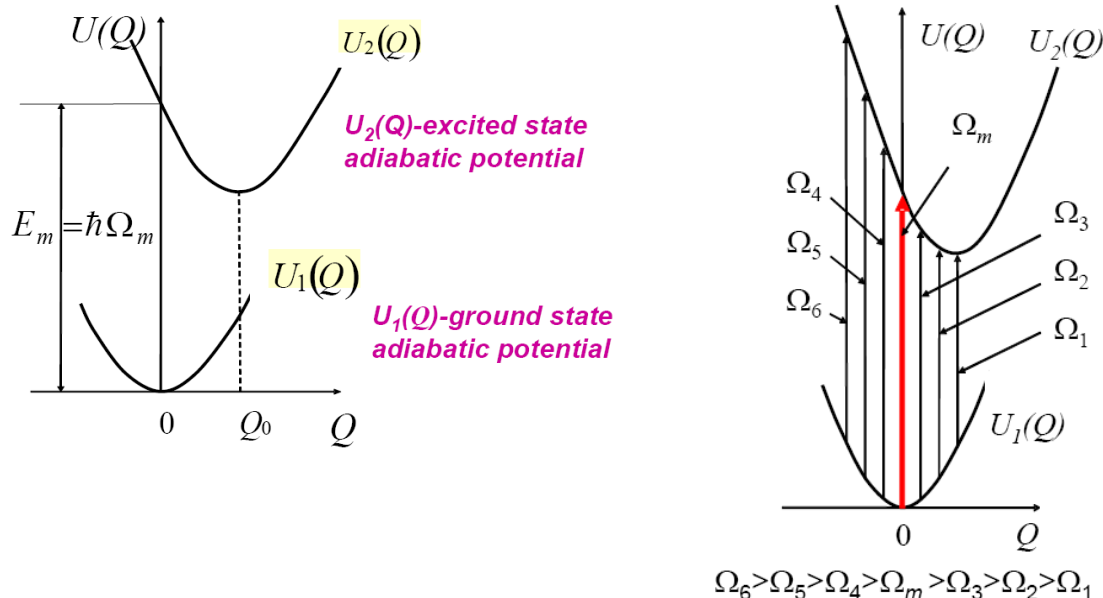
Figure 4 - 10: Origin of the *d-d* transitions. Series of transitions at different Q to form the absorption *d-d* band and $\Omega = 2\pi\nu$ is the frequency of the absorbed photon

The adiabatic potentials $U_1(Q)$ and $U_2(Q)$ for a two levels scheme are shown in Figure 4 - 10.

44

In case of the light absorption, the electronic state changes rapidly. During this electronic transition in the course of the photon absorption, the ligands have no time to change their positions in accordance with the Frank-Condon principle.

From this principle, it follows that only vertical transitions are allowed. Instead of one transition, a series of transitions at different Q contribute to the formation of the absorption d-d band.

The shape-function of the absorption band is defined by the following equation:

$$F(\Omega) = d_{21}^2 \sqrt{\frac{\eta^3 \, \omega}{2 \, \pi \, k_b \, T \quad (\nu_2 - \nu_1)^2}} \, \exp\left(-\frac{\eta^3 \, \omega \, (\Omega - \Omega_m)^2}{2 \, \pi \, k_b \, T \, (\nu_2 - \nu_1)^2}\right)$$

where $\eta \, \Omega_m = E_2 - E_1 + \dfrac{\nu_1 \, (\nu_1 - \nu_2)}{\eta \, \omega}$ and $d_{21} = \int \Psi_2^* (r) \, d \, \Psi_1 (r) \, d\tau$ is the dipole moment.

Thus, (i) the absorption band described by the equation for $F(\Omega)$ represents a Gaussian curve; (ii) the band which has a maximum intensity at $\Omega = \Omega_m$ can be observed only if the transition is dipole allowed, i.e. $d_{21} \neq 0$; the shape of the band and the position of the maximum depend on the vibronic parameters ν_1 and ν_2, on the temperature T and on the energy gap $(E_2 - E_1)$ between the electronic levels in the crystal field. The intensity of the band decreases with temperature rise as $F(\Omega_m) \sim \dfrac{1}{\sqrt{T}}$.

4.3.2. Charge transfer bands

Charge transfer bands arise as a direct consequence of an electron transfer under absorption of light. Actually this absorption occurs when an electron is transferred from an orbital primarily on the ligand to one primarily on the metal, or vice-versa. For the compounds under examination in the present thesis, charge transfer Ligand to Metal bands (LMCT) are observed. Besides the ligand – metal charge transfer bands the metal-ligand charge transfer can also take place and give rise to light absorption. The charge transfer transitions occur commonly at higher energies than the crystal field transitions. If the metal is easily oxidized and the ligand is simply reduced or vice-versa, the charge transfer may occurs at quite low energies. The intervalent transitions, when, under action of light, an electron is transferred from one metal ion to another, are known as well and are observed in complexes containing transition metal or lanthanide ions with different oxidation degrees. A colour visible to the human eye usually characterizes this transfer.

4.3.3. Hypothesis

The model was based on the following assumptions, supported by the experimental data: *a)* the latest results obtained by Giulio Lolli [ongoing work] showed that, in the low temperature range (from 128 K to 283 K) under vacuum (1 mbar), the maximum of the band at 580 nm did not change the position with increasing temperature. At the same time the intensity of the maximum of this band decreased with the temperature rise (Figure 4 - 11). These observations allowed us to assume that the bands at 580 nm and 680 nm arise from *d-d* transitions as described in 4.2.2.1. In our case, we have excluded the *d-d* transition of Zr^{3+} for the calculations. The Zr^{3+} ion belongs to the $4d$ group. The crystal field for the ions of the $4d$ group is much stronger than that for the $3d$ ions. Therefore, the *d-d* transitions of Zr^{3+} ion are strongly shifted to the "blue" side, in the range of 320-380 nm of the spectra. Thus, this band strongly overlaps with the oxygen-manganese charge transfer bands. Insofar as the *d-d* band of Zr^{3+} is narrow in comparison with the charge transfer bands, this *d-d* band cannot be distinguished from the charge transfer band. *b)* The band, in the range 300-400 nm in the UV region, is shifted to higher energies. This band results from a ligand-metal charge transfer (LMCT). LMCT requires more energy when the difference in oxidation state between the ligand and the metal is higher. This shift of the band to higher energy means that the charge transfer occurs with increasing temperature mainly between O^{2-} and Mn^{2+}; so that the number of Mn^{2+} ions is increased. The correlation of the band shift with the decrease of the intensity of the band at 680 nm gives an additional confirmation that the latter belongs to Mn^{3+} ions which are reduced at higher temperatures to Mn^{2+}; *c)* In favour of the assumption that the band at 680 nm belongs to Mn^{3+} while the band at 580 nm originates from Mn^{4+}, Sugano *et al.*[29] described a stronger crystal field for the Mn^{4+} than for the Mn^{3+} ion; thus the cation Mn^{4+} will be localized at higher energies than the Mn^{3+}.
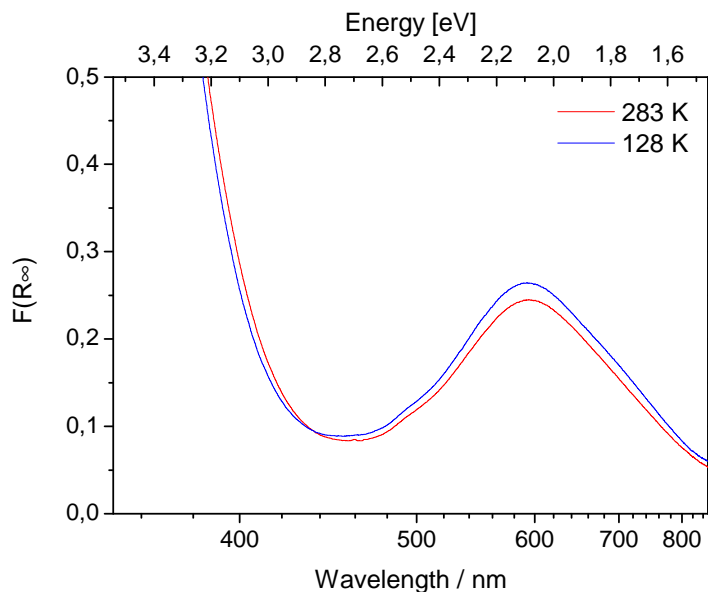
Figure 4 - 11: MnSZ (0.5 wt% Mn) at low temperature (283 to 128 K) and under vacuum (1 mbar) in the UV-Vis range. Evolution of the band at 580 nm

4.3.4. The Model

The Mn^{3+} ions in the zirconia lattice induce the generation of oxygen vacancies for charge compensation. Steele[30], Ishizawa[31] and Azzoni[32,33] described the oxygen vacancies close to the manganese cation. Based on these reports it was assumed in this study that the oxygen vacancies were also close to the Mn cation. These vacancies led to the displacement of the nearest neighbours of the impurity ion (Mn cation).
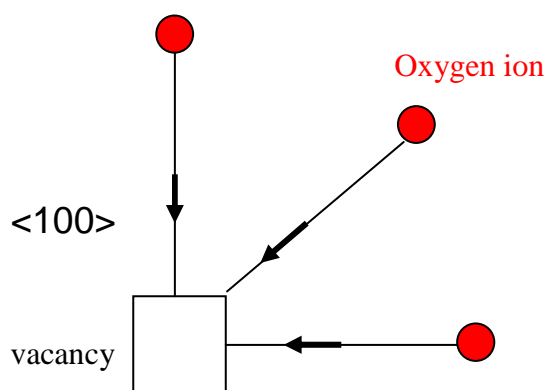
Figure 4 - 12: Oxygen ion displacements along the < 100 > directions towards the vacancy

On the basis of the experimental data (XAS, EXAFS, XRD, neutron-diffraction studies, EPR, optical spectra) it was possible to predict the number of vacancies in the nearest surroundings of the impurity ion, the number of its nearest neighbour oxygen ions, as well as the directions of the oxygen ions displacements, and finally the symmetry of the nearest surrounding of the impurity ion[30,31,32,33], Mn^{3+}. In the earlier paper[30], with the aid of neutron-diffraction measurements,

it was shown that the presence of oxygen vacancies causes oxygen ion displacements along the <100> directions towards the vacancies (Figure 4 - 12).

Recently, on the basis of the data obtained from single crystal X-ray diffraction using synchrotron radiation and EXAFS for yttrium doped cubic stabilized zirconia[31], it was suggested that the nearest surroundings of Y^{3+} consists of 6 oxygen ions, 2 missing oxygen ions were connected by the body diagonal of the cube (Figure 4 - 13).

Azzoni et al.[32,33] examined the EPR and optical spectra of Zr^{3+} in cubic stabilized zirconia. In reference[4,5] the observed EPR and optical spectra of Zr^{3+} were interpreted in the framework of a model that considered a six-fold coordinated Zr^{3+}. The local rearrangements of the anions were modelled as <100> displacements η_1 and η_2 of the two terns of oxygen towards each of the two vacancies (see Figure 4 - 13). Based on these experiments and findings, it was assumed in this model that the nearest Mn^{3+} surrounding in ZrO_2 also consisted of 6 oxygen ions, which were shifted towards the 2 oxygen vacancies (Figure 4 - 13).

Figure 4 - 13: Structural model of a metal Mn^{3+} centre in zirconia, showing the different displacements of the two terns of oxygen atoms towards the oxygen vacancies.

In this model the distances between the central Mn^{3+} ion and the two terns of oxygen ions were equal to:

$$R_1 = \sqrt{\left(\eta_1 - \frac{a}{2}\right)^2 + \frac{a^2}{2}} \text{ and } R_2 = \sqrt{\left(\eta_2 - \frac{a}{2}\right)^2 + \frac{a^2}{2}},$$
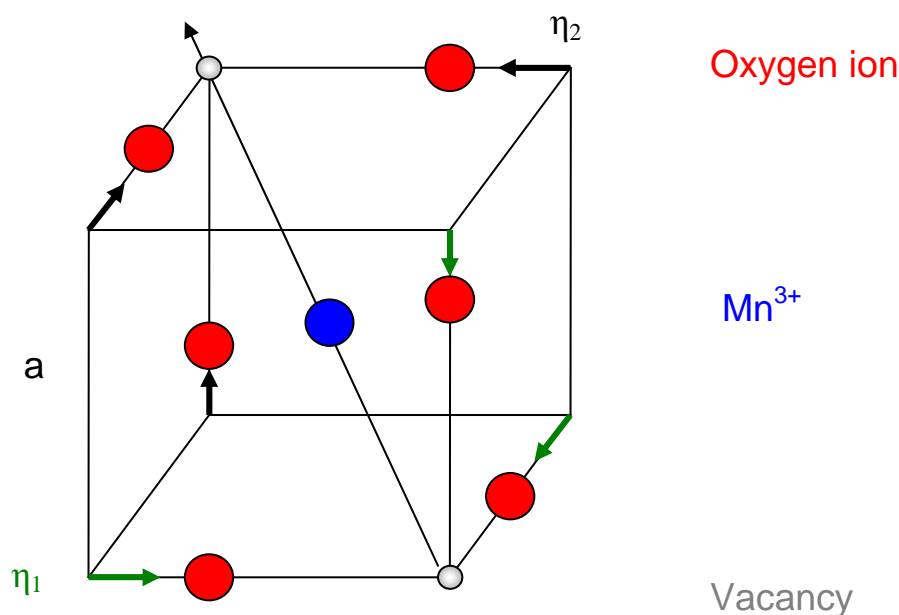
where a is the cube edge and η_1 and η_2 are the displacements of oxygen ions shown in Figure 4 - 13. The symmetry of the Mn^{3+} complex was supposed to be trigonal (because of the directions of the oxygen ions displacements) and it was described by the point group C_{3v}. In the trigonal ligand surroundings, the ground state of the Mn^{3+} ion is the $^5E^{(1)}$ term, while the excited states were the terms $^5E^{(2)}$ and $^5A_1$, arising from the splitting of the cubic $^5T_2$-term (Figure 4 - 14) by the crystal field. The indices "1" and "2" were introduced just to label the two different levels that transform according to the irreducible representation E of the C_{3v} point group. The total absorption band of the Mn^{3+} ion originated from the optical transitions $^5E^{(1)} \rightarrow ^5E^{(2)}$, $^5E^{(1)} \rightarrow ^5A_1$ (Figure 4 - 14).
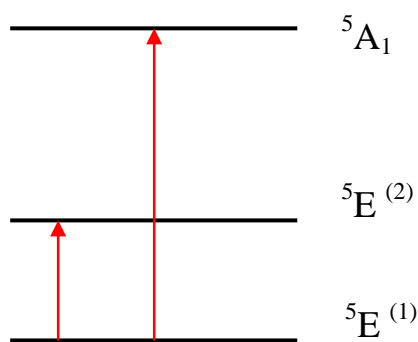
Figure 4 - 14: Energy levels of the Mn^{3+} ion in the trigonal ligand surroundings and the optical transitions contributing to the formation of the absorption band at 680 nm.

In correspondence with the neutron-diffraction measurements[30], the simulation of the absorption spectra of the Mn^{3+} ions was performed for η_1, η_2 values satisfying the inequalities $\eta_1 \leq 0.5$ Å, $\eta_2 \leq 0.5$ Å. From the calculations carried out for this work, it was found that the position and the shape of the Mn^{3+} absorption band at 680 nm could be satisfactorily reproduced for two sets of η_1 and η_2 parameters:

a) $\eta_1 = 0.16$ Å, $\eta_2 = 0.4$ Å

b) $\eta_1 = 0.15$ Å, $\eta_2 = 0.2$ Å

with $a = 2.57$ Å[32] being the cube edge (see Figure 4 - 13).

When Mn^{4+} substituted Zr^{4+}, no changes in the number of oxygen ligands surrounding the Mn^{4+} were supposed. Thus, for Mn^{4+} ions, the ligand surrounding was assumed to consist of 8 oxygen ions. The modelling of the oxygen surroundings of the Mn^{4+} ions was performed in the following way:

_____

> From X-ray data, the distances of 8 oxygen ions that surround the Zr^{4+} ion in tetragonal stabilized zirconia were taken. These distances were calculated from the structural data taken in the paper from Lutterotti[34].

O1: r = 2.366 Å, O2: r = 2.083 Å, O3: r = 2.366 Å, O4: r = 2.083 Å, O5: r = 2.083 Å, O6: r = 2.366 Å, O7: r = 2.083 Å, O8: r = 2.366 Å

The radius of Zr^{4+} ion is equal to R_{Zr4+} = 0.82 Å[35], whereas the radius of the O^{2-} ion is 1.36 Å. Thus, the mean distance between these ions is 2.18 Å. The radius of the Mn^{4+} ion is much smaller than that of Zr^{4+} ion, namely R_{Mn4+} = 0.52 Å, and thus the mean distance Mn^{4+}– O^{2-} is to be 1.88 Å.

> Under the assumption that the substitution of Zr^{4+} by Mn^{4+} only changed the distances between the metal ion and oxygen ions it was possible to write the following relations where the values are given in angstrom Å

$$1.88 / 2.18 = x / 2.366$$
$$1.88 / 2.18 = y / 2.083$$

For the complex $Mn^{4+}O_8$ the following distances were obtained: O1: r = 2.04 Å, O2: r = 1.796 Å, O3: r = 2.04 Å, O4: r = 1.796 Å, O5: r = 1.796 Å, O6: r = 2.04 Å, O7: r = 1.796 Å, O8: r = 2.04 Å. It should be mentioned that the values of the angles θ and φ for the ligands were taken as the same as for the complex $Zr^{4+}O_8$. The geometrical structure of the MnO_8 complex is shown in Figure 4 - 15.
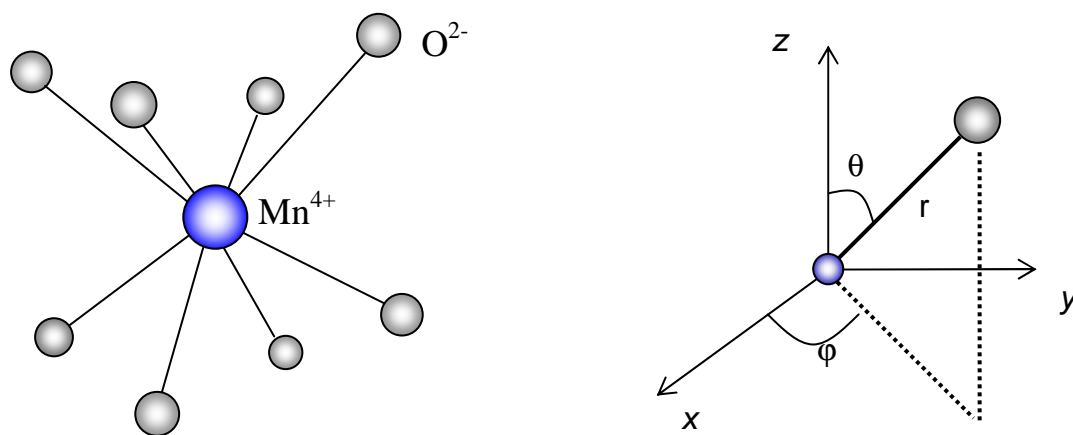
Figure 4 - 15: Geometrical structure of the Mn^{4+} complex

_____

The symmetry of the $Mn^{4+}O_8$ complex is very low. And the crystal field splits the ground cubic $^4T_1(t_2^2e)$ state into three levels (Figure 4 - 16). The same situation took place with the first excited $^4T_2$ (t_2^2e) state. In such a way, the band arising from Mn^{4+} was formed by 6 transitions [between the ground level that originates from the $^4T_1$ (t_2^2e) state and 6 excited levels: two from the state $^4T_1(t_2^2e)$, three from the state $^4T_2(t_2^2e)$ and the level $^4A_2(t_2^3)$, which was orbitally degenerate and cannot be split by a low symmetry crystal field].
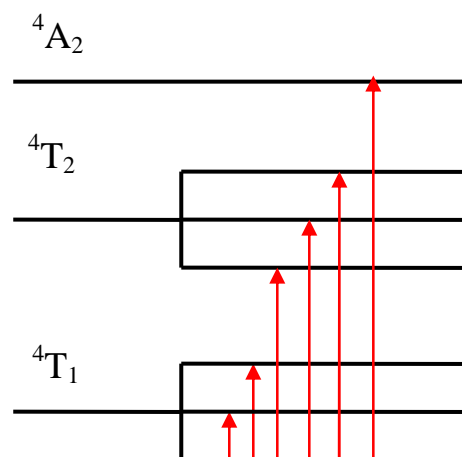
Figure 4 - 16: Energy levels of the $Mn^{4+}O_8$ complex and 6 optical transitions, which form the absorption band of the Mn^{4+} ions

For this work, the spectra of MnSZ containing 2 wt% of Mn were simulated. The simulation was carried out with two sets of parameters η_1 and η_2. The first set of parameters used for the simulation was: $\eta_1 = 0.16$ Å ,$\eta_2 = 0.4$Å, a = 2.57 Å. First it was calculated microscopically (electron-vibrational interaction and all above mentioned electronic states of the impurity manganese ions were taken into account in the theoretical model), the partial absorption spectra arising from Mn^{3+} and Mn^{4+} ions thanks to the first set of parameters η_1 and η_2 for the Mn^{3+} ions and the calculated bond lengths Mn^{4+}-O^{2-}. Then, from the fitting of the total calculated spectrum arising from Mn^{3+} and Mn^{4+} to the experimental spectrum, with the result that, at 373 K, the relative concentrations of Mn^{4+} and Mn^{3+} are calculated in the ratio,

$$x_{Mn4+} / x_{Mn3+} = 0.90$$

The corresponding experimental and theoretical spectra are shown in Figure 4 - 17.
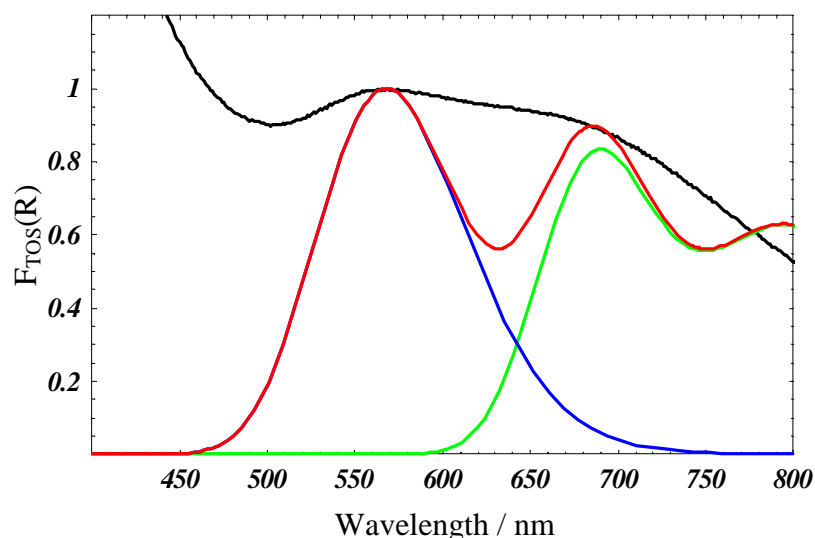
Figure 4 - 17: Apparent absorption spectra in the visible range, black line – experimental data (T = 373 K), Red line – theoretical curve calculated with $\eta_1 = 0.16\,\text{Å}$, $\eta_2 = 0.4\,\text{Å}$ and $x_{Mn4+}/x_{Mn3+} = 0.90$. In the blue line the partial contribution of the Mn^{4+} species to the total spectra is shown and in the green line the partial contribution of the Mn^{3+} species to the total spectra is shown.

Upon heating to 523 K, the shape of the apparent absorption spectrum in the visible range changed appreciably, as the band arising from Mn^{3+} and Mn^{4+} became broader. The fitting of the spectrum showed that the intensity of the *d-d* band arising from the Mn^{4+} ions exceeds that arising from the Mn^{3+} ions. At 523 K, the relative concentration was $x_{Mn4+}/x_{Mn3+} = 1.06$ (Figure 4 - 18).
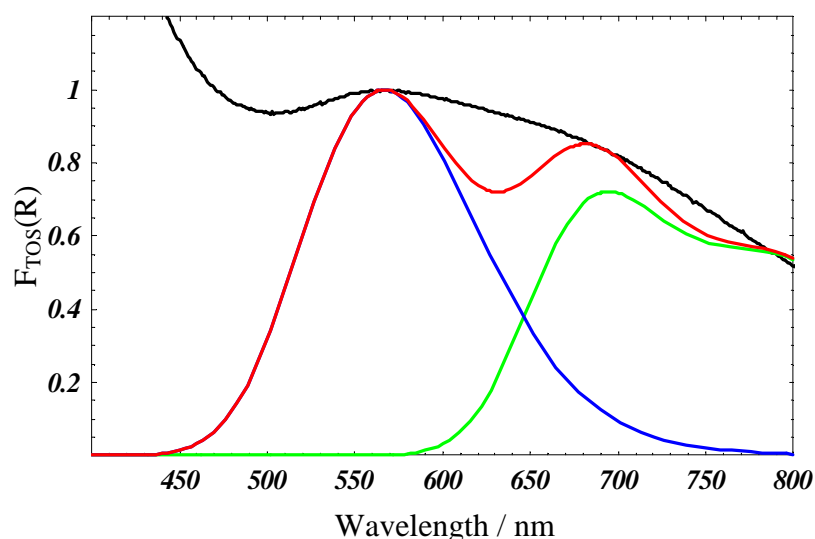
Figure 4 - 18: Apparent absorption spectra in the visible range, black line – experimental data (T = 523 K), Red line – theoretical curve calculated with $\eta_1 = 0.16\,\text{Å}$, $\eta_2 = 0.4\,\text{Å}$ and $x_{Mn4+}/x_{Mn3+} = 1.06$. In the blue line the partial contribution of the Mn^{4+} species to the total spectra is shown and in the green line the partial contribution of the Mn^{3+} species to the total spectra is shown.

Thus, the number of Mn^{4+} became higher than that of Mn^{3+} ions. This trend continued when the temperature was further increased to 623 K (Figure 4 - 19). The ratio x_{Mn4+} / x_{Mn3+} reached the value 1.18.
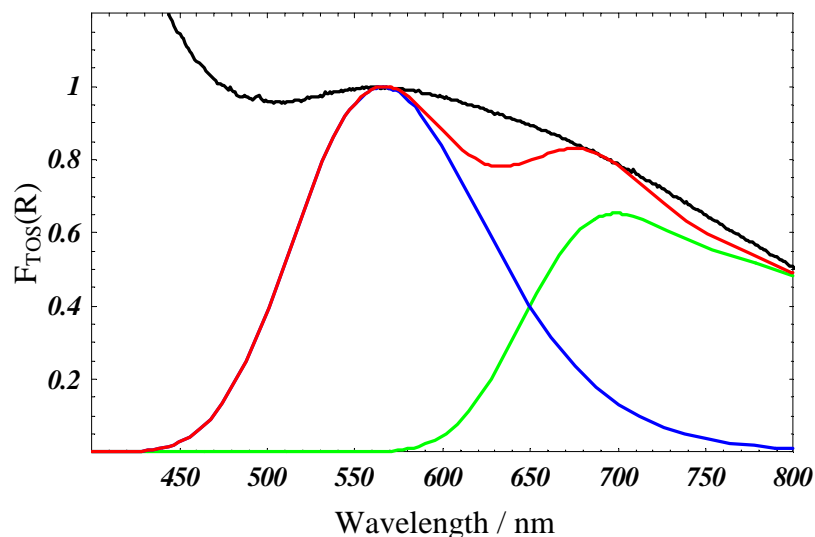
Figure 4 - 19: Apparent absorption spectra in the visible range, black line – experimental data (T = 623 K), Red line – theoretical curve, $\eta_1 = 0.16\,\text{Å}$, $\eta_2 = 0.4\,\text{Å}$ and x_{Mn4+}/ x_{Mn3+} = 1.18. In the blue line the partial contribution of the Mn^{4+} species to the total spectra is shown and in the green line the partial contribution of the Mn^{3+} species to the total spectra is shown.

With a further increase in temperature, the ratio x_{Mn4+} / x_{Mn3+} of relative concentrations continued increasing and, from the fitting of the calculated curve to the experimental curve at 723 K, the value x_{Mn4+} / x_{Mn3+} = 1.44 was obtained (Figure 4 - 20).
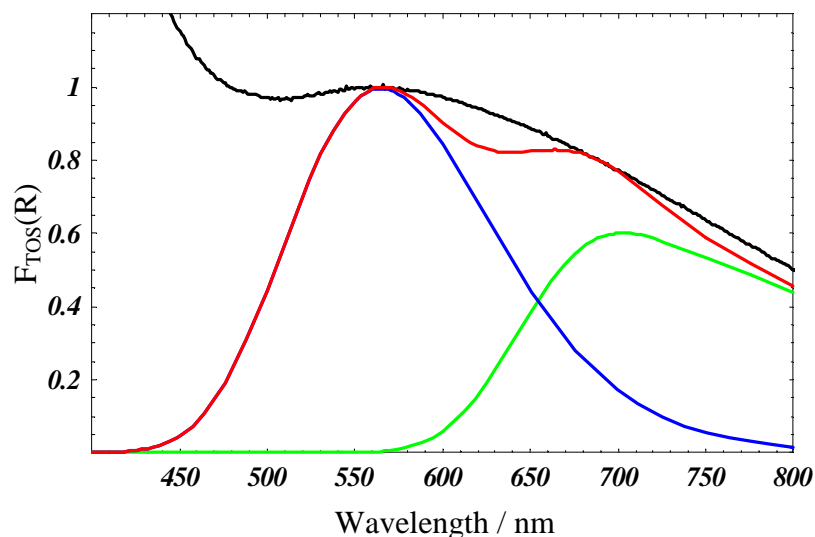
Figure 4 - 20: Apparent absorption spectra in the visible range, black line – experimental data (T = 723K) Red line – theoretical curve calculated with $\eta_1 = 0.16\,\text{Å}$, $\eta_2 = 0.4\,\text{Å}$ and x_{Mn4+}/ x_{Mn3+} = 1.44. In the blue line the partial contribution of the Mn^{4+} species to the total spectra is shown and in the green line the partial contribution of the Mn^{3+} species to the total spectra is shown.

_____

The x_{Mn4+}/ x_{Mn3+} values obtained for different temperatures were used further for the determination of the relative concentrations x_{Mn2+} , x_{Mn3+} and x_{Mn4+} of Mn^{2+}, Mn^{3+} and Mn^{4+} ions, respectively, in the catalyst at different temperatures. For this purpose a system of three equations was solved. The general form of this system of equations was as follows:

$$\left. \begin{array}{l} 2\,x_{Mn2+} + 3\,x_{Mn3+} + 4\,x_{Mn4+} = \alpha \\ x_{Mn2+} + x_{Mn3+} + x_{Mn4+} = 1 \\ x_{Mn4+}/\,x_{Mn3+} = \beta \end{array} \right\} \qquad (1)$$

The first equation represented the mean valence, α, of Mn ions in the catalyst. The second equation represented the normalization condition, and finally the third equation characterized the ratio of Mn^{3+} and Mn^{4+} species. In each case, the value β was obtained from the fitting of the calculated spectrum in the visible range to the observed one. For the determination of the values x_{Mn2+} , x_{Mn3+}, x_{Mn4+} from the system of equations (1), the mean valence, α, at different temperatures was taken from the paper[23] for samples MnSZ20 (20 stands for the amount of catalyst in gram calcined at once in synthetic air, and the loading of Mn was 2 wt%) activated in helium.

This α value varied with the experimental conditions at which the apparent absorption spectra had been measured. The values x_{Mn2+} , x_{Mn3+}, x_{Mn4+} determined using the mean valence, α, for the sample MnSZ20 are given in Table 4 - 1.

For $T = 373\ K$ the system of equations had the form $2\,x_{Mn2+} + 3\,x_{Mn3+} + 4\,x_{Mn4+} = 2.73$, $x_{Mn2+} + x_{Mn3+} + x_{Mn4+} = 1$, $x_{Mn4+}/\,x_{Mn3+} = 0.90$

The values obtained for the relative concentration of each cation were $x_{Mn2+} = 0.51$, $x_{Mn3+} = 0.26$ and $x_{Mn4+} = 0.23$.

T, K	α	x_{Mn2+}	x_{Mn3+}	x_{Mn4+}
373	2.73	0.51	0.26	0.23
523	2.62	0.59	0.20	0.21
623	2.58	0.63	0.17	0.20
723	2.53	0.67	0.13	0.20

Table 4 - 1: Relative concentrations x_{Mn2+} , x_{Mn3+}, x_{Mn4+} determined using the experimental data on the average valence, α, for the MnSZ20 in He and the calculated apparent absorption spectra in the visible range in the case of $\eta_1 = 0.16\,\text{Å}$, $\eta_2 = 0.4\,\text{Å}$

Similar systems of equations were compiled and solved for temperatures $T=523,\ 623$ and

_____

723 K. The corresponding relative concentrations x_{Mn2+}, x_{Mn3+}, x_{Mn4+} are given in Table 4 - 1 Similar calculations of the band shapes in the visible range and then of the relative concentrations x_{Mn2+}, x_{Mn3+} and x_{Mn3+} were performed in the case of the displacements $\eta_1 = 0.15$ Å, $\eta_2 = 0.2$ Å, which also provided the correct position of the Mn^{3+} band for $a = 2.57$ Å. However, for this set of parameters, the details of the description of the spectra calculation, as well as the details of the solution of equations (1), are dropped and only the obtained results are summarized in Table 4 - 2.

T, K	α	x_{Mn4+}/x_{Mn3+}	x_{Mn2+}	x_{Mn3+}	x_{Mn4+}
373	2.73	0.92	0.51	0.26	0.23
523	2.62	1.06	0.59	0.20	0.21
623	2.58	1.18	0.63	0.17	0.20
723	2.53	1.38	0.66	0.14	0.20

Table 4 - 2: Relative concentrations x_{Mn2+}, x_{Mn3+}, x_{Mn4+} determined using the experimental data on the average valence, α, for the MnSZ20 in He and the calculated apparent absorption spectra in the visible range in the case of $\eta_1 = 0.15$ Å, $\eta_2 = 0.2$ Å

The figures with the experimental and calculated spectra are not shown for the second set of parameters $\eta_1 = 0.15$ Å, $\eta_2 = 0.2$ Å. Table 4 - 2 also contains the ratio x_{Mn4+}/x_{Mn3+} determined from the comparison of the calculated and experimental spectra.

4.3.5. Conclusions for the theoretical calculations

First of all it should be underlined that for the two sets of the parameters η_1 and η_2, the obtained relative concentrations x_{Mn2+}, x_{Mn3+}, x_{Mn4+} were in good agreement for sample MnSZ20. The analysis of the data given in Tables 1-4 also showed that, with an increase temperature:

➤ The relative concentration x_{Mn2+} of Mn^{2+} ions increased from 0.51 to 0.67 for the sample; and this was in accordance with the temperature behaviour of the charge transfer band. The edge of the charge transfer band shifted to shorter wavelengths and higher energies, indicating an increase in the number of Mn^{2+} ions.

➤ The relative concentration of Mn^{3+} ions decreased from 0.26 to 0.13 in the sample used in this work; that also did not contradict the CT band behaviour and it was in agreement with the decrease of the intensity of the *d-d* band at 680 nm, which was assigned to Mn^{3+}.

_____

> ➤ The relative concentration of Mn^{4+} ions decreased very slightly for both samples in the range of temperature from 373 to 723 K. This result could be explained as follows: the helium stream did not change the structure of the oxygen surrounding of the Mn^{4+} ions. It did not remove the oxygen ions.

4.4. Conclusions

This Chapter showed how different the spectra of SZ and MnSZ were according to the activation atmosphere; and how decisive this activation procedure was in later the activity of the catalysts (Section 5). The activation helped to reduce the high concentration of water which was assumed to be one of the reasons of deactivation. Furthermore, the model developed in this work fits the obtained spectra well and explains why our assignments differ from the literature[27,28]. The bands at position 580 and 680 nm, which were ascribed to Mn^{3+} in the literature, can now be assigned to *d-d* transitions of Mn^{4+} and Mn^{3+}, respectively.

[1] M. Hino, S. Kobayashi and K. Arata, *J. Am., Chem. Soc*., 1979, 101, 6439

[2] X. Song and A. Sayari, *Catal. Rev. Sci. Eng*., 1996, 38, 329

[3] S. X. Song, R.A. Kydd, *J. Chem. Soc., Faraday Trans*., 94, 1998, 9, 1333-1338

[4] M.R. Gonzalez, J.M. Kobe, K.B. Fogash, J.A. Dumesic, *J. Catal.* 160,1996, 290-298

[5] J.M. Kobe, M.R. Gonzalez, K.B. Fogash, J.A. Dumesic, *J. Catal.* 164, 1996, 459-466

[6] C. Morterra, G. Cerrato, F. Pinna, M. Signoretto and G. Strukul, *J. Catal.* 149, 1994, 181-188

[7] R.A. Keogh, R. Srinivasan and B. H. Davis, *J. Catal*., 151, 1995, 292-299

[8] R.A. Comelli, C.R. Vera, J.M. Parera, *J. Catal.* 151, 1995, 96-101

[9] S.X. Song, R.A. Kydd*, Catal. Lett.* 51, 1998, 95

[10] T. Wang, A. Vazquez, A. Kato, and L.D. Schmidt, *J. Catal.* 1992, 78, 306

[11] P.G.Menon, G.B. Marin and G.F. Froment, *Ind. Eng. Chem. Prod. Res. Dev*. 1982, 21, 52

[12] F.C. Lange, T.-K. Cheung and B.C. Gates, *Catal. Lett*., 1996, 41, 95-99

[13] V. Adeeva, J.W. de Haan, J. Jänchen, G.D. Lei, V. Schünemann, L.J.M. van den Ven, W.M.H. Sachtler and R.A. van Santen, *J. Catal.* 1995, 151,364

[14] R.E. Jentoft and B.C. Gates, *Catal. Lett*., 2001, 72, 129-133

[15] B. Klose, F.C. Jentoft, R. Schlögl, I.R. Subbotina, V.B. Kazansky, *Langmuir* 21 (23), 2005, 10564-72

[16] K.T. Wan, C.B. Khouw, M.E. Davis, J. Catal. 1996, 158, 311-326

[17] Z. Hong, K.B. Fogash, R.M. Watwe, B. Kim, B.I. Masqueda-Jiménez, M.A. Natal-Santiago, J.M. Hill and J. A. Dumesic, J. Catal. 178,1998, 489-498

[18] C.R. Vera, C.L. Pieck, K. Shimizu, C. A. Querini and J.M. Parera, J. Catal. 187, 1999, 39-49

[19] X. Li, K. Nagaoka, L. J. Simon, R. Olindo, J. A. Lercher, A. Hofmann, J. Sauer, J. Am. Chem. Soc., 2005, 127, 16159-16166

[20] B.S. Klose, F.C. Jentoft, P. Joshi, A. Trunschke, R. Schlögl, I. R. Subbotine, V.B. Kazansky, Catal. Today 116, 2006, 121-131

[21] R.E. Jentoft, A. Hahn, F.C. Jentoft and T. Ressler*, J. Synchrotron Radiat*., 2001, 8, 563-565

[22], F.C. Jentoft, A. Hahn, J. Kröhnert , G. Lorenz, R.E. Jentoft, T. Ressler, U. Wild, R. Schlögl, C. Hässner and K. Köhler, *J. Catal*. 2004, 224, 124-137

[23] R.E. Jentoft, A.H.P. Hahn, F.C. Jentoft, T. Ressler, *Phys. Chem. Chem. Phys*., 2005, 7, 2830-2838

[24] B.S. Klose, *PhD dissertation*, Technische Universität Berlin, 2005

[25] A.S. Foster, V.B. Sulimov, F. Lopez Gejo, A.L. Shluger, R.M. Nieminen, *J. of Non-Crystalline Solids* 303, 2002, 101-107

[26] The dynamical Jahn-Teller effect in localized systems, *Jahn, H. A. Teller and Edward*, Editors: Perlin, Yurii Evgenevich. Wagner, Max., 1984

[27] W. S. Kijlstra, E. K Poels, A. Bliek,   B.M. Weckhuysen, R.A. Schoonheydt, *J. Phys. Chem. B*, 101, 1997, 309-316

[28] E. F. Lopez, V.S. Escribano, C. Resini, J.M. Gallardo-Amores, G. Busca, *Appl. Catal. B: Environmental*, 29, 2001, 251

[29] S. Sugano, Y. Tanabe, H. Kamimura, *Multiplets of Transition-Metal Ions in Crystals, Academic Press,* 1970, 124

[30] D. Steele, B.E.F. Fender, *J. Phys.C*, 1974, 7,1-11

[31] N. Ishizawa, Y. Matsushima, *Acta. Cryst. B*, 55,1999, 5, 726-735

[32] C.B. Azzoni, A. Paleari, *Phys. Rev. B*, 1991, 44, 6858-6863

[33] C.B. Azzoni, L. Bolis, A. Paleari, G. Samoggia, F. Scardina, *Phys. Rev. B*, 1995, 51, 15942-15946

[34] L.Lutterotti, P. Scardi, *J. Appl. Cryst. JACGA* 23, 1990, 246-252

[35] L.A. Sorin, M.V. Vlasova, V.D. Levandovsky, *Introduction into the radiospectroscopy of paramagnetic monocrystals*, Kiev, Naukova Dumka, 1969, 256

5.1 SZ as catalyst for *n*-butane isomerization

Sulfated zirconia (SZ) is a highly active catalyst for skeletal *n*-butane isomerization[1,2,3] at low temperatures; and as a matter of fact SZ always suffers from severe deactivation with time on stream, within very short initial time periods. So far, many studies were carried out to try to understand the reason for the high catalytic activity; but also why SZ deactivates that fast. Carbenium-type ions species have been proposed to be intermediates in the *n*-butane isomerization. However, the formation of this species is under discussion. Several groups support the idea that the carbenium ion is formed through butane oxidative dehydrogenation[4,5,6,7,8] (ODH). The *n*-butane ODH produces water and butene. The latter are easily protonated to carbenium ions, and thus serve as reaction chain carriers.

Water is one product of the ODH[9] and is speculated to act as a poison in the *n*-butane isomerization on SZ[10].

An alternative and the most reported explanation of deactivation in this reaction is the accumulation of hydrocarbon deposits on the catalyst surface.

Ahmad *et al*[11]. performed an *in situ* UV-vis diffuse reflectance spectroscopic study during *n*-butane isomerization on sulfated zirconia. They identified the surface deposits and correlated their temporal evolution with the catalytic performance of SZ for the first time.

For the present work, we have also used diffuse reflectance UV-vis-NIR spectroscopy to monitor, *in situ*, the catalyst surface during the activation of the catalyst and the *n*-butane isomerization on SZ at 373 K. To correlate the possible changes in the spectra and the activity of the catalyst, the effluent gases were analyzed by GC online.

The goal of this Chapter is to relate, on the basis of NIR and UV-vis spectra and online GC data, the evolution of water and carbon-containing deposits on the catalyst surface to the activity of the catalyst with time on stream. Water can be seen in the NIR range through a combination mode (deformation and stretching) and hydrocarbon deposits (unsaturated) can be detected and studied via their absorption bands in the UV-vis range.

Furthermore, it will be explained how decisive the feed composition is for the formation of the unsaturated species absorbing at 295 nm; species responsible, according to the literature, for the deactivation of the SZ during *n*-butane isomerization.

5.2 Experimental conditions

5.2.1. Activation

The catalyst of interest, SZ, was activated for 30 minutes at 723 K in 40 mL min^{-1} O_2 and cooled to the reaction temperature, 323 or 373 K, in O_2 flow or O_2 followed by a purge in He. More details were described in the previous chapter (see Section 4, Activation and Interpretation of the UV-vis spectra of Mn-promoted sulfated zirconia).

5.2.2. Reaction conditions

The reactant mixture was 5 kPa n-butane in inert gas (N_2 or He) with a total flow of $40\,mL$ min^{-1}. It was sent through the catalyst bed. The reaction took place at two different temperatures; 323 K and 373 K. In the course of this work, the importance of the feed composition will be demonstrated. According to the specifications of the n-butane and after dilution, up to 2500 ppm of impurities could be present in the feed. No cartridges were used to purify n-butane before entering the mass flow controller. However, the inert gases were dried by using oxy- and hydrosorb cartridges (Alphagas - purifier O_2-free and H_2O-free from Air Liquide) before entering the corresponding mass flow controller.

5.3 Results after activation of SZ in O_2

5.3.1 Catalytic activities overview

The reaction profile of the n-butane isomerization on non-promoted SZ consisted of an induction period, a maximum of rate of isomerization and a deactivation of the catalyst. These three stages of the catalytic activity were observed for the reaction carried out at 323 K whereas at 373 K, the induction period was not observed, most probably because of the lack of time resolution in the gas phase analysis. The catalytic profile started with a decline from the very beginning of the activity and the true maximum was missing as shown in Figure 5 - 1. The gas mixtures provided by different gas suppliers should not influence the catalytic performance.
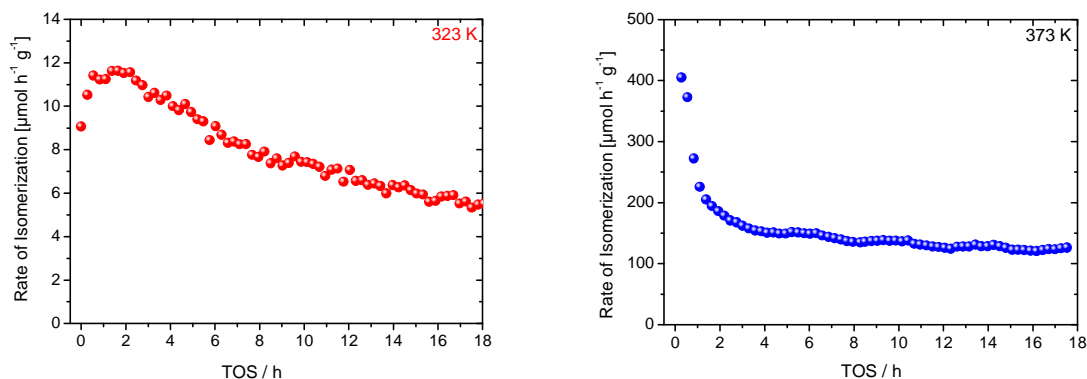
Figure 5 - 1: Rate of isomerization vs. time on stream. Reaction conditions: 5 kPa *n*-butane in N$_2$ on SZ (both using the industrial mixture from Linde) at 323 K (left) and at 373 K (right) with a total flow of 40 mL/min. The catalyst was activated under O$_2$ flow at 723 K for 30 min.

Figure 5 - 2 shows the catalytic performance of SZ using 5 kPa *n*-butane in N$_2$ from different gas providers.
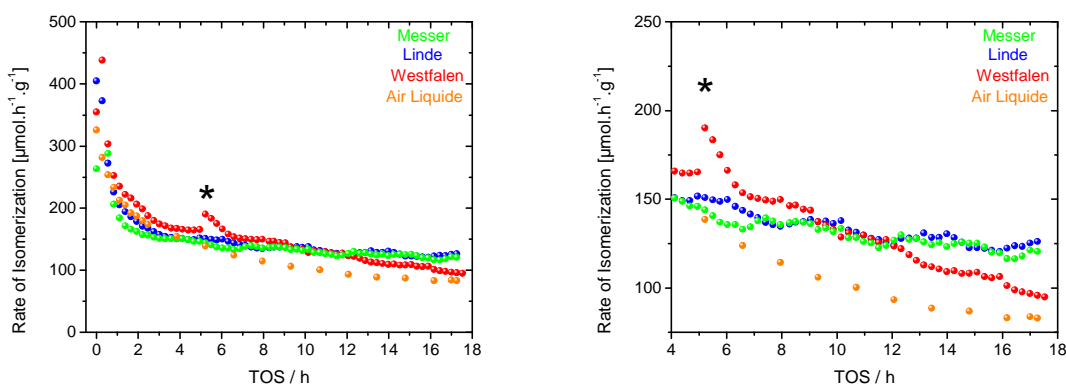
Figure 5 - 2: Rate of isomerization vs. time on stream. Overview of the activity on the left and zoom on the "steady state" on the right side with * artifact. The catalysts were all activated for 30 min in O$_2$ at 723 K. Reaction conditions: 5 kPa *n*-butane in N$_2$ on SZ by varying the gas providers at 373 K. The experiments performed with Linde and Westfalen are industrial mixtures whereas the one performed with Messer Griesheim and Air Liquide are obtained by diluting pure n-butane with N$_2$ in the laboratory.

The left plot shows a similar general trend for the catalytic performance of SZ at 373 K with all gas mixtures from the different gas providers. The catalytic activity started with a fast decline for the first 2 hours, followed by a constant slight loss during the "steady state". A zoom on the steady state part of the catalytic performance, Figure 5 - 2 right, showed that the experiments performed by using Messer Griesheim gas (self-mixed, in green) and Linde gas (industrial, in blue) as feed presented a similar trend within hours (same weak decline and rate of isomerization after 17 hours on stream of 132 $\mu mol \ g^{-1} \ h^{-1}$). Whereas, a stronger

deactivation and a lower rate of 89 - 102 $\mu mol\ g^{-1}\ h^{-1}$ after 17 hours for the experiments using Air Liquide gas (orange) and Westfalen gas (red) were observed respectively.

The trend of the activity followed an exponential decay (Figure 5 - 3) corresponding to the equation $r = S_1\ e^{-\frac{x}{t_1}} + S_2\ e^{-\frac{x}{t_2}}$, where r is the rate of isomerization in $\mu mol\ g^{-1}\ h^{-1}$, S_1 and S_2 the number of active sites responsible for the first and second deactivation phase respectively; and t_1 (0.89 h ± 0.25) and t_2 (23.75 h ± 4.27) are the time constant in hours.
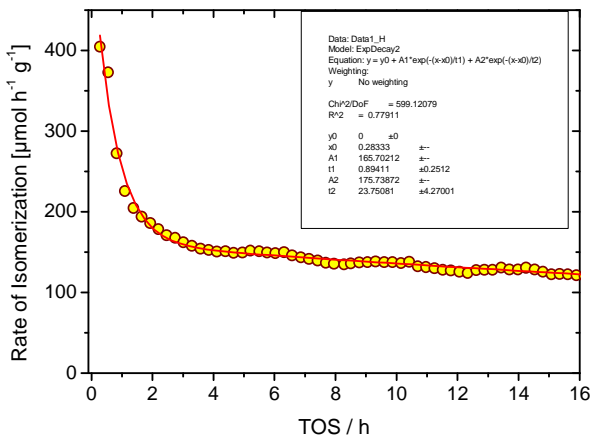
Figure 5 - 3: Fitting of the activity profile of 5 kPa *n*-butane in nitrogen (Linde gas mixture) isomerization on SZ at 373 K.

The experiments with self-mixed feed, using either pure *n*-butane from Messer Griesheim or Air Liquide, showed a different trend of the catalytic activity (Figure 5 - 4 left): a faster decline in activity was observed with the experiment performed with the Air Liquide gas. To discriminate the idea that this distinction was originated from the diluent gas, *n*-butane isomerization on SZ at 373 K using Air Liquide as gas provider was carried out either with He or N_2, diluent gas.
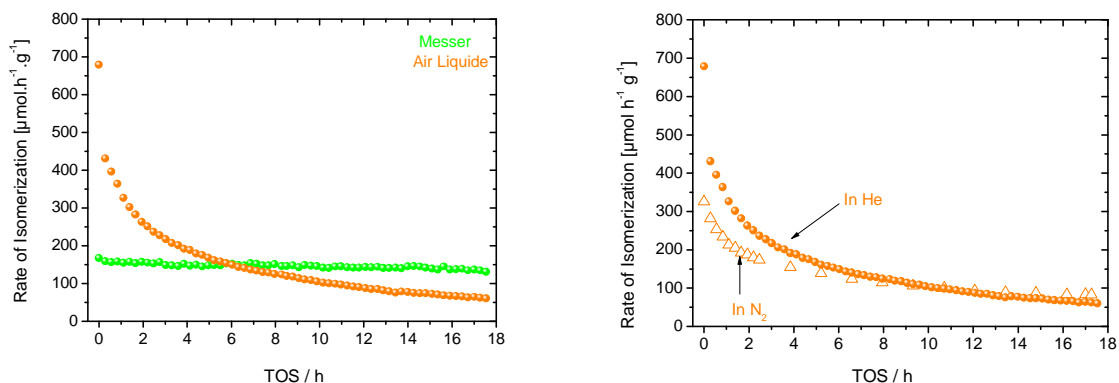
Figure 5 - 4: Rate of isomerization vs. time on stream. The catalysts were all activated at 723 K for 30 min in O$_2$. The reaction was performed under 5 kPa *n*-butane in He on SZ by varying the gas providers - Messer Griesheim and Air Liquide - at 373 K (left). On the right plot, the catalytic performance of the SZ is shown under a self-mixed gas from Air Liquide using He or N$_2$ as diluent.

The results showed, in Figure 5 - 4 right, a comparable deactivation process whatever the diluent was. It was clear from the catalytic data that some minor difference existed between the *n*-butane gas-mixtures.

5.3.2 Spectroscopic data observation and correlation with the activity

5.3.2.1 NIR region

The spectroscopic data were recorded in parallel with the activity of the catalyst during *n*-butane isomerization on SZ. In this part of the work, the attention will be focussed mainly on the NIR range of the spectra. The NIR range revealed the vibrations of species adsorbed on the surface of the catalyst. The spectra were recorded in reflectance and were converted into the Kubelka Munk function because of the proportionality which exists between the KM function and the concentration. After the activation of the catalyst in O_2, bands at 1423 nm and 1914 nm already existed in the catalyst spectra; the band at 1423 nm was more intense than the one at 1914 nm at 373 K in O_2 (Figure 5 - 5 spectrum in violet).
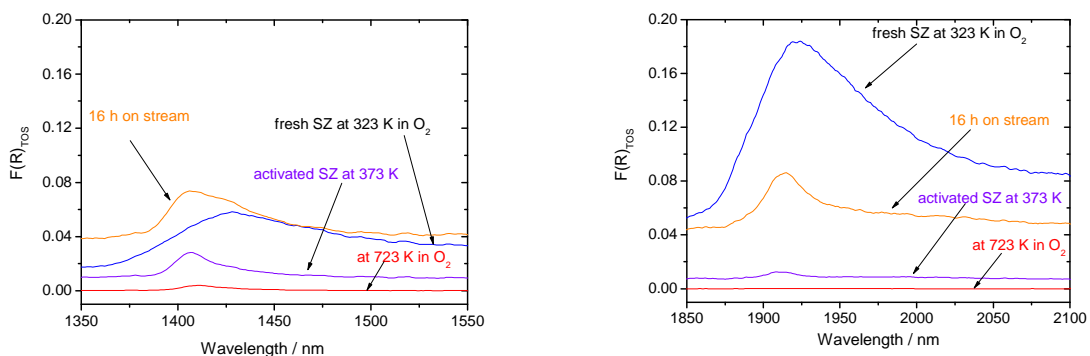
Figure 5 - 5: Species adsorbed at band positions ~1410 nm (left) and ~1920 nm (right) on the surface of a fresh SZ (blue), at 723 K in O_2, of the activated SZ at 373 K (violet) and after sixteen hours on stream (orange) for a reaction temperature of 373 K. Conditions: Activation in O_2 at 723 K for 30 minutes and reaction under 5 kPa *n*-C_4 (industrial mixture) at 373 K on SZ.

After one hour contact of the catalyst with the feed, the band at 1914 nm quickly grew and was more intense (Figure 5 - 6, spectrum in green). The maximum intensity of each spectrum at 1423 and 1914 nm and the rate of isomerization are plotted versus time on stream (Figure 5 - 7).
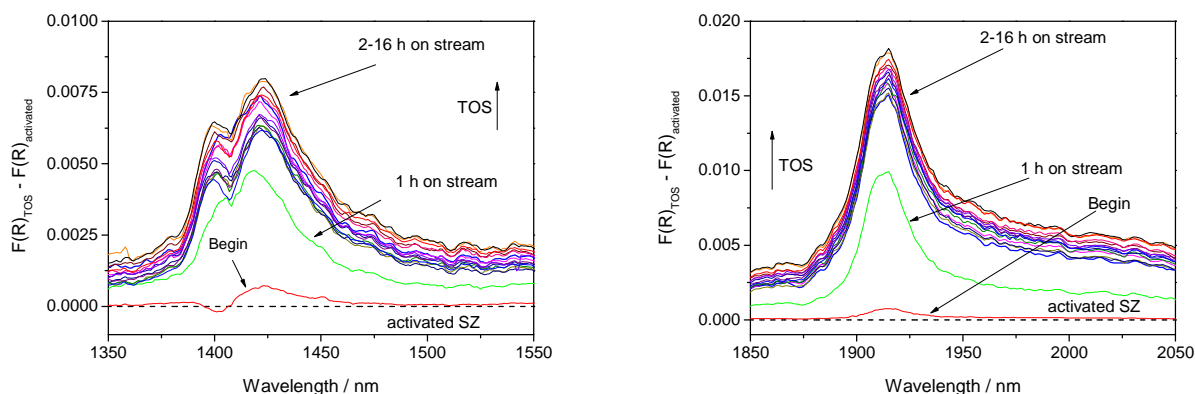
Figure 5 - 6: Left: band at 1420 nm, Right: band at 1914 nm. Conditions: Activation in O₂ at 723 K for 30 minutes and reaction under 5 kPa *n*-C₄ in N₂ at 373 K on SZ. Total flow of 40 mL/min with the Linde gas mixture.
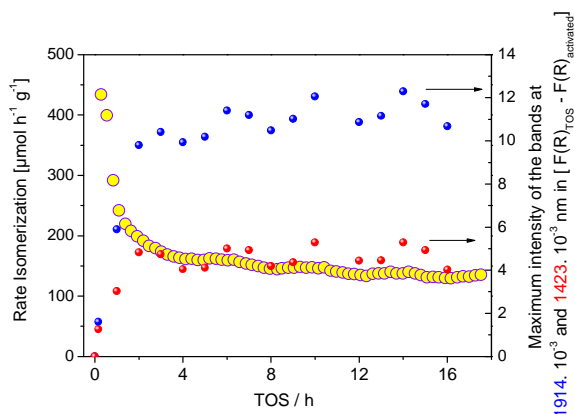
Figure 5 - 7: Activity and evolution of the species at band position 1423 and 1914 nm versus time on stream. Complete Figure 5 - 6. Conditions: Activation in O₂ at 723 K for 30 minutes and reaction under 5 kPa *n*-C₄ in N₂ at 373 K on SZ. Total flow of 40 mL/min with the Linde gas mixture.

During the first few (2-4) hours on stream the growth of the bands at 1423 and 1914 nm was fast, then the growth slowed down; and the intensity of the band at 1423 nm was twice weaker than the intensity of the band at 1914 nm.

The fast growth of the band at 1914 nm correlated, perfectly, to the drastic initial loss of activity as shown in Figure 5 - 8.

Similar results on the formation of the band at 1914 nm during the *n*-butane isomerization (5 kPa in N₂, at 373 K) were observed independent of the origin of the gas-mixture. The evolution of the spectra during reaction and the corresponding activity can be seen in the Appendix UV-vis of this work (Fig 1 and Fig 2).
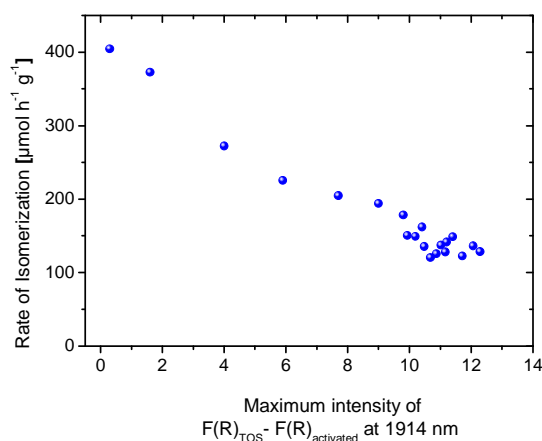
Figure 5 - 8: Complementary plot of the experiment described in Figure 5 - 7

For all gas mixtures used, the species of interest was formed fast during the first two hours on stream; and then the growth of this species slowed down. Moreover, the formation of the species absorbing at 1420 nm with time on stream, like the formation of the species absorbing at 1914 nm, was similar for all experiments regardless of the gas mixtures used. After sixteen hours on stream, the 1420 nm / 1915 nm intensity ratio was 0.37 for Linde, 0.36 for Westfalen and 0.30 for Messer Griesheim gas mixtures. Considering the error bars that exist when the maximum in intensity was plotted versus time on stream, the 1420 nm / 1915 nm intensity ratio was similar for the three different gas mixtures.

It should be mentioned that for this work only a comparison in the evolution of the species at band position 1914 nm was drawn. For a few experiments, normalization of the spectra in reflectance in the NIR range was compulsory to convert the data into KM. The KM function is strongly dependent on the reflectance, so that minor changes in the reflectance led to major changes in the KM function. The growth of the band at 1914 nm could be analyzed only qualitatively and not quantitatively. Nevertheless, our results showed that the initial loss in the activity of SZ correlated to the formation of the species absorbing at 1914 nm during the first few hours on stream.

5.3.2.2 UV-vis region

Similar to the catalytic activity, the spectroscopic data from experiments carried out with different sources of gas mixtures (industrial mixtures or self-mixed) showed some differences. The spectra during the reaction showed, in the UV-vis range: (i) no bands, (ii) one band at 295 nm (Figure 5 - 9) and (iii) three bands at 295, 370 and 450 nm (Figure 5 - 10). The three cases reflected three gas mixtures with the same specifications.

In the case when bands were detected in the UV-vis range, as soon as the catalyst was in contact with the feed, a band at 295 nm (Figure 5 - 9 right and Figure 5 - 10 left) was formed and continued to grow with time on stream.
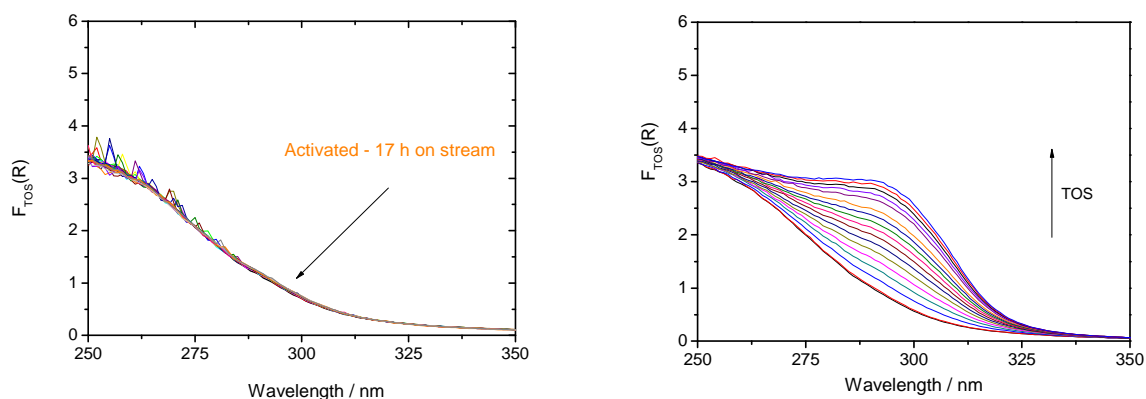
Figure 5 - 9: UV-vis spectra. The left plot shows no formation of bands with time on stream. The right plot shows the formation of one band at 295 nm with time on stream. Activation: 30 minutes at 723 K in O$_2$. Reaction conditions: 5 kPa *n*-butane in N$_2$ on SZ at 373 K during 16 hours on stream.
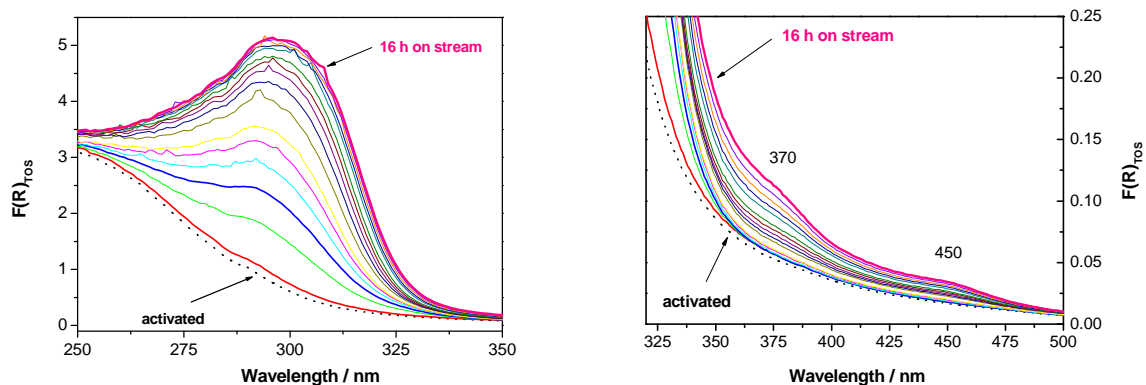
Figure 5 - 10: UV-vis spectra. Formation of three bands in time on stream at 295 nm (left), 370 and 450 nm (right). Activation: 30 minutes at 723 K in O$_2$. Reaction conditions: 5 kPa *n*-butane in N$_2$ on SZ at 373 K during 16 hours on stream.
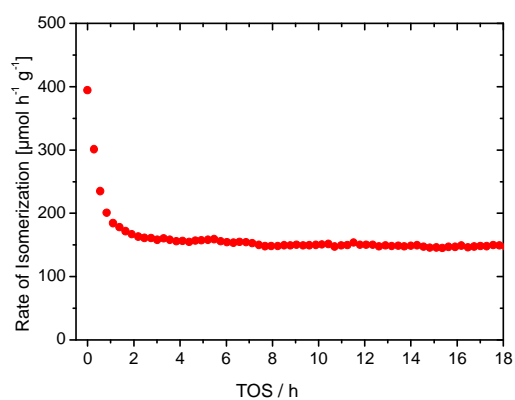
Figure 5 - 11: Activity of SZ in absence of bands in the UV-vis range. Activation: 30 minutes at 723 K in O$_2$. Reaction conditions: 5 kPa *n*-butane in N$_2$ on SZ at 373 K during 16 hours on stream.

In the absence of absorbing species in the UV-vis range, the SZ deactivated and the activity profile (Figure 5 - 11) was similar to the one obtained when the band at 295 nm was formed with time on stream (Figure 5 - 12 left).

When only the band at 295 nm was detected, the formation of the species responsible for this band was almost linear with time on stream (Figure 5 - 12 left). It is thus possible to conclude that the species at 295 nm cannot

explain the fast initial deactivation of SZ; these species are only spectators.

When three types of species were detected in the UV-vis range, the formation of the species characteristic of the band at 295 nm could be described in two steps: a fast formation within the first four hours on stream was followed by a slower growth within the next fourteen hours.
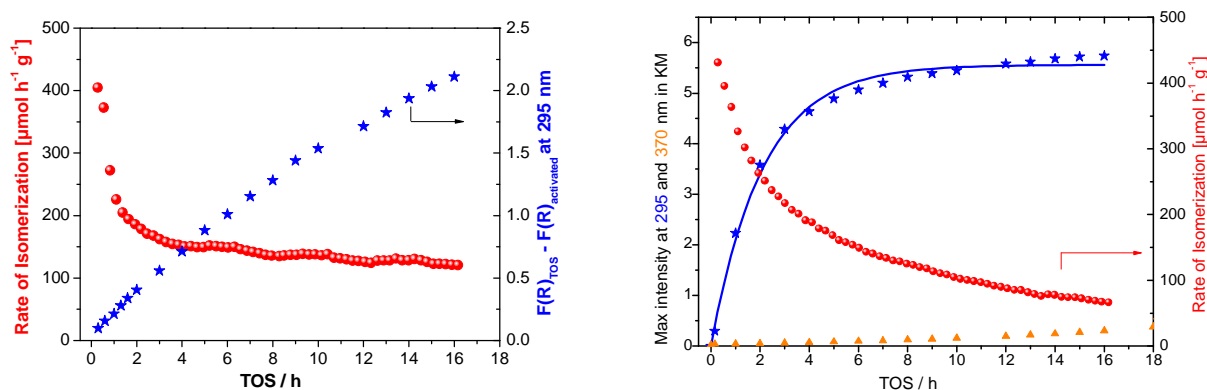
Figure 5 - 12: The rate of isomerization is plotted versus the time on stream. On the same graph, the maximum intensity in KM (corrected by subtracting the activated SZ) of the bands in the UV-vis range is plotted. On the left plot only the species at 295 nm (left) were detected while on the right plot in addition to the species at 295 nm , the one at 370 nm (right) were also detected within 16 hours. Activation: 30 minutes at 723 K in O_2. Reaction conditions: 5 kPa *n*-butane in N_2 on SZ at 373 K during 16 hours on stream.

In addition to the band at 295 nm, which grew – when it was present during the reaction – from the beginning of the reaction, two bands at 370 and 450 nm started to grow after 7 hours on stream (Figure 5 - 12 right). It should be mentioned that the second phase in the formation of the band at 295 nm did not decrease as the additional bands grew. Moreover, when the bands at 370 and 450 nm were detected, the rate of isomerization decreased continuously. The activity profile was thus different from the one observed in absence of any bands or only in presence of the band at 295 nm. This again shows that the species absorbing at 295 nm are not responsible for the catalyst deactivation.

In one gas mixture, propane was detected. The propane peak area obtained during reaction was larger than the one of the bypass measurement; that it is impossible to say if the amount of propane present in the feed reacted. Moreover, the performance (rate of isomerization) of SZ was equivalent independent of the presence or not of propane in the feed. In the case where propane was not present in the feed for two different gas mixtures, the spectra in the UV-vis range were not identical. For one gas mixture, only one band at 295 nm was forming during the reaction whereas with the other gas mixture three bands were observed. Propane cannot thus have a decisive influence on the formation of the bands in the UV-vis range and in the catalytic performance of SZ.

The bypass measurement of the one gas mixture showed an unidentified species at retention time 9.8 min. The peak area of this species did not change during the reaction so that it can be stated that these species never reacted.

Regarding these results, it can be concluded that the species at 295 nm are spectators in the deactivation of SZ.

5.4 Assignments of the bands

5.4.1 NIR region

The adsorbate responsible for the band at ~ 1915 nm is water (combination mode of OH stretching and deformation, 5185 cm^{-1} = 3590 + 1595 as reported already in previous literature[6,8,12]). The second band of interest at 1420 nm originates from the overtone of the stretching vibration of OH.

By performing *in situ* IR spectroscopy during *n*-butane isomerization at 373 K, Li *et al.*[6] showed an increase in the intensity of the OH vibration at 3580 cm^{-1}; in parallel with the increase in intensity of the water deformation band at 1600 cm^{-1} with time on stream. This band at 1600 cm^{-1} had been identified to be caused by the water deformation vibration through exposing SZ to H_2O. Klose *et al.*[8] also observed, bands at 1425 nm $\approx$ 7020 cm^{-1} and 1920 nm $\approx$ 5210 cm^{-1} in the NIR region, which arise from the overtone of the OH stretching vibration and a combination of H_2O stretching and deformation modes, respectively.

5.4.2 UV-vis region

The pronounced band at 295 nm in our experiments may suggest a $\pi - \pi^*$ transition of allylic cations. Alkyl group as substituent causes a shift of typically + 5 nm[13], which is not enough to properly identify the chain length of our allylic species.

In the literature, the deactivation of the SZ during *n*-butane isomerization was reported as being a result of the formation of allylic species. Chen *et al.*[14] studied the *n*-butane isomerization (9 kPa *n*-C$_4$ in N_2) on SZ at 523 K; and performed a UV-vis study of the sample after hours of time on stream. This *ex situ* study showed an intense band near 292 nm only on the deactivated catalyst. They assigned this band to allylic species which then block the active sites. Spielbauer *et al.*[15] studied also this reaction (8.5 kPa *n*-C$_4$ in He) on SZ in a temperature range of 393 - 473 K. After 90 minutes contact with the feed at 473 K, the sample was placed in the optical cell for the UV-vis diffuse reflectance spectroscopy measurement. Following

_____

Chen's arguments, they suggested that the absorption band at 306 nm (corresponding to the 292 nm in Chen *et al.*[14]) may be assigned to allylic cations.

Additionally to the formation of the species absorbing at 295 nm, they observed also the formation of two further bands at 366 and 400 nm, which were characteristic of polyenylic cations[16,17] and aromatic compounds[16].

Kiricsi *et al.*[18] adsorbed propene on zeolites and observed a band at 295 nm in UV-vis spectra which intensity increased with TOS and simultaneously the position of the band shifted to higher wavelengths. Following this idea, Chiappetta *et al.*[19] studied the interaction of propene with zeolites and reported a band at 310 nm for allylic monoenic cations. Moreover, increasing the temperature to 470 K, Kiricsi[18] also observed the formation of new bands at 320, 380 and 430 nm. They were thus consistent with previous works[18,20] where bands in the range 290-330, 350-380 and 430-460 nm were assigned to mono-, di- and trienylic carbenium ions. By adsorbing propene at 373 - 473 K, butadiene at 298 K and methanol at $\geq$ 473 K on H-ZSM-5 zeolites, Demidov *et al.*[21] showed that alkenyl carbenium ions were formed. These alkenyl carbenium ions have characteristic bands in the UV-vis spectra, namely at 290-310 nm (allyl), 350-380 nm (dienyl) and 430 - 450 nm (trienyl carbenium ions). Pazé *et al.*[22] exposed H-Ferrierite zeolite to 1-butene in the temperature range of 295 - 393 K and obtained bands at 1580 cm^{-1} and at 310 nm, which were ascribed to a monoenic allyl carbocationic species. They based their assignment on literature data of ions on zeolite surfaces[23] and in solution[24,25] and the fact that the band at 310 nm partially disappeared upon exposure to NH$_3$, which was presumed to neutralize the charge of the allylic cations. It is clear, based on their investigations on zeolites, Pazè[22] assigned bands at 370 and 435 nm to dienic and trienic ions; and Förster[23] assigned the bands at 370-390 nm to dienic and at 430-480 nm to trienic allylic cations, and suggested that initially formed monoenic species transformed to more highly conjugated species. Sommer *et al.*[26] performed the reaction of isobutane as starting material on D$_2$SO$_4$ at room temperature, and on D$_2$O-exchanged solid acid H-USY zeolite at 373 K. The UV spectrum of the D$_2$SO$_4$ solution after 1 hour exposure to the feed showed a broad band at 290 nm that they ascribed to a substituted cyclopentenyl cation. The cycloalkenyl ions overcame an hydride shift, followed by ring enlargement via protonated cyclopropane; deprotonation, hydride or deuteride transfer, aromatization and alkylation reaction. After numerous recirculation of the feed on the catalyst they observed the formation of polyenyl and aromatic ions (334, 385 and 435 nm) by following the UV visible spectra.

_____

The aromatic compounds were generated from the cycloalkenyl ions by consecutive hydride shift, deprotonation, hydride or deuteride transfer, aromatization and alkylations reactions (Figure 5 - 13).

Monoenic allylic species	**290-310 nm**	
Dienic allylic species	**350-380 nm**	
Trienic allylic species	**430- 440nm**	$\left[R_2C \text{------} CH \text{------} \left(CH \text{------} CH \text{------} \right)_n CR_2 \right]^+$
Demidov *et al.*[21]		Spielbauer *et al.*[15]

Formation of aromatic compounds from cycloalkenyl ions, Sommer *et al.*[26]
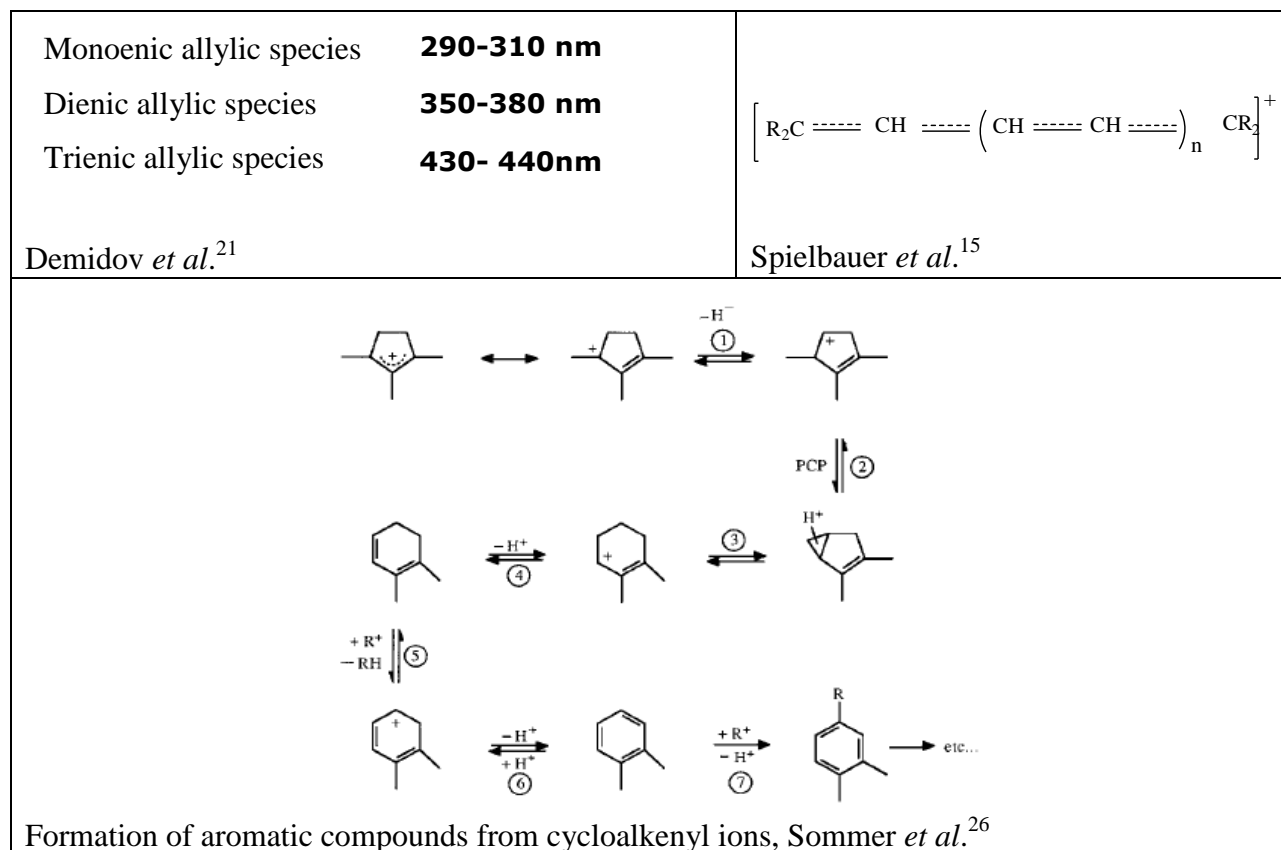
Figure 5 - 13: Scheme of the different compounds which were assigned to be the reason for SZ deactivation

The first *in situ* UV-vis-NIR experiment on this reaction was reported by Ahmad *et al.*[11]. They investigated the reaction of *n*-butane (5 kPa) at 358 and 378 K where they obtained a steady activity of 41 and 47 $\mu mol\ g^{-1}\ h^{-1}$ (isobutane formation). The spectra in the UV-vis range showed the formation of unsaturated surface deposits indicated by the band at 310 nm within the range of monoenic allylic cations. More highly conjugated allylic cations (bands at 370 and 430 nm) became evident during *n*-butane reaction at 523 K.

In our experiments, the band positions were too unspecific to exclude the presence of aromatic species on our samples; however, the positions matched the data reported for monoenic (295 nm), dienic (370 nm) and trienic (450 nm) allylic cations extremely well (Scheme showed in Figure 5 - 13). Propane and pentanes were detected by GC validating the bimolecular mechanism. The dehydrogenation of the longer hydrocarbons chain obtained

_____

through the bimolecular mechanism results in the formation of dienic- and trienic- allylic species. Table 5 - 1 gathers the different assignments reported in the literature.

Catalyst	Temp (K)	Hydrocarbon	Bands / nm	Assignments	References
Zeolite	298	Propene	310	allylic monoenic cation	Chiappetta[19]
NaZSM-5	298	Propene	295, 320	mono-	Kiricsi[18]
	470		380	di-	
			430	trienylic carbenium	
H, ZSM-5	373-473	Propene	290-310	allyl	Demidov[21]
	298	Butadiene	350-380	dienyl	
	> 473	Methanol	430-450	trienyl	
H-Ferrierite	295-393	1-butene	310	monoenic	Pazè[22]
			370	dienic	
			435	trienic allyl carbocationic	
SZ	523	9 kPa n-C$_4$ in N$_2$	292	Allylic species	Chen[14]
SZ	393-473	8.5 kPa n-C$_4$ in He	306	Allylic cation	Spielbauer[15]
			366	Polyenylic cations and aromatic compounds	
			400		
H-USY and D$_2$SO$_4$	373	isobutane	290	Cycloalkenyl – monoenic allylic cation	Sommer[26]
			334	Polyenyl and aromatic ions	
			385		
			435		
SZ	358-523	5 kPa n-C$_4$ in He	310	monoenic	Ahmad[11]
	523		370	dienic	
			430	trienic allylic cation	
SZ	373	5 kPa n-C$_4$ in N$_2$	295		This work
			370		
			450		

Table 5 - 1: Different assignments for the bands in the UV-vis range in the literature.

As it was impossible to distinguish clearly in our case the allylic species from the aromatic compounds, the species absorbing light over 320 nm will be named as polyunsaturated species. The extinction coefficients of allylic cations are in the order of magnitude of $10^4 l.mol^{-1}.cm^{-1}$[24]; and as with polyenes, the coefficients should increase with conjugation (up to a factor of 2 per additional double bond[13]). The spectra could thus be deceiving with respect to the amount of dienic and trienic allylic cations on the surface.

5.5 Effect of oxygen or propene addition to the feed

Summary of the observations described above and results from the experiments:

(i) The initial loss of activity is due to the formation of water during the first few hours on stream.

(ii) The band at 295 nm originated from monoenic allylic species[11,14,15,21,26] and did not play a role in the trend of the deactivation. Whether or not they are formed, the rate of isomerization was "quasi constant" within hours.

The monoenic allylic species absorbing at 295 nm are then only spectators in the deactivation process of the catalyst.

(iii) The second step of deactivation is faster when the polyunsaturated species[11,21,26] at 370 and 450 nm are detected with time on stream. They are good candidates to explain the loss of activity of SZ.

From the experiments in this work, it was also found that the reaction atmosphere and the feed composition plays an important role in the activity of the catalyst and in the spectra during reaction. The diverse species, monoenic and polyunsaturated species, detected in the UV-vis range of the spectra during reaction can (i) be present in the feed[33] and not detected by GC, or (ii) be the consequence of some impurities that the feed contains which react further with the catalyst.

Li *et al.*[6] reported that it was possible to enhance the catalytic activity by adding a small amount of O_2 to the feed. Lohitharn *et al.*[27] also increased the activity of the catalyst by adding some amount of alkene to the feed. We investigated also the role of these two compounds, O_2 and olefins to understand their impact not only on the catalytic activity, but also on the species formation on the catalyst surface.

5.5.1 Addition of oxygen to the feed

The following strategy was carried out to try to understand the effect of oxygen in the feed during *n*-butane isomerization (5 kPa from Air Liquide, diluted in He) at 373 K on SZ:

  1a. Activation in O_2, 30 min at 723 K

  1b. Cooling down in O_2 to 373 K followed by 40 min purge with He

  2. Reaction of 5 % *n*-C_4 in He (18 h)

  3. Reaction of *n*-butane in He in presence of 1.5 vol%. O_2 in the feed (15 h)

  4. Purge with He (4 h)

The number ascribed to each step of the experiment is used in Figure 5 - 14.

After the activation of the catalyst in O_2, the tubing and the cell containing the SZ was purged with helium till no oxygen was detected by TCD of the GC. The reaction could then start. The catalytic performance and the corresponding spectroscopic data from every step of this switching experiment are shown in Figure 5 - 14. During the *n*-butane isomerization on a fresh activated SZ (Phase 2), unsaturated species absorbing at 297, 370 and 450 nm (higher band intensity for the monoenic allylic species at 297 nm) developed with time on stream.
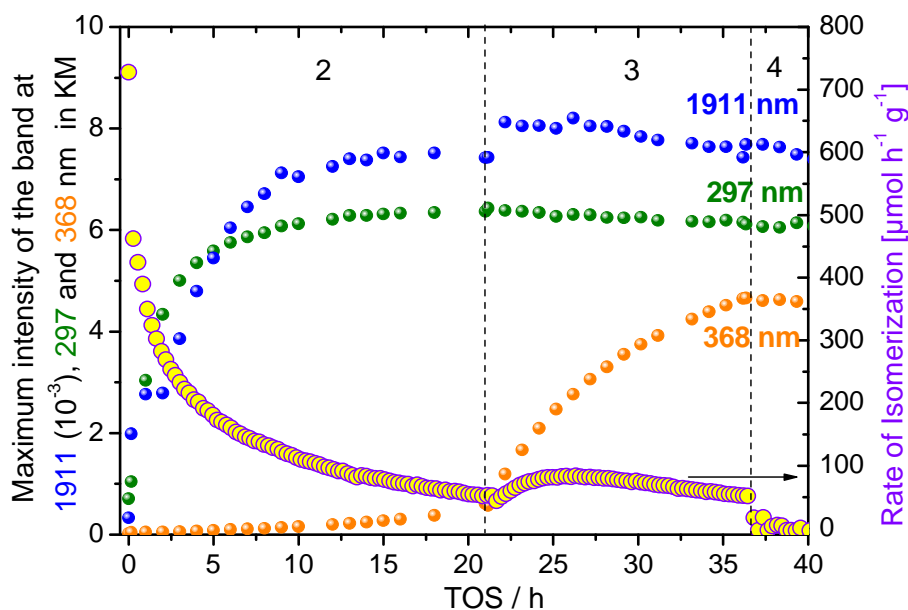
Figure 5 - 14: The catalytic performance is plotted versus time on stream. On the same plot, the evolution of the water (1911 nm) and hydrocarbon deposits are plotted. Conditions: Activation at 723 K for 30 minutes in O_2 followed by 40 minutes purge with He at 373 K. Conditions: (2) 5 kPa *n*-C_4 from Air Liquide in He at 373 K. (3) addition of 1.5 vol. % O_2 to the feed at 373 K. (4) Purge with flow of He. For all treatments, a total flow of 40 mL/min is used.

The increase of the water concentration on the surface of the catalyst slowed down after ten hours on stream. The amount of adsorbed water was relatively stable within the next ten hours. The deactivation of SZ occurred in parallel with the growth of the band characteristic of adsorbed water during the first 2-10 hours.

The addition of 1.5 vol. % O_2 to the feed (Phase 3) led to an enhancement of the activity over a time period of three hours with a presence of an induction period. The amount of water adsorbed on the surface increased as a direct consequence of the O_2 addition to the feed. In addition to the increase of the amount of water, the band ascribed to polyunsaturated species at 370 nm grew fast (the intensity was nearly ten times higher after eighteen hours on stream) while the intensity of the band characteristic of the monoenic species at 295 nm decreased

_____

slightly. After the reaction in the presence of oxygen in the feed, the system was purged with helium flow (Phase 4) for four hours until little *n*-butane was detected by chromatography. The *n*-butane peak area after the purge represented less than 0.02 % of the *n*-butane peak area at the end of the oxygen addition to the feed. Within this purge, only a permanent slight decrease in the amount of water and a negligible change in intensity of the band at 295 nm characteristic of the monoenic allylic species were observed. The amount of polyunsaturated species absorbing at 370 nm remained constant.

In this work, the addition of O_2 to the feed influenced the catalytic activity positively. The latter increased and reached a maximum followed by a slow deactivation of the SZ catalyst. These results were thus consistent with the literature[6] as shown in Table 5 - 2. Li *et al.*[6] explained the high activity after oxygen addition to the feed by the formation of very reactive sulfate groups and the reoxidization of sulfite groups. They assumed that the formation of reactive sulfate groups led to an enhanced production of olefins, which not only produced more carbenium type intermediates but also alkylated the existing carbenium ions, leading to the longer chain species on the surface. This once again brings us back to the double role of olefins in the *n*-butane isomerization. To prove and understand better the effect of olefins on the deactivation of SZ, we have performed additional experiments.

TOS	Rate ($\mu mol\ g^{-1}\ h^{-1}$) without O_2		Rate ($\mu mol\ g^{-1}\ h^{-1}$) with O_2	
	This work	Li *et al.*	This work	Li *et al.*
After 7 h	147	68	87	79
After 16 h	74	65	no data	57

Table 5 - 2: Comparison of rate of isomerization without or with the addition of 1.5 % O_2 to the feed. Reaction conditions: 40 mL/min of 5 kPa *n*-butane in helium at 373 K on SZ. Li *et al.*[6] used 20 mL/min of 5 kPa *n*-butane in He at 373 K to performe their experiment.

5.5.2 Addition of propene to the feed

In the literature[27] it was reported that the addition of alkene to the feed during the *n*-butane (5 kPa + 1% Ar in a balance of He) isomerization on SZ at 373 and 423 K had a positive influence on the induction period of the activity. In our case, we performed the following experiment.

    1a. Activation in O_2, 30 min at 723 K

    1b. Cooling down in O_2 to 373 K followed by 300 min purge with He

2. Reaction of 5 % n-C$_4$ in He (25 h) at 373 K

3. Purge with He (5 h)

4. Reaction of 5 % n-butane in He with 5000 ppm of propene in the feed (15 h)

The number ascribed to each step of the experiment is used also in Figure 5 - 15.

During the first reaction on the fresh catalyst (Phase 2), in the UV-vis spectra, all the species at 295, 370 and 450 nm were present after nineteen hours on stream (Figure 5 - 15). In the NIR region the band ascribed to water was growing for three hours on stream before the growth slowed down. Propene was then added to the feed (Phase 4) and the rate of isobutane formation was enhanced by a factor of 1.5 in comparison to the one after 20 hours on stream (end of Phase 2). Parallel to the enhancement of the rate of isomerization, the amount of polyunsaturated species at 370 and 450 nm increased drastically. The increase of the rate was followed by a fast loss of activity, resulting in a quasi non-active catalyst. The amount of monoenic allylic species also increased (one unit) when propene was added to the feed but was less pronounced than the increase of the amount of polyunsaturated species (4 units). The presence of highly conjugated species can be thus correlated to the decline of SZ activity. Moreover, adding propene to the feed led to the decline of the water concentration (band at 1911 nm) on the catalyst surface.

Phase 2	Phase 4
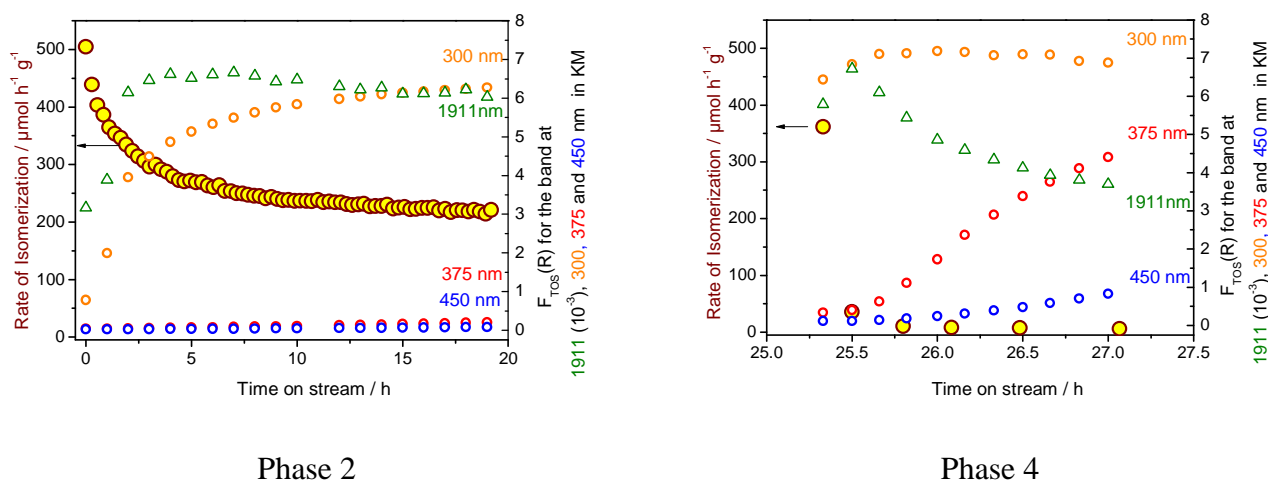
Figure 5 - 15: The catalytic performance is plotted versus time on stream. On the same plot, the evolution of the water (1911 nm) and hydrocarbon deposits are plotted. Conditions: Activation at 723 K for 30 minutes in O$_2$ followed by 300 minutes purge in He at 373 K. Conditions: (2) 5 kPa n-C$_4$ in He at 373 K using a pure n-C$_4$ cylinder from Air Liquide. (3) Purge under flow of He (4) addition of 5000 ppm of propene to the feed at 373 K. For all treatments, a total flow of 40 mL/min is used.

The positive effect of olefins on the isomerization reaction was reported in the literature[27]. However, increasing the olefins concentration, beyond a molar ratio of 0.009 (corresponding to a maximum rate of $576 \, \mu mol \, g^{-1} \, h^{-1}$) for propene, only accelerated catalyst deactivation

and decreased the isobutane selectivity. The same behaviour was observed in the experiments reported here. This acceleration of the deactivation was expected, as olefins also form coke precursors.

5.5.3 Post reaction treatment: role of oxygen in SZ regeneration

Deactivation of sulfated zirconia catalysts can be avoided by doping the catalyst with Pt and adding hydrogen to the feed. Alternatively, the catalyst can be regenerated. As carbonaceous deposits on the catalyst surface are supposed to be the main reason for its deactivation, their removal should restore the activity of the catalyst. Therefore, the reactivation takes place under an oxidizing atmosphere. And under a temperature program similar to the activation procedure. Li and Gonzalez[28] completely recovered the activity of sulfated zirconia used for n-butane isomerization at 473 K by treatment in air at 723 K. Jackson[29] reported a complete recovery of the activity of an alumina-supported vanadia catalyst after n-butane dehydrogenation. This regeneration was possible at room temperature under 2% O_2/Ar.
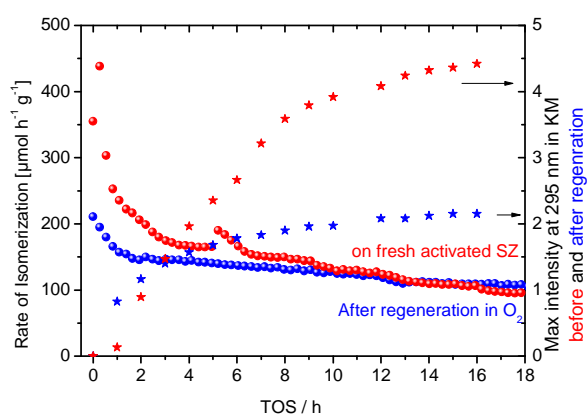
Figure 5 - 16: Catalytic activity before and after regeneration in oxidizing atmosphere (40 mL/min O_2) at 723 K with a temperature ramp of 5 K/min; n-butane isomerization (5 kPa in N_2) at 373 K using Westfalen gas mixture. Evolution of the species absorbing at 295 nm before and after regeneration (the maximum of the band intensity from spectra in Kubelka Munk function).

In this case, the catalyst was regenerated under 40 mL/min O_2 at 723 K for 30 min. The activity of the catalyst under 5 kPa n-butane in N_2 at 373 K, was mainly recovered (Figure 5 - 16), specifically in the steady state; monoenic allylic species were formed but in smaller amounts in comparison with the fresh catalyst.

In Figure 5 - 17, two graphs, one for the UV range (left) and the second one for the Vis range (right), show the evolution of the allylic species during regeneration of the deactivated catalyst. With increasing the temperature, the intensity of the bands at 295 nm decreased, whereas a constant increase of the intensity of the bands at 370 and 450 nm was observed. Similar to the experiment performed with O_2 in the feed (See section 5.3.6.1), the transformation of monoenic allylic species to polyunsaturated species was observed. Thus, in this case, the monoenic allylic species were transformed to the polyunsaturated species (isosbestic point in the spectra). Furthermore, at 333 K, H_2O and CO_2

were detected with the help of a mass spectrometer. At this temperature, combustion of the monoenic allylic species occurs and produces heat. This heat favours the formation of polymers.

In contrast to the other experiment, *n*-butane was not supplied and the species absorbing at 295 nm were not formed anymore. Moreover, at higher temperature and in presence of O_2, it was possible to remove the polyunsaturated species from the surface.
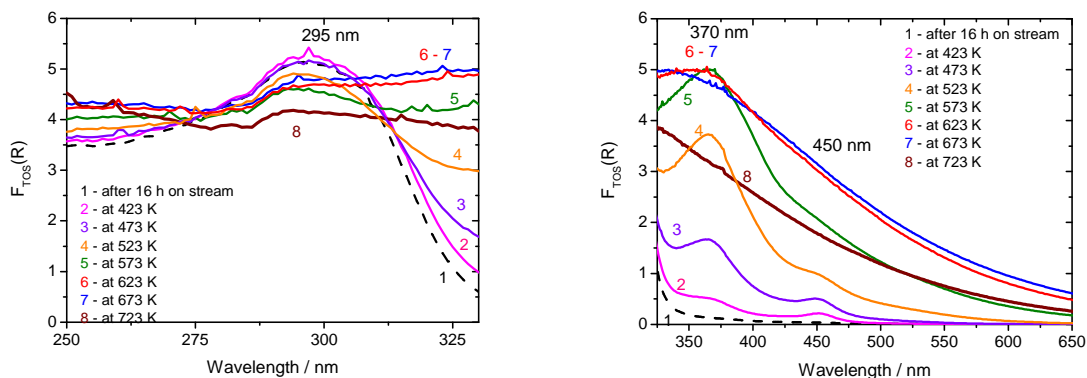
Figure 5 - 17: Regeneration in oxidizing atmosphere (40 mL/min O_2) at 723 K with a temperature ramp of 5 K/min; after *n*-butane isomerization (5 kPa in N_2) at 373 K using Westfalen gas mixture

At 623 K (spectrum in red in Figure 5 - 17), the band at position 295 nm did not exist anymore. As no allylic species were present on the surface of the catalyst, the transformation to polyunsaturated species cannot happen. Upon 623 K, the bands at 370 and 450 nm were also not detected in the spectra. The polyunsaturated species are also removed from the surface, and the initial catalytic activity was recovered. These results confirm the statement that polyunsaturated species on the surface of the catalyst cause the deactivation of SZ.

5.5.4 Similarities with platinum modified H-mordenite zeolite

Investigating zeolites, Kiricsi[18], Demidov[21] and Pazè[22], observed bands at 290-310 nm, 350-380 nm and 430 - 450 nm that they assigned to allyl, dienyl and trienyl carbenium ions respectively. The formation of these highly conjugated species should be avoided by promoting the zeolite with platinum and using hydrogen as diluent gas and not an inert one. Supported by this idea, Tzolova-Müller *et al.*[30], in the group, investigated platinum mordenite, Pt-MOR, under 15 kPa *n*-butane in H_2 or He at 623 K. The catalyst was reduced for 2 hours at 623 K before starting reaction at the same temperature.

When the hydrocarbon was diluted with H_2, after several hours of reaction, none of the three bands described earlier were formed on the Pt-MOR, and the rate of isomerization

(1900 $\mu mol\ g^{-1}\ h^{-1}$) was stable (Figure 5 - 18 left). Switching to He as diluent gas (no longer H_2) led to the formation of the unsaturated species (295, 400 and 458 nm) and concomitantly the rate of isomerization was rapidly decreased (70 $\mu mol\ g^{-1}\ h^{-1}$ or loss of 96%). Coming back to H_2 as diluent gas, only the band at 295 nm disappeared, whereas the two others at 400 and 458 nm remained (Figure 5 - 18 right). A slight increase in the rate of isomerization (240 $\mu mol\ g^{-1}\ h^{-1}$) was observed, but the initial rate was not recovered.
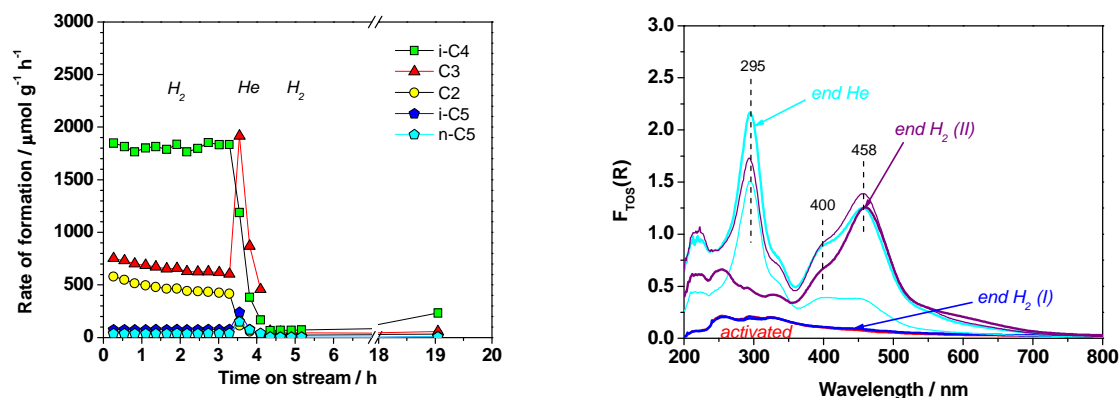
Figure 5 - 18: Catalytic activity (left) and evolution of the different species in the UV-vis range (right) by switching H_2 to He. Reaction conditions: Self-mixed (Messer Griesheim gas) 15 kPa of *n*-C$_4$ in H_2 or He at 623 K on Pt-Mordenite.

The absence of any of these three species under H_2 flow and their formation under helium implied that under reductive atmosphere and in presence of platinum, the formation of these species could be avoided. However, coming back to reductive atmosphere only the allylic species at 295 nm disappeared but not the species absorbing at higher wavelength; in the absence of the allylic species and the presence of polyunsaturated species, the activity was not recovered.

5.6 The roles of water and unsaturated species in the isomerization mechanism

5.6.1 Water

The present work has shown that the initial drastic loss in the catalytic activity corresponds to the formation of water. Water was formed only during the first few hours (2-4) on stream. After longer times on stream, the amount of water detected remained constant, meaning that at this stage, water was not a product of reaction anymore. The role of water is debated, as water (i) is a vital component in the initiation part of the *n*-butane isomerization, but (ii) can

act as a poison when it is in excess. Several reports were published to explain the role of water in alkane isomerization on SZ at low temperature. Wen[31], Dumesic[32,33] and Song[34,35] reported the positive effect of water on the initiation part of the reaction. The three groups agree that a small amount of water on non-promoted SZ[32,33,34] and Pt-doped SZ[31] in the reaction system enhances the catalytic activity of the catalysts. Song[34] explained that an active catalyst should contain a ratio of Brønsted to Lewis acid sites, 2:1 respectively. This ratio could be achieved in the presence of certain amount of water. Dumesic *et al.*[32,33] showed the importance of the water content by varying the temperature of calcination; and by adding successively a certain amount of water (74 $\mu mol\ g^{-1}$ H_2O) until a maximum catalytic activity (5256 $\mu mol\ g^{-1}h^{-1}$) was reached during *n*-butane isomerization (10 kPa at 423 K). Wen *et al.*[31] explained the enhancement of the catalytic activity of Pt-doped SZ in the hydroisomerization and hydrocracking of *n*-heptane by the transformation of Lewis sites into Brønsted sites. Besides being an important component for an active catalyst in the *n*-butane isomerization on SZ at low temperature, water is also a product of alkane activation via ODH[4-9,34]. Li *et al*[6]. demonstrated that the gradual formation of water, on SZ, was primordial for building up the active sites, which corresponded to the period of increasing activity in the *n*-butane isomerization. The detection of water confirmed the oxidative dehydrogenation route[5,6,9] proposed as the initiation step of *n*-butane isomerization. However, when the steady state of the isomerization reaction had been reached, the rate of accumulation of water was significantly slower[6]. This phenomenon could be explained by the strong perturbation of sulfate/SO_3 groups by the water formed[36]. The activity of the catalyst could be recovered by SO_3 sulfation of crystalline zirconia materials. Nevertheless, water can also act as a poison[6,10,12,32,33,34,37] because the water adsorbed over the catalyst blocks the access to the active Lewis sites[9]. For this reason, an excessive catalyst hydration leads to low catalytic activity[32,33,35].

A general statement cannot be made about the exact hydration state which gives the maximum initial activity of the catalyst. Song and Kydd found that small amounts of water had a positive effect, whereas larger amounts had a negative effect on the performance of SZ[35]; the best performance was reported for 200 $\mu mol\ g^{-1}$ of water[34]. Gonzalez *et al.*[32] claimed that a water concentration of 75 $\mu mol\ g^{-1}$ was optimal while Klose *et al.*[8] found that small variations of the water content by 2.5-5%, clearly visible in the IR region, did not affect the catalytic activity of the manganese promoted sulfated zirconia (2 wt% Mn loading).

_____

5.6.1 Unsaturated species

In sulfated zirconia which contains few (5 %)[38] redox active sites, ($S_2O_7^{2-}$) provides the acidity to catalyze the *n*-butane isomerization at low temperatures. This reaction is initiated by the oxidative dehydrogenation of *n*-butane to butene, water and SO_2[38,39]. The formed butene is further protonated by the Brønsted acid site of sulfated zirconia to form the carbenium ions[34]. As reported by Li *et al.*[39] the term carbenium ion is frequently used to describe the stable surface intermediates; but they emphasized that alkoxy groups and not carbenium ions are the stable species in the ground state. The skeletal rearrangement can proceed through intramolecular or bimolecular mechanism. The bimolecular mechanism takes place via the alkylation of the secondary butyl carbenium ion with another olefin. It results in a secondary or tertiary octylcarbenium ion, which is isomerized and cracked, forming a smaller olefin. The obtained olefin is re-adsorbed on a Brønsted acid site and finally desorbs via hydride transfer from *n*-butane. In this scenario, olefin – here butene – plays a major role in the formation of alkoxy groups, intermediate in the further skeletal isomerization.

However, the alkoxy groups can also react further to form side products blocking the access to the active sites of SZ; and leads to the deactivation of the catalyst. The experiment where propene was added to the feed led not only – after an increase of the rate of isomerization – to the drastic loss of activity but also to the formation of more polyunsaturated on the catalyst surface. The propene addition to the feed leads to further reactions in competition with the bimolecular pathway. The higher concentration of olefin in the reaction chamber induced a various possible reactions, including oligomerization. The oligomers detected in the UV-vis range of the spectra at 370 and 450 nm blocked the access to the active sites deactivating sulfated zirconia. The same deactivation process can take place when the feed contains olefin impurities, even not detected by the methods used in the course of this thesis. The presence of olefins in some of the gas mixtures, used to perform the experiments, unfortunately cannot be discriminated and can explain why sulfated zirconia deactivates faster when absorption bands of polyunsaturated species were detected in the UV-vis range of the spectra.

A similar correlation between the deactivation and the formation of highly conjugated species was observed when *n*-butane isomerisation was performed in presence of O_2. In this case, the polyunsaturated species were the result of additional heat produced by the combustion of hydrocarbon deposits.

The regeneration procedure of a deactivated sulfated zirconia corroborates our interpretation. With increasing temperature during the regeneration in O_2, polyunsaturated species were formed while the amount of monoenic species decreased (isosbestic point in the spectra).

Moreover, at higher regeneration temperature (above 623 K) it was possible to remove from the catalyst surface both the monoenic allylic and polyunsaturated species.

Among the three types of unsaturated species detected on the catalyst surface during reaction, only a correlation between the polyunsaturated species and the loss of activity was proven. No evidence correlating the catalyst deactivation and the formation of the monoenic species at 295 nm was found. The SZ performance was identical in presence or absence of these allylic species. The comparison with the *n*-butane isomerization on Pt-MOR study validates that the monoenic allylic species are only spectators in SZ deactivation while the polyunsaturated species play a role in this deactivation.

5.7 Effect of the temperature

5.7.1 NIR region and activity of SZ
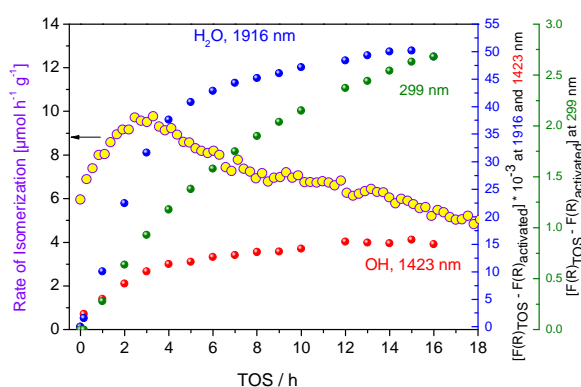
Figure 5 - 19: Temporal evolution of the species at bands position 299, 1423 and 1916 nm. Reaction conditions: 5 kPa *n*-C$_4$ in N$_2$ at 323 K on SZ. Total flow of 40 mL/min with gas mixture from Linde.

At lower reaction temperature (323 K), with the same activation procedure and the same feed, the growth of the bands indicative of water and OH groups at 323 K followed the same scheme as at 373 K (Figure 5 - 19).

The formation of the species at 299 nm and the accumulation of the adsorbates – water – were observed with a lower rate of isomerization at 323 K (6 against 123 $\mu mol \; g^{-1} \; h^{-1}$ at 373 K and after 16 hours on stream) as shown in Table 5 - 3.

T [K]	Rate [μmol g^{-1} h^{-1}]	[F(R)$_{TOS}$- F(R)$_{activated}$] at 295 nm	[F(R)$_{TOS}$ - F(R)$_{activated}$] * 10^{-3}
323-1	8	2	29 (at 1918 nm)
323-2	6	2.5	49 (at 1916 nm)
373-1	87	3.8	20 (at 1914 nm)
373-2	123	2.5	11 (at 1912 nm)

Table 5 - 3: Rate of isomerization and maximum of the intensity of the bands at 295 nm and 1915 nm after 16 hours on stream. Reaction conditions: 5 kPa *n*-C$_4$ in N$_2$ at 323 and 373 K on SZ with gas mixture from Linde.

The intensity of adsorbed water at sixteen hours on stream was normalized to one (323-1 or 373-1 stands for the first experiment and 323-2 or 373-2 and 323-3 or 373-3 stand for the reproducibility). The trend in the water formation at each reaction temperature could thus be evaluated as shown in Figure 5 - 20.
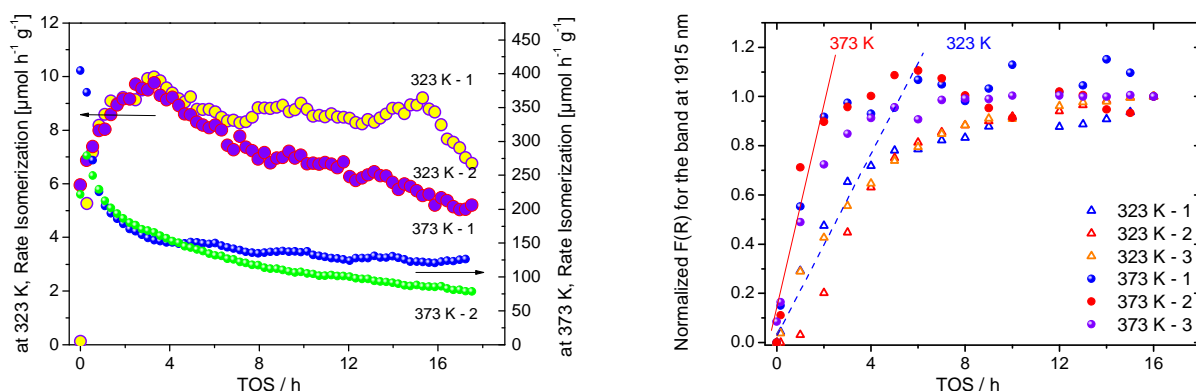
Figure 5 - 20: Comparison of the catalytic performance at 323 K and 373 K of two experiments on SZ for each reaction temperature with 5 kPa *n*-C$_4$ in N$_2$ gas mixture from Linde. Normalization to 1 of the maximum band intensity of adsorbed water after 16 h on stream vs. TOS for three experiments at each temperature (right); included the four experiments showed on the left side.

At 373 K, the curve representing the water adsorbed during the reaction had a steeper slope during the induction period than that observed for the reactions performed at 323 K; which indicated that the formation of water was faster at this reaction temperature. As explained in Section 4.2.1.1, water started desorbing at 473 K, implying that whatever the amount of water adsorbed on the catalyst surface during the *n*-butane isomerization at 323 or 373 K remained there. At these two reaction temperatures, water adsorbed on the catalyst was most probably a product of reaction; but could also be present in the feed and adsorbed on the surface of the catalyst, which is highly hydrophilic.

_____

However, the normalization procedure of the spectra was relevant, as the evaluation of water formed during the reaction was not affected. The ratio OH/H$_2$O (evolution of H$_2$O and OH groups during the activation is shown in Appendix, Fig 3 and Fig 4, respectively) calculated for two experiments, 373 K - 1 and 323 K – 2 was different for the fresh SZ and the one activated in O$_2$; as shown in Table 5 - 4. This difference in the ratio value validated also that water was removed from the SZ surface during the activation.

OH / H$_2$O	Fresh SZ	Activated SZ
373 K - 1	0.3	2.3
323 K - 2	0.2	35.1

Table 5 - 4: OH/H$_2$O ratio for *n*-butane (5 KPa) isomerization on SZ at 323 and 373 K with gas mixture from Linde. Activation in O$_2$ at 723 K for 30 minutes.

5.7.2 Is water a product of reaction or present in the feed?

SZ was activated in oxygen at 723 K and most water should be removed after such a treatment (See Section 4.2). Indeed, the spectrum at 723 K in Appendix, Fig 3 did not show the water band. However, upon cooling to the reaction temperature, water was adsorbed on the surface of the catalyst.

It cannot be excluded that a small amount of water could be adsorbed from the gas phase on the hydrophilic catalyst.
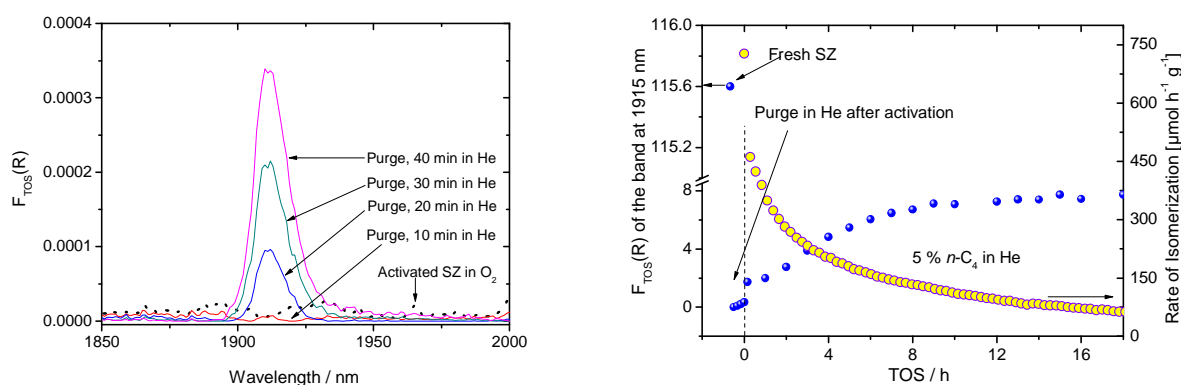
Figure 5 - 21: Evolution of the adsorbed water on SZ at 373 K during 40 min purge in He, after activation for 30 min at 723 K and cooling to 373 K in O$_2$ (left). The amount of water initially present in the fresh SZ, adsorbed on the activated SZ during the purge at 373 K in He and the evolution of water formation vs. time on stream during the *n*-butane isomerization, and the corresponding catalytic performance are showed in the right plot.

_____

It should moreover be mentioned that, for the same experiment presented in Figure 5 - 21, the TCD of the GC was used during the bypass measurement and reaction; and no water was detected. Nevertheless, the intensity of water re-adsorbed from the gas phase was far lower than the intensity of water adsorbed on the catalyst surface after sixteen hours on stream. The intensity of water initially adsorbed on the fresh catalyst surface without any oxidizing treatment was not reached. Water could also be a product of reaction via oxidative dehydrogenation, the suspected initiation step of the mechanism, and could come in parallel from the gas phase; however as shown in Figure 5 - 21, the gas phase contribution could be neglected.

5.7.3 UV-vis region and activity of SZ

Working at lower temperature (323 instead of 373 K), with in this case the industrial Linde gas mixture, led to some changes in the catalytic performance but also on the formation of allylic species at position 295 nm, on the catalyst surface. Low temperatures are desired for *n*-butane isomerization, as the equilibrium is shifted towards the branched alkanes. However, a too low temperature of reaction reduced the rate of isomerization. Indeed, when the reaction took place at 323 K, the maximum rate was almost 40 times lower (12 $\mu mol\ g^{-1}\ h^{-1}$ against 408 $\mu mol\ g^{-1}\ h^{-1}$ at 323 and 373 K respectively) and the steady state rate was almost 20 times lower (6 $\mu mol\ g^{-1}\ h^{-1}$ against 124 $\mu mol\ g^{-1}\ h^{-1}$ after sixteen hours on stream at 323 and 373 K, respectively) than for the reaction (5 kPa *n*-butane in N_2) at 373 K (Figure 5 - 1). At a reaction temperature of 323 K, a maximum value of the intensity was obtained (1) after sixteen hours on stream, whereas at 373 K, the maximum value was around 2, i.e. twice as many allylic species were formed on the surface of the SZ at higher temperature. More values of the maximum in intensity after sixteen hours on stream could be given from experiments carried out several times, or using different gas mixtures (Table 5 - 5), or performed at different reaction temperature (Table 5 - 6).

At 373 K	Gas-mixtures from different gas providers		
	Linde	Westfalen	Air Liquide
Rate ($\mu mol\ g^{-1}\ h^{-1}$)	124	107	74
Maximum intensity at 295 nm after 16 h on stream	2	5	5.8

Table 5 - 5: Evolution of the maximum intensity of the band at 295 nm formed during *n*-butane isomerization on SZ with different gas mixtures of 5 kPa *n*-butane in nitrogen

At 323 K	Reaction 1	Reaction 2	Reaction 3
Rate($\mu mol\ g^{-1}\ h^{-1}$)	6	8	4
Maximum intensity at 295 nm after 16 h on stream	1	1.9	2.4

Table 5 - 6: Evolution of the maximum intensity of the band at 295 nm formed on SZ with gas mixture of 5 kPa *n*-butane in nitrogen (Linde). Reaction 1 to 3 represents different experiments carried out at different time under the same conditions

The data in Table 5 - 5 and Table 5 - 6 prove that the maximum intensity of the band at 295 nm is not directly correlated to the rate of isomerization, but to the gas-mixture composition. This observation could thus support the argument that the monoenic allylic species, at 295 nm, are just spectator in the deactivation of the SZ. The formation of these species is believed to be dependent on the gas mixture composition used for the experiment of isomerization.

We have seen that the formation of water varied with the reaction temperature, while the formation of unsaturated species was due to the gas mixture. The role of the activation and reaction atmosphere on the catalyst activity will be now discussed.

5.8 Influence of activation and reaction atmosphere on SZ activity

5.8.1 Effect of reaction atmosphere

SZ was activated following the usual procedure. The *n*-butane isomerization was carried out at 373 K under flow of hydrogen (5 kPa *n*-butane diluted in hydrogen to reach atmospheric pressure). The catalytic performance was affected by the reaction atmosphere as the maximum rate was 16 $\mu mol\ g^{-1}\ h^{-1}$ vs. 200 $\mu mol\ g^{-1}\ h^{-1}$ obtained for the same reaction but with nitrogen as diluent and the pure *n*-butane provided from Messer Griesheim. However, the deactivation of the catalyst was similar after sixteen hours on stream, a loss of about 60 % of the maximum rate was observed in both cases (10 vs. 130 $\mu mol\ g^{-1}\ h^{-1}$) as shown in Figure 5 - 22.
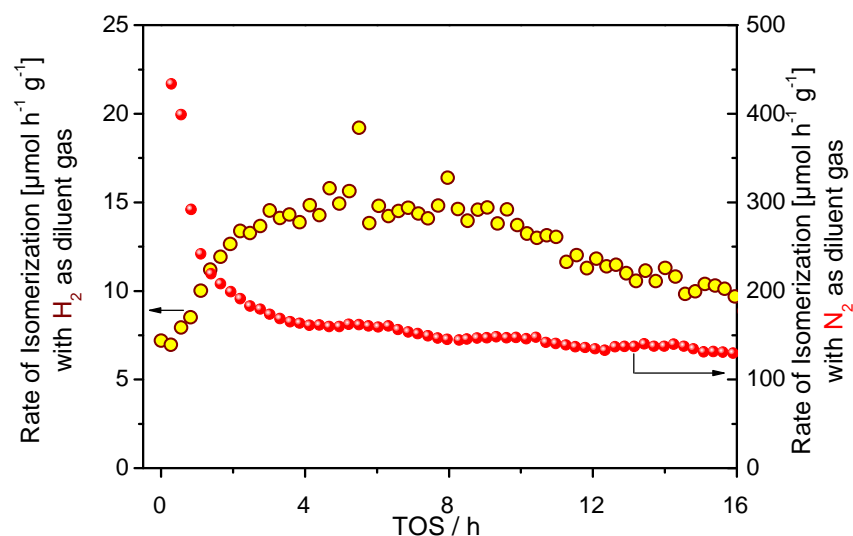
Figure 5 - 22: Comparison of catalytic performance versus time on stream. Activation: 30 min in O$_2$ at 723 K and a purge with N$_2$. Reaction: 5 kPa *n*-C$_4$ in H$_2$ at 373 K (yellow) and 5 kPa *n*-C$_4$ in N$_2$ at 373 K (red). Total flow of 40 mL/min.

Besides the low activity of the catalyst, the formation of unsaturated species was not detected and the band of water grew for the first 2 hours before the growth slowed down and reached a stable level (not shown here). The growth of the water band the first two hours implies that ODH occurred as initiation step; but the reductive atmosphere of the reaction did not lead to a performance comparable with the reaction in inert atmosphere. The unsaturated species were not detected in the UV-vis region and this could be explained (i) by a gas-mixture which would be cleaner that the others although all of them fulfil the same specifications, or (ii) by the presence of hydrogen in the feed. Hydrogen has the possibility to hydrogenate unsaturated species which could be deposited on the surface of the catalyst blocking the active sites.

5.8.2 Effect of activation atmosphere

Figure 5 - 23 shows that activating SZ at 523 K in H$_2$ for 120 minutes led to more water adsorbed on the SZ surface, compared to the amount observed on SZ activated at 723 K for thirty minutes in O$_2$.
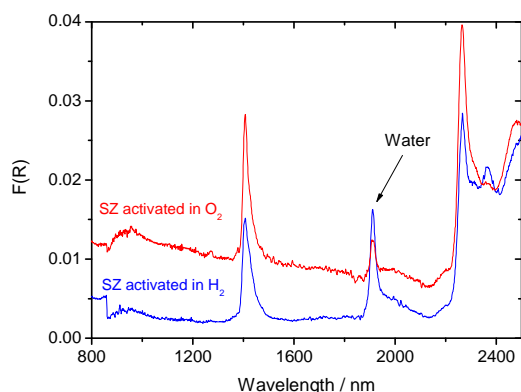
Figure 5 - 23: Comparison between SZ activated for 30 min at 723 K in O_2 (red) and SZ activated for 120 min at 523 K in H_2 (blue). The spectra represent the activated SZ at 373 K.

Figure 5 - 24 shows that water was not formed. The slight increase of the band intensity could be explained by the background shift that occurred while the detector changed from the NIR to the UV-vis range. The absence of water formed during the reaction could be explained by (i) the lower activation temperature than for the activation in O_2, which results in a higher level of SZ hydration so that SZ is not active (ii) the lack of oxygen on the SZ surface so that no ODH can happen. Moreover, the catalytic activity was relatively low considering a maximum rate of isomerization of 12 $\mu mol\ g^{-1}\ h^{-1}$.
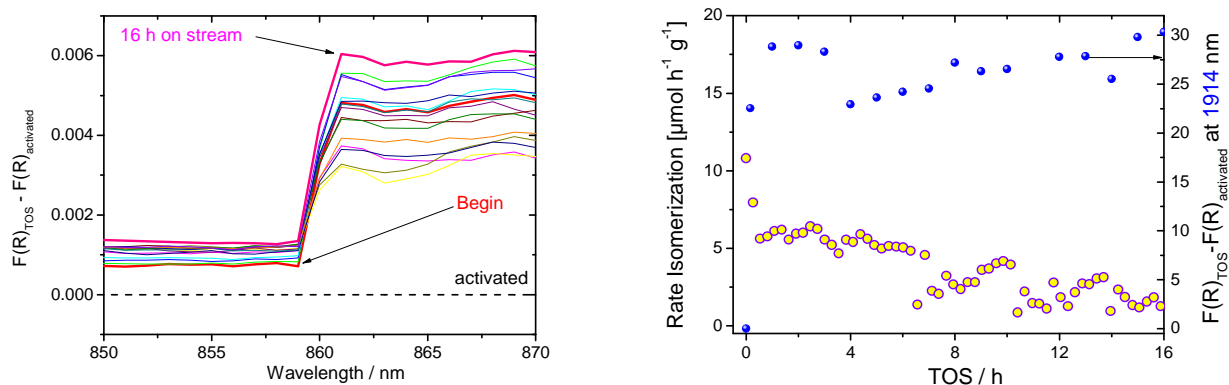
Figure 5 - 24: The evolution of adsorbed water on the surface is plotted versus time on stream. Behaviour at the detector change (left) and activity with evolution of adsorbed water versus time on stream (right). Conditions: 5 kPa n-C_4 in H_2 at 373 K after activation in H_2. Total flow of 40 mL/min. Additional plot in Appendix, Fig 5.

This low activity could be clarified by the activation procedure carried out for this experiment. The reductive activation atmosphere and the temperature applied to this activation (523 K) were not appropriate to remove the excess of water adsorbed on the surface of the catalyst. As reported previously by Wen[31], Dumesic[32,33] and Song[34,35], the amount of water initially adsorbed on the catalyst is of great importance for its activity. Moreover, as described in 5.3.5.1, the reductive atmosphere applied to the reaction of isomerization was not favourable for an active catalyst. Comparing the experiments described in 5.3.5.1 and 5.3.5.2,

_____

it was proved that the activation conditions of the catalyst play a major role in the initiation step of the mechanism, *i.e.* ODH during which H_2O is formed. Activation in O_2 at 723 K led to the growth of the water band during the reaction i.e. the amount of water adsorbed on the catalyst surface although H_2 was used as diluent gas for the feed.

5.9 Conclusions for SZ

To have an active SZ catalyst in the *n*-butane isomerization at low temperature, it is important to have the appropriate balance of the amount of water adsorbed on the surface of the catalyst and of the concentration of olefin in the gas phase.

This Chapter has shown that when this appropriate balance is not respected, the compounds which are participating in the feasibility of the oxidative dehydrogenation of butane on sulfated zirconia can also be responsible for the deactivation of the catalyst.

Water was produced by ODH during the initiation phase of the mechanism and was accumulated on the SZ surface. The higher concentration of water on the surface led to the initial drastic loss in activity of the catalyst.

Once butane is converted to butane via ODH on the labile sulphate species, it forms *sec*-butyl carbenium ion / alkoxy group in the presence of Brønsted acid sites. This carbenium ion / alkoxy group which is necessary for the skeletal isomerization step is demonstrated to act additionally as poison at higher concentration.

Mono allylic and polyunsaturated species were observed on SZ during *n*-butane isomerization. However, the role of these different species could be distinguished. It has been shown that the monoenic allylic species (band at 295 nm) are not responsible for SZ deactivation as it was reported in the literature; they are spectators in the deactivation of SZ. The more highly conjugated allylic species (bands at 370 and 450 nm) most likely play the role of a poison for the catalytic activity. Finally, the regeneration of the deactivated catalyst was possible by removing these surface deposits under O_2 and high temperature.

[1] C.-Y. Hsu, C.R. Heimbuch, C.T. Armes and B.C. Gates, *J. Chem. Soc. Chem. Commun*. 1992, 1645

[2] M. Hino, S. Kobayashi and K. Arata, *J. Am. Chem. Soc*. 101, 1979, 6439

[3] M. Hino and K. Arata, *J. Chem. Soc. Chem. Commun*. 1980, 851

[4] C.R. Vera, C.L. Pieck, K. Shimizu, C.A. Querini, J.M. Parera, *J. Catal*. 187, 1999, 39-49

[5] Z. Hong, K.B. Fogash, R.M. Watwe, B. Kim, B.I. Masqueda-Jiménez, M.A. Natal-Santiago, J.M. Hill and J. A. Dumesic, *J. Catal*. 178, 1998, 489-498

[6] X. Li, K. Nagaoka, L. J. Simon, R. Olindo, J. A. Lercher, A. Hofmann, J. Sauer, *J. Am. Chem. Soc*. 127,2005, 16159-16166

[7] B.S. Klose, F.C. Jentoft, R. Schlögl, *J. Catal*. 233, 2005, 68-80

[8] B.S. Klose, F.C. Jentoft, P. Joshi, A. Trunschke, R. Schlögl, I. R. Subbotina, V.B. Kazansky, *Catal. Today* 116, 2006, 121-131

[9] B. Klose, F.C. Jentoft, R. Schlögl, I.R. Subbotina, V.B. Kazansky, *Langmuir* 21 (23), 2005, 10564-72

[10] R.A. Comelli, C.R. Vera, J.M. Parera, *J. Catal*. 151, 1995, 96-101

[11] R. Ahmad, J. Melsheimer, F.C. Jentoft, R. Schlögl, *J. Catal*. 2003, 218 (2), 365-374

[12] C. Morterra, G. Cerrato, F. Pinna, M. Signoretto and G. Strukul, *J. Catal*. 149, 1994, 181-188

[13] M. Hesse, H. Meier, B. Zeeh, „Spektroskopische Methoden in der Organischen Chemie", Georg Thieme Verlag, Stuttgart, 1984

[14] F.R. Chen, G. Coudurier, J-F. Joly, J.C. Vedrine, *J. Catal*., 143 1993, 616-626

[15] D. Spielbauer, G. A. H. Mekhemer, E. Bosch and H. Knözinger, Catal. Lett., 1996, 36, 59-68

[16] H.G. Karge, M. Laniecki, M. Ziolek, G. Onyestyak, A. Kiss, P. Kleinschmitt and M. Siray, in: *Zeolites: Facts, Figures*, Future; eds. P.A. Jacobs and R. van Santen (Elsevier, Amsterdam, 1989) p.1327

[17] T.S. Sorensen, *J. Am. Chem. Soc*. 87, 1965, 5075

[18] I. Kiricsi, G. Tasi, H. Förster, P. Fejes, *J. Mol. Structure*, 218, 1990, 369-374

[19] R. Chiappetta, S. Bodoardo, F. Geobaldo, F. Fajula, E. Garrone, *Res. Chem. Intermed*. 25, 1999, 111

[20] I. Kiricsi and H. Förster, *J. Chem. Soc. Faraday Trans*. I , 84, 1988, 491- 499

[21] A.V. Demidov, A. A. Davydov, *Materials Chem. Phys*. 39, 1994, 13-20

[22] C. Pazè, B. Sazak, A. Zecchina and J. Dwyer, *J. Phys. Chem. B*, 103, 1999, 9978-9986

[23] H. Förster, J. Seebode, P. Fejes, I. Kiricsi, *J. Chem. Soc., Faraday Trans*. I, 83, 1987, 1109-1117

[24] N.C. Deno, J. Bollinger, N. Friedman, K. Hafer, J.D. Hodge, J.J. Houser, *J. Am. Chem. Soc*. 87, 1963, 2998-2950

[25] G.A. Olah, C.U. Pittman Jr, R. Waack, M. Doran, *J. Am. Chem. Soc*. 88, 1966, 1488-1495

[26] J. Sommer, A. Sassi, M. Hachoumy, R. Jost, A. Karlsson and P. Ahlberg, *J.Catal*. 171, 1997, 391-397

[27] N. Lohitharn, J.G. Goodwin Jr, E. Lotero, *J. Catal*. 234, 2005, 199-205

[28] B. Li and R. D. Gonzalez, Appl. Catal. A : General 165, 1997, 291-295

[29] S.D. Jackson, S. Rugmini, *J. Catal*. 251, 2007, 59-68

[30] G. Tzolova-Müller, F.C. Jentoft, J.I. Villegas, Mürzin

[31] M.Y. Wen, I. Wender, J. W. Tierney, *Energy Fuels*, 1990, 4, 372

[32] M.R. Gonzalez, J.M. Kobe, K.B. Fogash, J.A. Dumesic, *J. Catal*. 160,1996, 290-298

[33] J.M. Kobe, M.R. Gonzalez, K.B. Fogash, J.A. Dumesic, *J. Catal*. 164, 1996, 459-466

[34] S. X. Song, R.A. Kydd, J. Chem. Soc., *Faraday Trans*., 94, 1998, 9, 1333-1338

[35] S.X. Song, R.A. Kydd, *Catal. Lett*. 51, 1998, 95

[36] X. Li, K. Nagaoka, R. Olindo, J.A. Lercher, *J. Catal*. 238, 2005, 39-45

[37] R.A. Keogh, R. Srinivasan and B. H. Davis, J. *Catal*., 151, 1995, 292-299

[38] R.W. Lloyd, *PhD dissertation*, Freie Universität Berlin, 2008

[39] X. Li, K. Nagaoka, L. J. Simon, R. Olindo, J.A. Lercher, *J. Catal*. 232, 2005, 456-466

_____

6.1 Manganese promoted-sulfated zirconia as catalyst

Several groups studied the impact of adding main group metals such as Al[1,2] and Ga[3], or transition metals like Pt[4,5] to the SZ. First row transition metals[6,8] in cationic form, in particular, act as promoters in skeletal isomerization reactions. Among them, iron and manganese were most intensely studied, as they were reported to enhance the activity[7] (1-2 order of magnitudes) and the presence of Fe or Mn oxides increased both the number and the strength of SZ surface acid sites[7]. In the present work, manganese-promoted sulfated zirconia was studied to (i) confirm the enhancement of the activity, (ii) compare the deactivation procedure of the manganese promoted sulfated zirconia and (iii) to compare the surface changes using UV-vis NIR spectra with those obtained with the non-promoted SZ (See Chapter 4).

6.2 Experimental conditions

6.2.1. Activation

MnSZ was activated for 30 minutes at 723 K in 40 mL/min O_2 and cooled to reaction temperature, 323 or 373 K, in O_2 flow or He. More details are given in the previous chapter (see Section 4).

6.2.2. Reaction conditions

Similar conditions like for SZ were applied to MnSZ (Section 5.2.2). The reaction gas consisting of 5 kPa *n*-butane in N_2 was obtained by using industrial gas mixtures or by using the self-mixed one.

6.3 Results

6.3.1. Manganese loading of 0.5 wt%

6.3.1.1 Catalytic activities overview

During the *n*-butane isomerization at 323 K on manganese-promoted SZ, an increase in the catalytic activity, as described elswhere[8,9], was observed. The MnSZ was active with a maximum rate of isomerization at 323 K of 160 $\mu mol\ g^{-1}\ h^{-1}$, independent of the gas mixture used, vs. 12 $\mu mol\ g^{-1}\ h^{-1}$ for the non-promoted SZ (Figure 6 - 1). A drastic loss in the activity followed this maximum in rate and after sixteen hours on stream, the Mn-promoted SZ

exhibited a rate of isomerization of 40 $\mu mol\ g^{-1}\ h^{-1}$ vs. 6 $\mu mol\ g^{-1}\ h^{-1}$ for the non-promoted catalyst. Non-promoted SZ had a lower rate of isomerization in comparison to MnSZ. Nevertheless; after sixteen hours of reaction, the loss in activity for MnSZ was more pronounced than for the SZ (75 % and 50 % for MnSZ and SZ respectively).
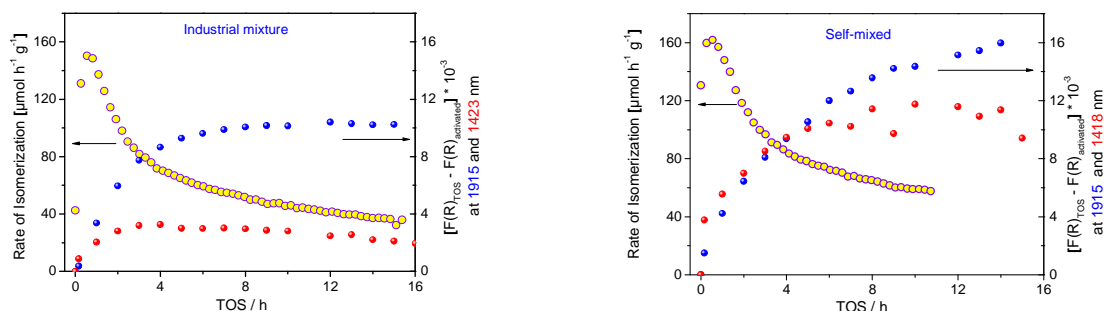
Figure 6 - 1: Catalytic data versus time on stream. In the same plot evolution of adsorbed water (1915 nm) and OH group (~1420 nm) by using industrial mixture (Left), or self-mixed feed (Right). Conditions: Activation at 723 K in O_2 for 30 minutes. Reaction: 5 kPa n-C_4 in N_2 at 323 K on MnSZ (0.5 wt% Mn). Total flow of 40 mL/min.

6.3.1.2 Spectroscopic data

The spectroscopic data were different to those obtained with non-promoted SZ. In the UV-vis range, two bands characteristic (Figure 6 - 2) of charge transfer (300 nm) and d-d transition at 580 nm related to manganese were observed.
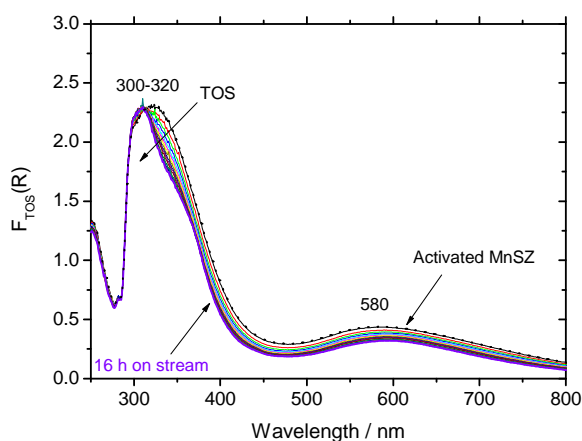
Figure 6 - 2: Evolution with time on stream of the charge transfer and d-d transitions. Conditions: Activation in 40 mL/min O_2 and reaction in 5 kPa n-C_4 in N_2 from gas provider Linde at 323 K on MnSZ (0.5 wt% Mn) with a total flow of 40 mL/min for 16 h of reaction.

With this loading of manganese, the d-d transition at 680 nm was not observed implying thus that Mn cations were at the highest oxidation state Mn^{4+}.

These two phenomena were intensively described in the Section 4.2.2. Similar to SZ, formation of adsorbates on the surface of the catalyst, namely water, was also observed (Figure 6 - 1). With the industrial gas mixtures, the increase in water concentration was observed during the first few (six) hours and then slowed down and stayed at a constant level for several hours. With the self-

mixed feed the amount of water formed was somehow constant, implying that water (i) was constantly produced by ODH within sixteen hours on stream, (ii) was re-adsorbed from the gas phase or (iii) manganese was reducing since the beginning of the reaction (in orange in Figure 6 - 3). The second assumption was less likely as all experiments were performed with similar conditions.
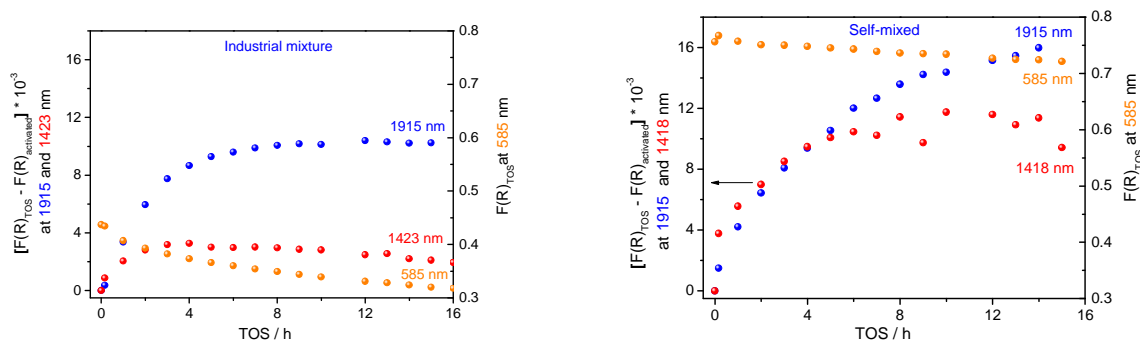
Figure 6 - 3: Complete Figure 6 - 1. The evolution of the concentration of Mn^{4+} cations during the *n*-butane isomerization on MnSZ (0.5 wt% Mn) at 323 K was shown in parallel with the formation of water.

The inert gas of dilution could contain some traces of water although cartridges were used to dry the gas (see section 5.3.4.2) but not in that large concentration to justify the constant growth of the water band during the reaction (Figure 6 - 3 right in blue).
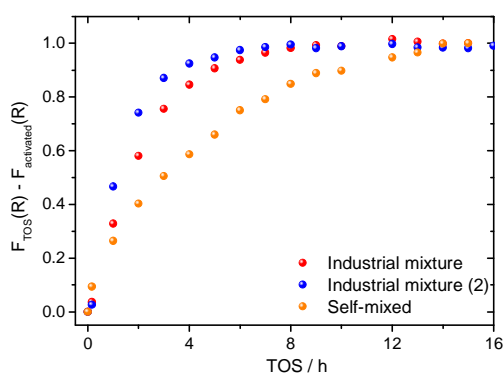
Figure 6 - 4: Complete Figure 6 - 3 on the evolution of water concentration adsorbed on MnSZ (0.5 wt% Mn) at 323 K. Here the concentration of water after 15 hours on stream was normalized to 1 for the experiments carried out with the three different gas mixtures.

To compare the trend of the water formation during the *n*-butane isomerization performed with the three different gas mixtures, the concentration of water after fifteen hours on stream was normalized to 1 (Figure 6 - 4).

Using the industrial gas mixtures led to a similar trend in the water formation which consisted in a growth of the water band the first four hours followed by a stable level.

However, with the self-mixed feed, the increase in water concentration on the catalyst

surface was more or less continuous and did not reach a stable level; and could neither explain the fast loss in activity during the first two hours on stream or the second part of the deactivation. Except with this case, concentration of water and OH groups adsorbed during

reaction on MnSZ (0.5 wt% Mn), were comparable to that formed on SZ (Chapter 5). Moreover, no formation of the bands ascribed to the unsaturated species, monoenic or polyunsaturated species, were formed like it was the case with SZ (Chapter 5), but a faster decline in the catalytic performance was noticed. These results could thus corroborate that these unsaturated species were only spectators in the deactivation process and the role of water was questionable. A further difference with SZ was also noticeable: the band at 1410 nm corresponding to the OH stretching vibration did show a growth during the first two hours on stream before decreasing in intensity for the rest of the reaction.

6.3.2. Manganese loading of 2 wt%

6.3.2.1 Catalytic activities overview

At higher loading of Mn (2 wt %) the maximum rate of isomerization at 323 K was improved (Figure 6 - 5) with respect to that obtained using 0.5 wt % Mn.
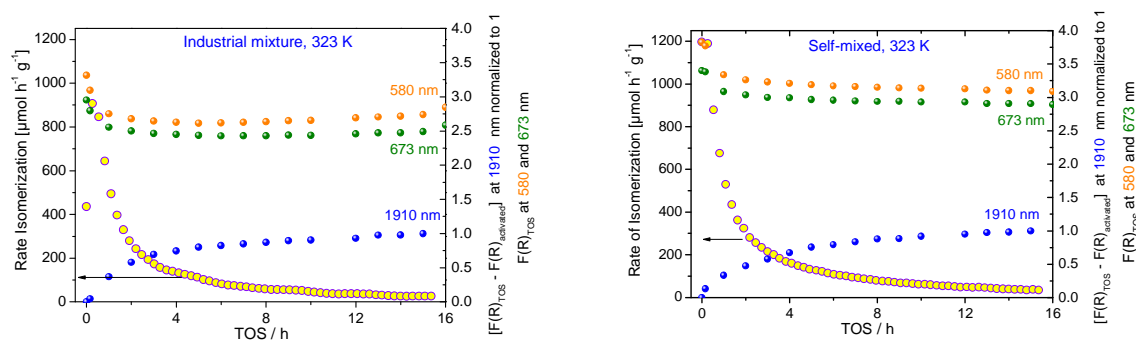
Figure 6 - 5: Catalytic data versus time on stream. In the same plot evolution of adsorbed water normalized to 1 after 15 h on stream, the evolution of the concentration in manganese cations Mn^{4+} (at 561 nm) and Mn^{3+} (at 673 nm) is shown. The three different gas mixtures were used to carry out these experiments. Reaction conditions: 5 kPa n-C$_4$ in N$_2$ at 323 K on MnSZ (2 wt% Mn). Total flow of 40 mL/min.

The rapid decrease following the maximum rate of isomerization was, with a higher loading in Mn, more drastic (loss of about 100 %) than that observed with 0.5 wt% Mn and much faster and more pronounced than that observed with SZ. Manganese-promoted sulfated zirconia (0.5 wt % Mn) showed the rate of isomerization of about 35-50 $\mu mol\ g^{-1}\ h^{-1}$ after sixteen hours on stream; whereas the 2 wt % MnSZ had around 14-35 $\mu mol\ g^{-1}\ h^{-1}$.

6.3.2.2 Spectroscopic data

The *n*-butane isomerization on MnSZ (2 wt% Mn) at 323 K showed a different increase of the water formed and adsorbed on the surface (Figure 6 - 6), and the growth was different from one feed to the other. The reactions performed with the feed using the industrial gas-mixtures showed that the concentration of water adsorbed on the surface reached a stable level after two and four hours on stream.
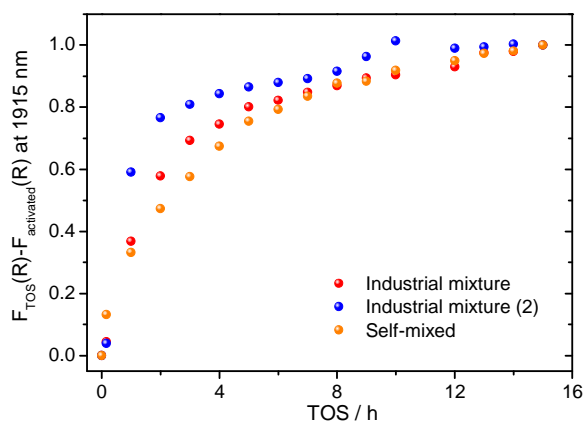
Figure 6 - 6: Complete Figure 6 - 5 on the evolution of water concentration adsorbed on MnSZ (2 wt% Mn) at 323 K. Here the concentration of water after 15 hours on stream was normalized to 1 for the experiments carried out with the three different gas mixtures.

In case of the reaction performed with a self-mixed feed, the growth of the water band was almost constant as a stable level of water adsorbed on the surface was not reached after sixteen hours on stream. With this higher loading of manganese, the monoenic and polyunsaturated allylic species were not formed, independently to the feed used. Confirming the observation with MnSZ (0.5 wt% Mn), the unsaturated species were not detected in the presence of manganese and one could here confirm again the role of these species as a spectator in the deactivation process. Some species that cannot be detected by the available technique and conditions used in this work should be present and responsible for the loss in activity.

6.3.2. Effect of the reaction temperature

The *n*-butane isomerization on MnSZ (2 wt % Mn) at 373 K with the industrial gas mixture, led to a lower value of the maximum rate of isomerization ($34 \, \mu mol \, g^{-1} \, h^{-1}$) than the one observed with SZ ($410 \, \mu mol \, g^{-1} \, h^{-1}$) at the same temperature; or than the one observed on the same Mn loading at 323 K ($900 \, \mu mol \, g^{-1} \, h^{-1}$). Besides a lower maximum rate of isomerization at 373 K, the induction period was not observed and after only three hours on stream, the rate reached a value close to zero (about $1 \, \mu mol \, g^{-1} \, h^{-1}$). These results were observed with experiments performed with the different gas mixtures; but only the experiments carried out with the industrial gas mixture were shown here (Figure 6 - 7). A

reaction temperature of 373 K, for the higher manganese loading led to a faster deactivation process.
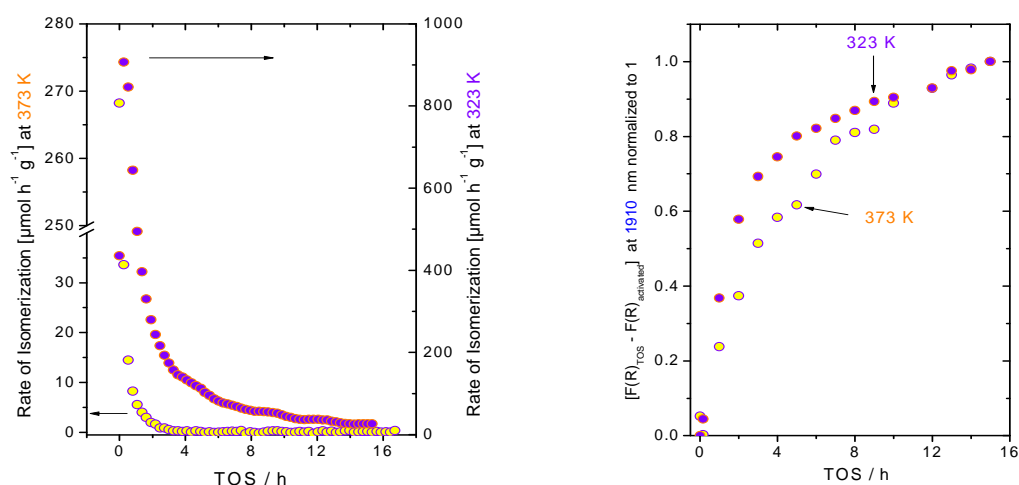
Figure 6 - 7: Catalytic data using gas mixture from Linde versus time on stream are shown on the left. The evolution of the corresponding adsorbed water at 323 K and 373 K is shown on the right. Conditions: Activation in O_2 at 723 K for 30 minutes. Reaction under 5 kPa n-C_4 in N_2 at 323 K and 373 K on MnSZ (2 wt% Mn). Total flow of 40 mL/min.

The GC used to analyze the effluent gas could not record the true maximum rate. The use of a micro GC could have avoided this situation.

The analysis of the spectroscopic data showed that the concentration of water adsorbed on the surface did not reach a stable value; implying that water was constantly produced or re-adsorbed form the gas phase (?) during the reaction of isomerization at higher temperature (373 K). Water is a product of reaction, but the increase in the concentration of water adsorbed on the surface was slower than the one observed with SZ. During the n-butane isomerization on MnSZ, the role of water in the first rapid part of deactivation was questionable. No obvious correlation between the catalytic data and the evolution of water formation could be drawn.

6.3.2. Effect of the activation and reaction temperatures on MnSZ

The n-butane isomerization took place either in an industrial gas mixture (5 kPa n-butane in nitrogen) or in a self-mixed feed (5 kPa n-butane in H_2). These two experiments were probably missing the true maximum rate because the reaction temperature was too high (Figure 6 - 8 left and right); thus no comparison on these values could be done. To compare the general trend of water formed during several experiments, normalization of spectra was needed, that the water band intensity after 15 hours on stream was set to one. That is the

reason why a quantitative study of the amount of water adsorbed on the surface of the catalyst was not relevant.
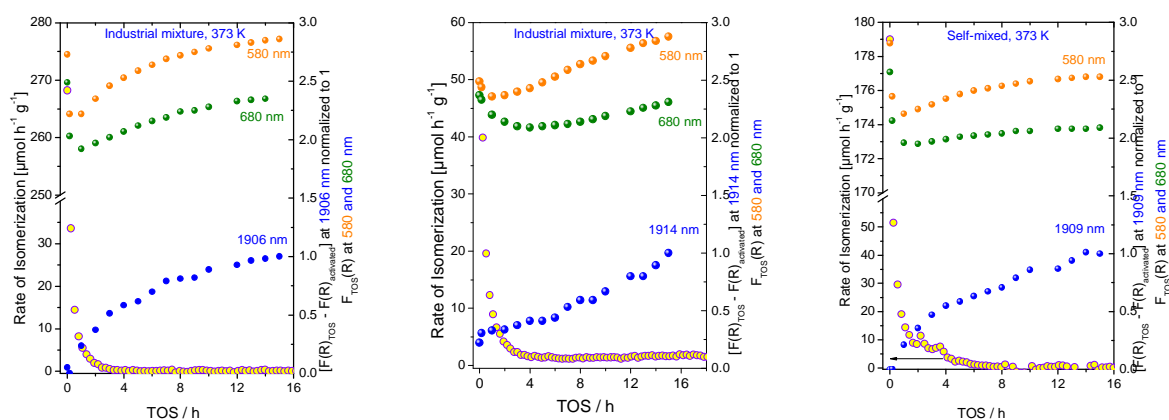
Figure 6 - 8: Catalytic data versus time on stream at 373 K on MnSZ (2 wt% Mn). In the same plot evolution of adsorbed water by using a industrial gas mixture with 5 kPa n-C$_4$ in N$_2$ after activation in O$_2$ (left), industrial mixture 5 kPa n-C$_4$ in N$_2$ after activation in H$_2$ (middle) and self-mixed feed of 5 kPa n-C$_4$ in H$_2$ after activation in O$_2$ (right). Total flow of 40 mL/min; the concentration of water formed was normalized to 1 after 15 h on stream. Total flow of 40 mL/min.

The growth of the water band could thus be compared for the two experiments. The amount of water was increasing similarly the first four hours implying for both cases that ODH occurred as initiation step; and then the growth of the band slowed down faster in the case of a reductive feed (right). In these two cases, the activation temperature in O$_2$ was optimized (see section 4.1) that not too much water was initially adsorbed on the surface. The fact that the growth of the water band occurred after four hours on stream, could signify that water was continuously produced or that the feed contains traces of water. The manganese cations Mn^{4+} and Mn^{3+} were reduced because of the reaction gas which is a reducing atmosphere. After four hours on stream, an increase of the intensity of bands characteristic of the two *d-d* transitions (580 and 680 nm) was observed. This means, that the oxidation state of the different manganese cations slightly increases. The increase can be explained by the few amount of water that the diluent gas contains. Keeping similar the reaction atmosphere and varying the activation one (Figure 6 - 8 left and middle), the increase of the water amount adsorbed on the surface of the catalyst was also different. In the case of activation in H$_2$, a lower activation temperature (523 K) was required to avoid the sulfur reduction (section 4.1), that the level of initial hydration was not the required one for an active catalyst.

6.4 Conclusions for MnSZ

Our results have shown that like sulfated zirconia, manganese-promoted sulfated zirconia deactivates drastically during the *n*-butane isomerization. In the case of the promoted catalyst, none of the bands assigned to unsaturated species, namely monoenic and polyunsaturated species, were observed. However, MnSZ deactivated more severely than the non-promoted SZ. These results corroborate thus that the monoenic allylic species are spectators in the deactivation process of SZ catalysts. Concerning the polyunsaturated species which were supposed to act as poison in the deactivation of SZ, they were not observed here that no conclusions about their possible role in the MnSZ deactivation could be drawn. Moreover, it should be emphasized that for many experiments, the rapid formation of water adsorbed on the catalyst surface was always observed in parallel with the reduction of the manganese Mn^{4+} and Mn^{3+} cations. ODH, one of the initiation route proposed for the *n*-butane isomerization results on water formation, reduction of the catalyst, here the manganese cations, and butene formation. We have shown here two of the three conditions which are necessary to validate an ODH.

[1] Z. Gao, Y. Xia, W. Hua, C.Miao, *Top.Catal*. 1998, 6(1-4), 101-106

[2] M. Perez-Luna, A. Cosultchi, J. Toledo-Antonio, E. Aree-Estrada, *Catal. Lett*. 2005 (102) 1-2, 33-38

[3] M. Signoretto, M.A. Stefano, F. Pinna, S. Polizzi, G. Cerrato, C. Morterra, *Microporous Mesoporous Matter*, 2005, 81(1-3), 19-26

[4] S. Baba, Y. Shibata, T. Kawamura, H. Takaoka, T. Kimura, K. Kousaka, Y. Minato, N. Yokoyama, K. Lida, T. Imai, *Eur. Patent EP0174836*, 1986

[5] F. Garin, D. Andriamasinoro, A. Abdulsamad, J. Sommer, *J. Catal*. 1991, 131(1), 199-203

[6] F.C. Lange, T.-K. Cheung, B.C. Gates, *Catal. Lett*. 1996, 41(1-2), 95-99

[7] S.X. Song, R.A. Kydd, *Catal. Lett*. 1998, 51(1-2), 95-100

[8] C.Y. Hsu, C.R. Heimbuch, C.T. Armes, B.C. Gates, *J. Chem. Soc. Chem. Commun*. 1992, 1645.

[9] F.C. Lange, T.-K. Cheung and B.C. Gates, *Catal. Lett*. 1996, 41, 95-99

To obtain an active manganese promoted or unpromoted sulfated zirconia catalyst, the way in which the catalyst is activated plays an important role. In inert or oxidative atmosphere, more than 95 % of water initially present in the catalyst is removed, that water does not act as poison by blocking Lewis acid sites necessary for the initiation step of the reaction. SZ activated in O_2 is more active. Furthermore, SZ during activation in reductive atmosphere shows an absorption band at 400 nm which can correspond to a single charged oxygen vacancy V^+ but more investigations need to be carried out to clarify this point.

For the unpromoted sulfated zirconia, two deactivation steps were observed during the *n*-butane isomerization at 373 K. The first one occurs during the reaction initiation validating oxidative dehydrogenation as a possible mechanism for that. Water, as product of the reaction mechanism, is detected during the first hours on stream simultaneously with a decline in the catalytic activity. The second stage, longer term deactivation, is reported to be due to formation of monoenic allylic species absorbing at band position 295 nm. Their formation can be linked to the presence of some impurities (olefins) in the feed. However, this work has clearly shown that the absence of these species does not prevent the catalyst from longer term deactivation. They can be formed or not during the reaction, the catalyst shows the same deactivation. This result can thus bring to the conclusion that the monoenic allylic species are only spectators in the loss of activity of the catalyst. However, the catalyst deactivates a longer term on stream implying that other allylic species, highly conjugated, are also deposited on the catalyst surface (see cartoon at the end of the conclusion).
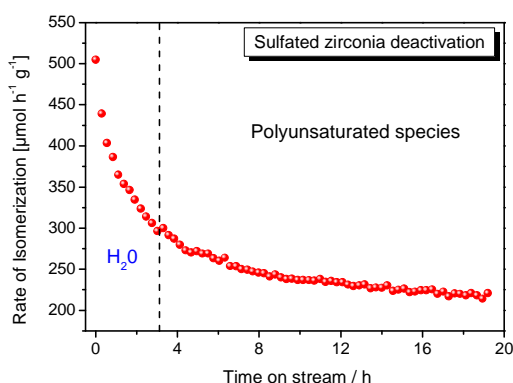
When the highly conjugated species absorbing at 370 and 450 nm are formed, SZ deactivates more than without these species. The formation of these highly conjugated species can be explained by (i) oligomerization resulting from a high concentration of olefins present in the feed or (ii) polymerization in presence of O_2 in the feed. In the latest case, the combustion of the allylic species takes place and produces heat that the polymers can be formed. Based on all our results, we can thus conclude that polyunsaturated species are most likely the poison for the *n*-butane isomerization than the monoenic allylic species which are only spectators.

A dual role of water and olefins for *n*-butane isomerization on sulfated zirconia has to be considered for understanding SZ deactivation. Water, which is a vital component in the initiation step, was revealed to act as poison during the skeletal isomerization. The carbenium ion / alkoxy groups are intermediates for the skeletal rearrangement and isobutane formation. They take also part in reactions, which products (polyunsaturated) can block the active sites and lead to SZ deactivation.

The poisoning effect of water and olefins can be avoided when clean feed (oxygen- and olefin-free) or large batch of SZ catalyst is used.

In the case of the manganese promoted sulfated zirconia, the catalyst deactivates even faster than SZ. However besides the formation of water during the initiation step, none of the unsaturated species - monoenic or highly conjugated, are detected. Moreover, manganese was not significantly reduced to ascribe the deactivation to manganese.

The UV-vis spectra of the manganese promoted sulfated zirconia are different from the spectra of unpromoted SZ by the fact that ligand to metal charge transfer and *d-d* transitions occur at band positions 580 and 680 nm for the latter and 300 - 400 nm for the former one, in this colored catalyst. In inert or oxidizing atmosphere, manganese cations in two oxidation states coexist, Mn^{3+} and Mn^{4+} (Mn^{2+} being spin forbidden). In reducing atmosphere, only one absorption band at 580 nm is observed in the spectra. That means only one type of manganese cation is present. By increasing the temperature, in the inert and oxidant atmosphere, the charge transfer is shifted to higher and lower energy respectively. In inert atmosphere, the oxidation state of Mn is not the highest possible. The charge transfer occurs at higher energy than that observed in oxidative atmosphere where Mn is at its higher oxidation state. In reducing atmosphere, the charge transfer similar to the *d-d* transition does not change in intensity or in energy; implying that Mn does not change its oxidation state. Based on our experimental results we assumed that the band at 580 nm belongs to Mn^{4+} while the band at 680 nm is due to Mn^{3+}. To confirm these assignments, theoretical calculations were performed based on a model where Mn^{3+} ions in the zirconia lattice induce the generation of oxygen vacancies for charge compensation leading to the displacements η_1 and η_2 of the oxygen atoms towards the oxygen vacancies; and the symmetry of the Mn^{3+} complex is supposed to be trigonal. When Mn^{4+} ions substitute Zr^{+4} ions, the position of 8 oxygen ligands surrounding the Mn^{4+} is supposed not to be changed. Based on this model and using two sets of parameters for the O^{2-} displacements, we have clearly shown that the absorption band at 580 nm belongs to Mn^{4+} while the one at 680 nm to Mn^{3+}.

Possible Poisons
(Polyunsaturated allylic species and H_2O)

Spectators (Monoenic allylic species)

Active sites
($S_2O_7^{2-}$, labile SO_3...)
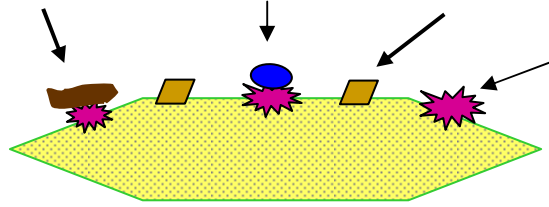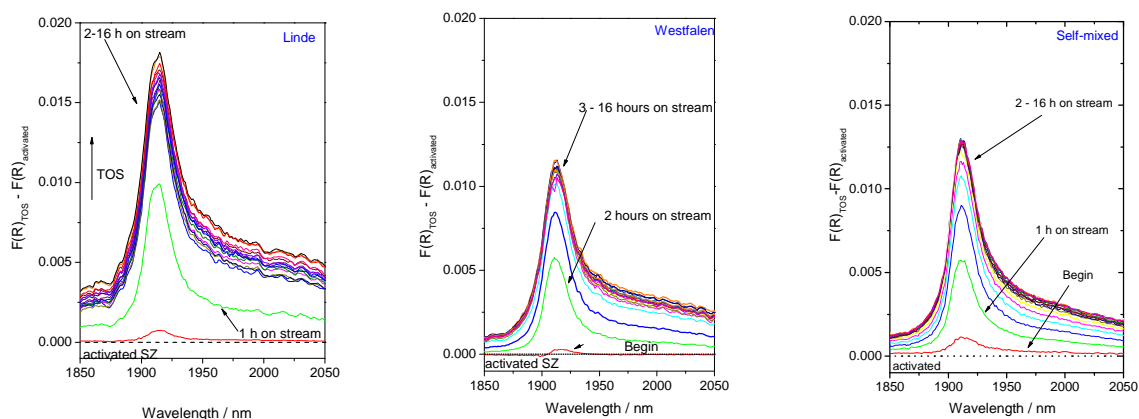
Appendix, Fig 1: Evolution of the species adsorbed on the surface (band at 1914 nm) with different gas-mixtures provided from Linde (left), Westfalen (middle) and Messer-Griesheim (right). Conditions: Activation in O_2 at 723 K for 30 minutes and reaction under 5 kPa n-C_4 in N_2 at 373 K on SZ. Total flow of 40 mL/min.
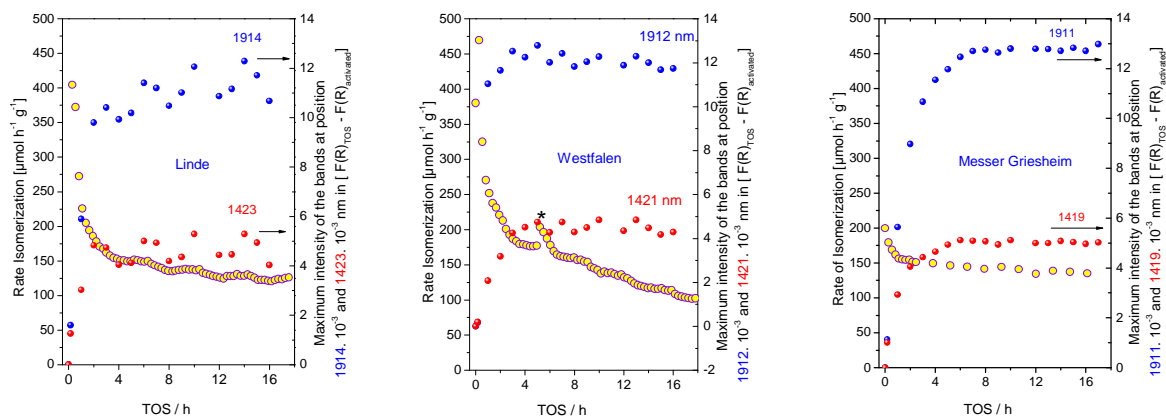
Appendix, Fig 2: Each plot represents the activity of the catalyst versus time on stream. On the same plot the evolution of adsorbed OH (~ 1420 nm) and water (~1910 nm) versus time on stream (shown also in Appendix, Fig 1) are added. Conditions: Activation in O_2 at 723 K for 30 minutes and reaction under 5 kPa n-C_4 in N_2 at 373 K on SZ. Total flow of 40 mL/min.
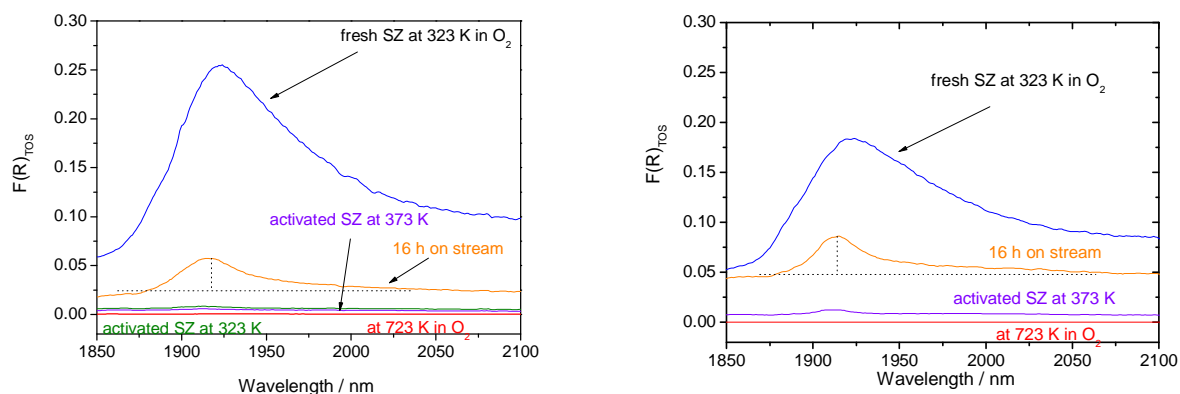
Appendix, Fig 3: Water adsorbed on the surface (at 1915 nm) of fresh SZ (blue), at 723 K in O$_2$ (red), on the activated SZ at 373 K (violet) and after sixteen hours on stream (orange) for a reaction temperature of 323 K (left) and 373 K (right). Activation: 30 minutes at 723 K in O$_2$. Reaction conditions: 5 kPa n-C$_4$ in N$_2$ (Linde) at 323 K and 373 K on SZ.
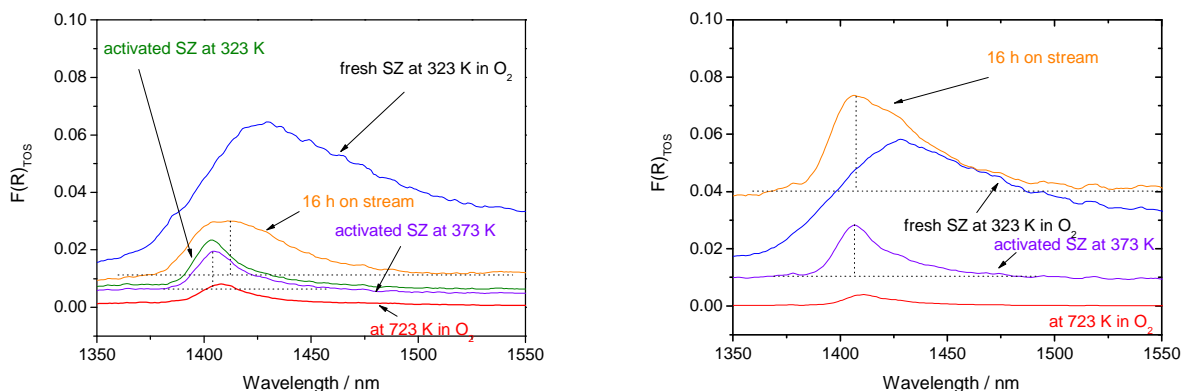
Appendix, Fig 4: OH adsorbed on the surface (at 1406 nm) on fresh SZ (blue), at 723 K in O$_2$, on the activated SZ at 373 K (violet) and after sixteen hours on stream (orange) for a reaction temperature of 323 K (left) and 373 K (right). Activation: 30 minutes at 723 K in O$_2$. Reaction conditions: 5 kPa n-C$_4$ in N$_2$ from gas provider Linde at 323 K on SZ, complementary to Appendix, Fig 3
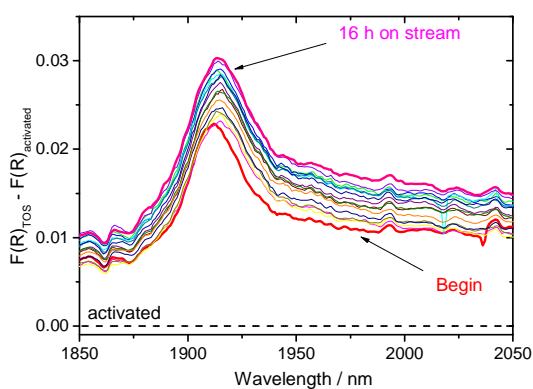
Appendix, Fig 5: The evolution of adsorbed water on the surface. Conditions: 5 kPa n-C$_4$ in H$_2$ at 373 K after activation in H$_2$. Total flow of 40 mL/min. Complete Figure 5 - 24

In the framework of ELCASS, this thesis was carried out in two different and complementary laboratories. The initial motivation was to carry out some isotope labelling experiments to study the reaction mechanisms for *n*-butane, *n*-hexane and *n*-heptane. The use of isotopes such as ^{18}O, D and ^{13}C would have been useful. It would have also been interesting to evaluate the influence of the hydrocarbon partial pressure and flux. However, due to technical problems, these experiments were not performed.

8.1. Motivation for a kinetic scheme for deactivation

Sulfated zirconia suffers from deactivation during *n*-butane isomerization at low temperature (373 K). Among several reasons, coke deposits on the surface of the catalyst can be a candidate in the deactivation process. To avoid this deactivation, several groups[1,2,3] speculated on the role of H_2 in the *n*-butane isomerization on SZ. The accepted idea is that hydrogen in the feed inhibits this reaction by decreasing the butene concentration on the catalyst surface. Taking into consideration that at lower temperatures, *n*-butane isomerization on SZ is thought to occur via a bimolecular mechanism in which the formation of butene is primordial, Song *et al.*[4] agreed additionally that the presence of hydrogen can limit the number of butene molecules present, thus limiting the activity. Platinum modified zeolite and platinum modified sulfated zirconia, in the presence of hydrogen, are used as stable catalysts for commercial alkane isomerization[5,6]. Many papers reported the positive effect of promoting the SZ with some transition metal cations[7] such as Mn, or a metal, Pt[8,9] for example. The presence of hydrogen in the feed with a Pt promoted SZ (PtSZ) catalyst is essential to maintain the catalytic activity[10]. Many studies concerning the catalytic behaviour of SZ and PtSZ have been published but the results are much debated[11,12,13,14], particularly for the reaction mechanism of alkanes on such system. The experimental conditions also influence the mechanism in which the isomerization will occur. Inert or reductive atmospheres, during *n*-butane isomerization on SZ, play a major role in the mechanism. In the absence of a metal, Pt for instance, the conversion into isobutane at 453 K is more than one order of magnitude lower in H_2 than in He[28]. At 523 K, Chen *et al.*[15] and Garin *et al.*[10] studied the effect of hydrogen on the same reaction and on SZ. The presence of hydrogen reduces the deactivation of the catalyst, although the initial activity is low. They explain the positive effect of hydrogen by the hydrogenation of the coke precursors which could be formed during the reaction. The influence of hydrogen is complex. This gas can (i) rehydrogenate (hydro)carbon residues under the condition that a metal, which is able to dissociatively chemisorbed H_2, is present. Furthermore, (ii) during the alkane isomerization reactions on metals for instance, the

presence of hydrogen has an inhibiting effect on the reaction. The inhibiting effect of H_2 could be explained following two general mechanisms in kinetics. Whatever the model chosen, associative as Eley-Rideal (1) or dissociative as Langmuir-Hinshelwood (2), hydrogen is produced; and by increasing the P_{H2} the reverse reaction is favoured.

Associative mechanism

$$C_nH_{2n+2} + H_{ads} \longleftrightarrow (C_nH_{2n+1})^+_{ads} + H_2 \qquad (1)$$

Dissociative mechanism

$$C_nH_{2n+2} + 2\,free\,sites \longleftrightarrow (C_nH_{2n+1})_{ads} + H_{ads}$$

$$C_nH_{2n+1} + 1\,free\,site \longleftrightarrow (C_nH_{2n})_{ads} + H_{ads}$$

$$H_{ads} \longleftrightarrow H_2 + 2\,free\,sites$$

$$C_nH_{2n+2} + 1\,free\,site \longleftrightarrow (C_nH_{2n})_{ads} + H_2 \qquad (2) \qquad Metal$$

$$(C_nH_{2n})_{ads} + H^+ \longleftrightarrow (C_nH_{2n+1})^+$$

$$(C_nH_{2n+1})^+ \longrightarrow Isomers + cracking\ products \qquad Acid$$
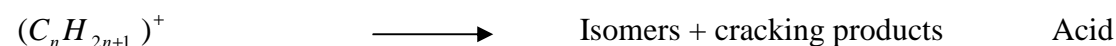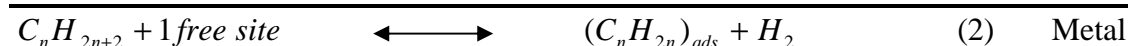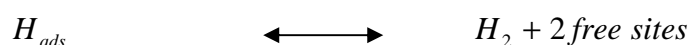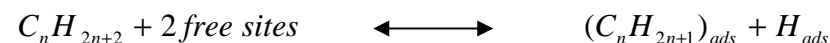
Besides platinum, ruthenium is used alternatively, because, contrary to platinum, which can isomerize n-alkanes[16,17], it will not contribute to the product formation as it does not catalyze alkane isomerization (it has hydro cracking properties). Industrially, ruthenium is used to promote the activity of the catalysts in the Fischer-Tropsch reaction, because the cobalt is better reduced[18]; but ruthenium also allows the decomposition of ammonia[19]. Hino and Arata[20,21] claimed that ruthenium promoted sulfated zirconia (RuSZ) is a highly active superacid catalyst for the isomerization of butane to isobutane with He as carrier gas. Most studies have been focussed on the isomerization of n-butane to iso-butane[13,12,13,22,23,24,25,26,27,28]. Some questions about the mechanisms involved on acid catalysts, are not yet well answered, similar to the question about the molecularity. At present, the skeletal rearrangement of alkanes is still under debate, as different reports proposed this rearrangement can proceed through a unimolecular (intramolecular or monomolecular) or / and a bimolecular (intermolecular) mechanism. The mechanism of n-butane isomerization on sulfated zirconia takes place through an intramolecular rearrangement as suggested by Garin $et\ al.$[25] followed by Tomishige $et\ al.$[29] who studied platinum modified sulfated zirconia. However, this mechanism is contradicted by Adeeva $et\ al.$[28] who are in favour of the bimolecular rearrangement. The intramolecular mechanism seems to be accepted for

_____

hydrocarbons having more than five carbon atoms[24],[30,31]. Few papers are available on the isomerization of *n*-hexane[32,33] and *n*-heptane[34,35] on PtSZ. *n*-Heptane and *n*-Hexane are chosen because the mechanism of isomerization is better understood than that of *n*-butane; thus the wish to obtain more information about the mechanism and intermediates of the reaction.

8.2. Tools for taking into account the deactivation effect

A poisoning effect can be concomitant with the presence of H_2 or He/ N_2. Stabilizing the catalyst activity during *n*-butane isomerization can be prevented by doping the catalyst with platinum and adding hydrogen to the feed. Moreover, when the deactivation cannot be avoided with or without the presence of the noble metal, a way to regenerate the catalyst is investigated. As the idea is to remove carbonaceous deposits which block access to the active sites, these species can be burnt under an oxidizing atmosphere following a temperature program similar to the activation procedure.

To sum up, the entire catalytic reactions can be represented under a general scheme as described bellow.
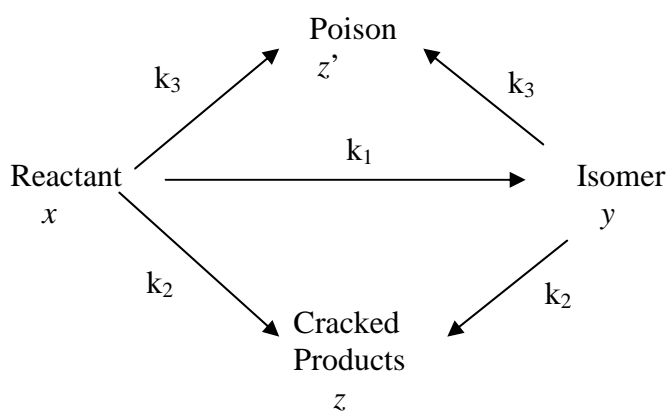
Figure 8 - 1: General kinetic scheme

x, *y*, *z* and *z'* are molar fractions and at t = 0, $x = x_0 = 1$

$$\frac{dx}{dt} = -(k_1 + k_2 + k_3)\,x = -\left(\sum k_i\right) x$$

$$\frac{dy}{dt} = k_1\,x - (k_2 + k_3)\,y$$

$$\frac{d(x+y)}{dt} = -(k_2 + k_3)\,(x+y)$$

$$\frac{dz}{dt} = k_2\,(x+y)$$

$$\frac{dz'}{dt} = k_3\,(x+y)$$

The resulting equations are:

$x = e^{-(k_1+k_2+k_3)t}$, the total conversion is $\alpha_T = 1 - x$

$x + y = e^{-(k_2+k_3)t}$, y is the amount of isomer formed

$z = \dfrac{k_2}{k_2 + k_3}\left[1 - e^{-(k_2+k_3)t}\right]$, z represents the amount of cracked products

$z' = \dfrac{k_3}{k_2 + k_3}\left[1 - e^{-(k_2+k_3)t}\right]$, z' represents the sum of the "poison"

From these 4 equations, the values of the rate constant can be determined. In addition, the poisoning process will be also discussed in this chapter.

The aim of this chapter is to investigate the isomerization reactions of *n*-hexane and *n*-heptane on SZ, PtSZ, RuSZ and RuMnSZ and to contribute to a better understanding of the mechanism through which these reactants are rearranged.

8.3. Experimental conditions

8.3.1. Set-up

Figure 8 - 2 shows a scheme of the set-up used to perform these experiments; which consists of a gas dosing system, a cold trap to obtain a set partial pressure for the hydrocarbon used (*n*-hexane and *n*-heptane), thermal conductivity detectors, a quartz reactor (30 cm length and internal diameter of 10.5 mm) which is heated by a spiral oven, a pressure controller and a GC to detect and separate the products of reaction. The tubing is made of stainless steel.
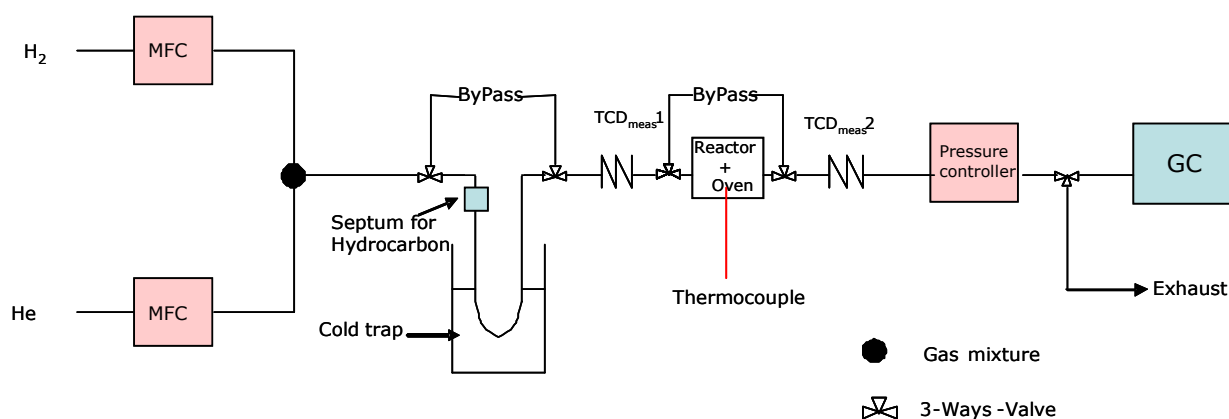
Figure 8 - 2: Experiment set-up

The gas was followed by thermal conductivity detectors located before and after the reactor. The detector delivers a rectangular-type signal, the height of which is proportional to the

partial pressure of the hydrocarbon injected. The contact time of the hydrocarbon on the catalyst is obtained directly from the signal (Figure 8 - 3)
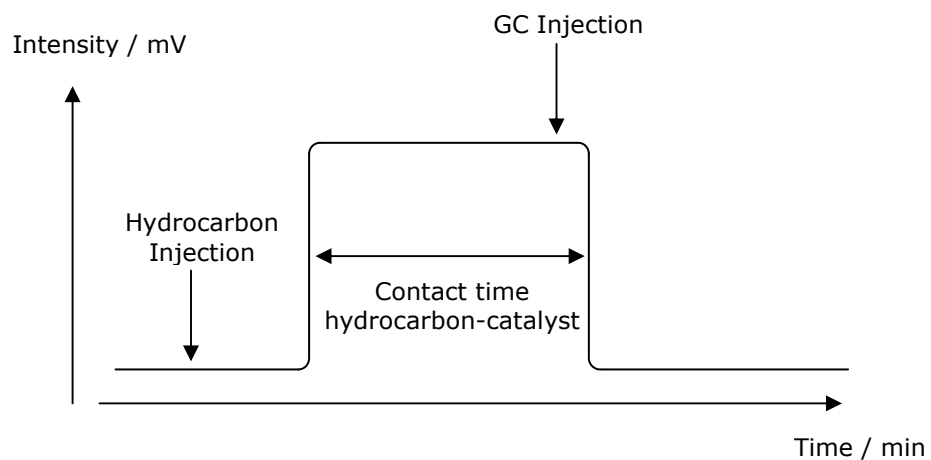
Figure 8 - 3: Thermal conductivity signal

Anisole mixed with liquid nitrogen to get a temperature of 236 K was used as cold trap for *n*-hexane to obtain a partial pressure of 4 Torr equivalent to 0.5 hPa; while benzyl alcohol mixed with liquid nitrogen to obtain a temperature of 255 K was used for *n*-heptane to obtain a partial pressure of 3.5 Torr equivalent to 0.46 hPa. The effluent gas from the reactor is analyzed on line by GC. The GC is a CE Instruments - GC8000 Top equipped with a capillary column (CPSil 5CB) which is 60 m length and 0.32 mm inner diameter.

8.3.2. Activation

The catalysts (200 mg) were activated either under $40\,mL\,\text{min}^{-1}$ H_2 for two hours at 523 K (a ramp of 5 K/min). The catalysts were cooled to the reaction temperature under the same activation atmosphere.

8.3.3. Reaction

The catalytic reactions were carried out in a pulse flow system with a fixed bed reactor working at atmospheric total pressure. In each run 5 μL of *n*-hexane or *n*-heptane (Fluka, puriss.) were introduced into the gas flow of H_2 (Air Liquide, 99.999 % purity) at constant hydrocarbon partial pressure (around 5 Torr or 0.5 hPa) thanks to a cold trap kept at constant temperature. The reaction takes place at 473, 453, 423 or/and 373 K. After four successive injections of hydrocarbon at each reaction temperature, a pulse of 5 mL of air is added to the reactor at 473 K to study the possible impact of air on the catalytic performance afterwards.

8.4. Results

8.4.1. *n*-Hexane and n-heptane on SZ or MnSZ (0.5 wt% Mn)

Several injections of hydrocarbons were performed at constant temperatures, varying from 473 K to 373 K, on the same catalyst to observe the deactivation process. For each set of temperatures, new catalyst was loaded in the reactor and activated before the reaction was performed.

In the case of *n*-hexane, at high reaction temperature, 473 K, for both catalysts, SZ (Table 8 - 1) and MnSZ (Table 8 - 2), the total conversion increases when the reaction temperature increases, but the selectivity in isomers is decreased when the reaction temperature is increased. At lower reaction temperature the selectivity in isomers increases to 100 %. Previously, a continuous addition of O_2 (Section 5 and 6) increased the catalytic activity. In these experiments, the addition of a pulse of 5 mL air does not improve the catalytic performance.

On SZ, at different reaction temperatures, the results obtained are presented in the following tables:

T (K)	α_T (%)	$S_{isomers}$ (%)	$k_1t. 10^{-2}$		T (K)	α_T (%)	$S_{isomers}$ (%)	$k_1t. 10^{-2}$
473	21.9	21.5	5.9		453	7.8	55.9	4.6
473	7.3	34.9	2.7		453	1.0	80.2	0.8
473	4.9	37.0	1.9		453	0.9	74.2	0.7
473	4.5	37.7	1.8		453	0.7	73.1	0.5
5 mL of Air added					5 mL of Air added			
473	3.9	20.5	0.8		453	1.8	27.6	0.5

T (K)	α_T (%)	$S_{isomers}$ (%)	$k_1t. 10^{-2}$		T (K)	α_T (%)	$S_{isomers}$ (%)	$k_1t. 10^{-2}$
423	13.2	23.1	3.4		373	2.2	92.8	2.0
423	0.3	100.0	0.3		373	1.7	98.6	1.7
423	0.3	100.0	0.3		373	1.2	85.2	1.0
423	0.1	100.0	0.1		373	0.7	100	0.7
5 mL of Air added					5 mL of Air added			
423	0.2	100	0.2		373	0.5	55.3	0.3

Table 8 - 1: *n*-hexane (pulse of 0.7 kPa) total conversion at different temperatures. Reaction flow is 40 mL/min H_2 on SZ. k_1t represents the amount of isomers formed as defined in Fig.7-1. α_T is the total conversion; $S_{isomers}$ the selectivity of isomers is determined as $\dfrac{\alpha_{isomers}}{\alpha_T} \times 100$

The same experiments are performed on MnSZ at different reaction temperatures,

T (K)	α_T (%)	$S_{isomers}$ (%)	$k_1 t \cdot 10^{-2}$		T (K)	α_T (%)	$S_{isomers}$ (%)	$k_1 t \cdot 10^{-2}$
473	7.8	23.8	2.0		453	3.7	48.6	1.8
473	2.8	38.0	1.1		453	1.8	45.9	0.9
473	2.4	24.0	0.6		453	1.6	50.5	0.8
473	2.1	25.9	0.5		453	1.1	45.9	0.5
5 mL of Air added					5 mL of Air added			
473	2.5	11.3	0.3		453	1.2	25.7	0.3

T (K)	α_T (%)	$S_{isomers}$ (%)	$k_1 t \cdot 10^{-2}$		T (K)	α_T (%)	$S_{isomers}$ (%)	$k_1 t \cdot 10^{-2}$
423	4.4	69.4	3.2		373	1.0	100.0	1.1
423	1.2	80.8	1.0		373	1.0	100.0	1.0
423	0.9	81.3	0.75		373	0.8	100.0	0.8
423	0.1	59.5	0.4		373	0.7	100.0	0.7
Add 5 mL of Air					Add 5 mL of Air			
423	0.7	83.9	0.6		373	0.38	33.6	0.1

Table 8 - 2: *n*-hexane (pulse of 0.7 kPa) total conversion at different temperatures. Reaction in a flow of 40 mL/min H$_2$ on MnSZ (0.5 wt% Mn).

Under the same reaction conditions with *n*-heptane as the reactant, the total conversion is higher than that obtained with *n*-hexane. This higher reactivity with *n*-C$_7$ than with *n*-C$_6$ can be explained by the fact that, at the same reaction temperature, more *n*-C$_7$ will be adsorbed on the surface reactive sites (Table 8 - 3). Furthermore, there is no selectivity in isomers as only cracked products are detected. As an acidic mechanism takes place, carbenium ions are formed and the β scission reaction may also take place with *n*-C$_7$ cation isomers, initially formed in the adsorbed phase, which do not desorb as isomers but as cracked products.
In the case of *n*-C$_6$ we may have:

β-scission impossible
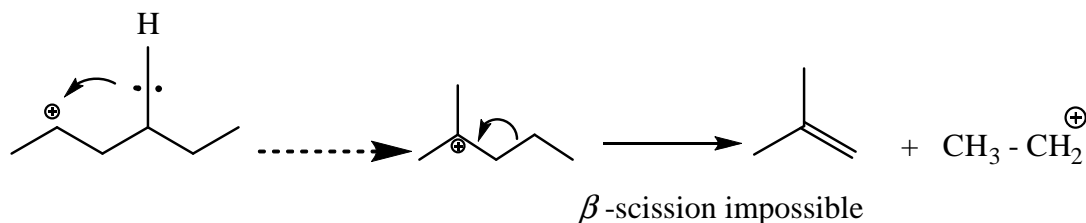
The β-scission cannot take place on the carbenium ion formed, as it involves the formation of a thermodynamically unstable primary carbenium ion.
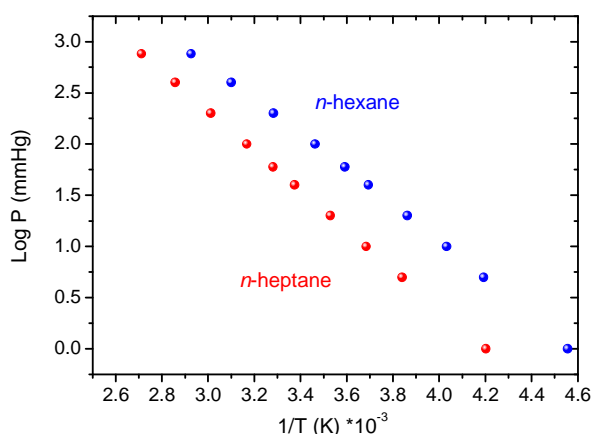
Table 8 - 3: Partial pressure curves of *n*-hexane and *n*-heptane calculated from the Clapeyron equation $\dfrac{d \ln P}{d(1/T)} = -\dfrac{\Delta H_v}{RT^2}$ **, where** ΔH_v **[36] is the molar enthalpy of vaporisation and T the temperature in Kelvin.**

And in the case of *n*-C$_7$
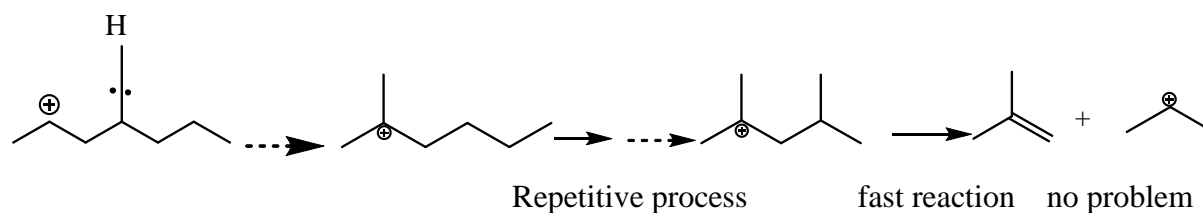
For instance, at 473 K, on SZ, the total conversion is 22 % with *n*-hexane against 80 % with *n*-heptane.

The conversion and selectivity obtained on SZ and MnSZ with *n*-C$_6$ and *n*-C$_7$ are consistent with the literature. Carbon deposition during the reaction blocks the active site then no conversion or low conversion can occur. This carbon deposit is one of the reasons for catalyst deactivation. However, the presence of hydrogen in the feed should avoid any accumulation of carbon on the surface of the catalyst if the unsaturated species formed are hydrogenated. Calculation of the rate constant shows that k$_3$ can not be calculated as *z'* can not be easily quantified. Another approach will be taken next.

8.4.2. *n*-Heptane on RuSZ (0.5 wt% Ru)

During the different injections, at the 4 different reaction temperatures, the catalytic performance of the RuSZ decreases and no selectivity in isomers is observed. The addition of the pulse of air does not lead to any increase in the catalytic activity, but at 473 and at 453 K

it leads to the formation of some isomers (Table 8 - 4). The catalyst deactivates with time on stream due to carbon deposition on the active surface of the catalyst. At high temperature (473 and 453 K) and when the catalyst is treated under air, isomer is formed. Ruthenium has no capability to isomerize alkanes; Ru can only contribute to the cracking of the hydrocarbon. Loften[37] reported that, by performing a temperature programmed reduction of RuSZ (0.75 wt% Ru, 1.3 wt% sulfur content and 132 m^2/g of surface area), a reduction at 468 K corresponding to the reduction of sulfate groups is obtained.

T(K)	α_T (%)	S $_{isomers}$ (%)	T(°C)	α_T (%)	S $_{isomers}$ (%)
473	11.3	-	453	16.8	-
473	8.7	-	453	16.3	-
473	7.3	-	453	18.2	-
473	6.5	-	453	-	-
473	8.2	9,3%	453	4,8	6,1%
T(°C)	α_T (%)	S $_{isomers}$ (%)	T(°C)	α_T (%)	S $_{isomers}$ (%)
423	7.1	-	373	1.1	-
423	6.0	-	373	0.3	-
423	5.1	-	373	0.3	-
423	5.7	-	373	0	-
423	4.5	-	373	-	-

Table 8 - 4: *n*-heptane (pulse of 0.7 kPa) total conversion at different temperatures on RuSZ (0.5 wt% Ru). Reaction in a flow of 40 mL $\min^{-1}$ H₂. The highlighted data are obtained after air treatment.

The presence of isomers could be explained by the character acid of the catalyst which has been reactivated by the addition of air into the feed. At high temperature, and after the addition of air into the feed, Ru loses its cracking capability, as oxygen atoms block the active sites of Ru responsible for the C-C bond rupture. However, a second hypothesis can be made. During the first injection of hydrocarbon by the pulse, the catalyst was always exposed to a reducing atmosphere, so that when air was injected into the reactor at 473 K, the Ru is not fully oxidized; thus only a mixture of Ru/O exists rather than an ordered oxide. This phenomenon is also observed at higher reaction temperature where oxide islands are formed but some disordered Ru/O regions exist inbetween, as explained by Blume *et al.*[38]. Furthermore, the selectivity in isomers after the addition of air can be compared to the results obtained by Blume *et al.*[39] in the methanol oxidation on Ru catalysts. On Ru metallic catalyst (O₂-free), methanol dehydrogenation takes place. The desired products, CH₂O and H₂O, were obtained after a moderate amount of oxygen had been incorporated, forming thus the surface oxide RuO$_x$.

8.4.3. *n*-Hexane and *n*-heptane on RuMnSZ (0.5 wt% Ru and 0.5 wt% Mn)

It cannot be worthwhile to explain the hydrocracking patterns. The initial assumption is to consider that all carbon-carbon bonds are broken. The carbon balance starting with *n*-hexane molecule can be written as following.

$$6\,[C_6]^0 = C_1 + 2\,C_2 + 3\,C_3 + 4\,C_4 + 5\,C_5 + 6C_6{}^{isom} + 6C_6{}^{t}$$

Where $[C_6]^0$ = initial concentration of the reactant

$[C_6]^t$ = concentration at time t of the reactant

$[C_6]^{isom}$ = concentration of the isomers

The amount transformed is:

$$[C_6]^0 - [C_6]^t = \frac{C_1}{6} + \frac{C_2}{3} + \frac{C_3}{2} + \frac{2C_4}{3} + \frac{5C_5}{6} + C_6{}^{isom}$$

The conversion is defined by $\alpha_T = \dfrac{[C_6]^0 - [C_6]^t}{[C_6]^0} \times 100$ and can be generalized as:

$$\alpha_T = \frac{\sum\limits_{i=1}^{6} \cdot \sum\limits_{j, j \neq k} i \cdot C_i^{j}}{\sum\limits_{i=1}^{6} \cdot \sum\limits_{j, j \neq k} i \cdot C_i^{j} + \cdot 6 \cdot C_6^{k}} \times 100$$

where C_i denotes the concentration of a hydrocarbon with *i*-carbon atoms. Summation over *j* is performed over all detected compounds for each C_i hydrocarbon; the subscript k denotes the hydrocarbon in the feed. This procedure can be applied when repetitive cracking processes take place. It is now possible to set the hypothesis that, on the surface, only one C-C bond rupture during the reaction occurs. It means that from *n*-C_6, the same number of moles is expected for C_1 and C_5, C_2 and C_4, and 2 moles for C_3. Then, if this hypothesis is verified, the stoichiometric product distributions in moles can be written as follows;

$\dfrac{1}{2} \cdot (C_1 + C_5)$, $\dfrac{1}{2} \cdot (C_2 + C_4)$, $2\,C_3$ and $C_6{}^{isom}$. Sometimes C_1 and C_5, as well as C_2 and C_4, are not equal and there is an excess of C_1 and C_2 written as $6\,C_1$ and $3\,C_2$ which represent the extensive hydro cracking. These amounts are calculated as the excess of C_1 and C_2, divided by 6 and 3 respectively; it was already the case for $2\,C_3$ which is equal to the number of moles of C_3 divided by 2. In the following tables the calculations were done for the case of the non repetitive process. The following stoichiometric data are given in moles for the product distributions. The reaction temperature, the total conversion and the isomer selectivity are added in Table 8 - 5. With *n*-hexane, at the three different reaction temperatures, the total

conversion is relatively low (from 0.5 to 2 %) and the selectivity in isomers is high (over 90 %) as shown in Table 8 - 5. All values are given in percentage.

T (K)	α_T (%)	$S_{isomers}$ (%)	$6C_1$	$3C_2$	$2C_3$	$(C_1+C_5)/2$	$(C_2+C_4)/2$	2,2dmb	2,3dmb	2mp	3mp
473	0.9	90.6	0.0	1.7	0.0	7.3	0.6	0.0	11.4	17.9	61.3
453	1.2	93.7	0.0	1.0	0.0	3.3	2.2	2.0	11.9	41.2	38.6
423	0.6	96.9	0.0	0.0	0.0	3.1	0.0	0.0	6.6	32.0	58.3

Table 8 - 5: *n*-hexane (pulse of 0.7 kPa) total conversion and selectivity in isomers at different temperatures on RuMnSZ (0.5 wt% Ru and 0.5 wt% Mn). Reaction in a flow of 40 *mL* min^{-1} H$_2$.

With *n*-heptane, the results are different. At different reaction temperatures, the total conversions are much higher than those obtained with a shorter alkane, the *n*-C$_6$, and can reach more than 90 % at 473 and 463 K (Table 8 - 6). It is observed that the selectivity in isomers increases when the reaction temperature decreases. This result shows that in the adsorbed phase, the isomers formed also give cracked products.

Discussion

From these results, *n*-C$_7$ is more reactive over RuMnSZ than *n*-C$_6$. This result highlights the acid character of the reaction and the predominance of the secondary carbenium formation as already seen on SZ and MnSZ. Such information demonstrates that a possible influence of the metal character on the reactivity does not take place on the global activity. On a catalyst with an exclusive metal character, 0.2 wt % Pt on Al$_2$O$_3$ inert, *n*-C$_6$ and *n*-C$_7$ react at the same rate[17,40,41,42]. What is surprising here is that the cracking pattern seems to follow a "metal" character; *C$_1$* and *C$_2$* are formed. This apparent contradiction can only be explained by the presence of an adduct site composed of [Ru + acid sites] and if this ensemble is reactive. Starting with *n*-C$_7$, at low temperature (373 K), only isomerization reaction takes place. C-H bond rupture may take place on Ru surface atoms and the skeletal rearrangement of the alkane takes place on acid sites, where the C-C bond rupture and recombination occur. When the reaction temperature increases, another more activated process takes place, the hydrocracking reaction. A part of this reaction takes place on Ru; *C$_1$* and *C$_2$* as well as *C$_6$* and *C$_5$* are formed, but the main process is always present on the acid sites and the more internal *C-C* fission reaction is favoured with the formation of *C$_3$* and *C$_4$*.

_____

T (K)	α_T (%)	$S_{isomers}$ (%)	Distribution of products in %										
n-heptane			$7C_1$	$(7C_2)/2$	$(7C_3)/3$	$(C_4+C_3)/2$	$(C_5+C_2)/2$	$(C_6+C_1)/2$	2,4dmp	3,3dmp	2mhex	2,3 dmp	3 mhex
473	98.1	1.1	13.0	5.4	2.3	68.04	8.3	1.8	0.0	0.2	0.3	0.2	0.4
463	97.0	4.1	9.1	4.2	2.0	68.68	7.4	4.4	0.4	0.7	1.2	0.6	1.2
453	87.6	15.6	7.1	3.8	2.1	58.92	6.9	5.4	1.2	2.7	4.8	1.6	5.3
443	49.7	43.2	4.7	2.7	1.7	39.14	5.2	3.4	1.8	4.7	15.8	4.2	16.7
433	30.0	57.0	3.5	2.4	1.3	26.50	5.7	3.6	1.7	5.7	21.6	5.2	22.8
423	24.2	59.3	4.2	2.5	0.7	16.67	9.1	7.6	1.5	7.4	21.4	5.6	23.4
413	11.6	57.3	4.7	3.0	1.4	14.64	10.3	8.6	1.5	6.1	21.6	4.2	23.9
393	2.0	63.5	2.1	0.0	2.4	9.47	12.7	9.7	0.0	2.0	27.0	2.5	32.0
373	0.3	100							0.0	0.0	66.7	0.0	33.3

Table 8 - 6: *n*-heptane (pulse of 0.7 kPa) total conversion at different temperatures on RuMnSZ (0.5 wt% Ru and 0.5 wt% Mn). Reaction in a flow of 40 *mL* $\min^{-1}$ H₂.

In Table 8 - 5, besides the cracking reaction which can be seen as a "dual reaction" able to take place on two different sites, isomerization reaction occurs only on acid sites. At low temperature 2-methylhexane and 3-methylhexane are exclusively formed and after, when increasing the temperature, di-substituted heptanes are formed.

8.4.4. Study of the deactivation process

In addition to isomerization and hydro cracking processes, it is compulsory to take into account the deactivation underlined below. Following the O. Levenspiel[43] approach the activity, a, of a catalyst at any time is:

$$a = \frac{\text{rate at which the catalyst converts A}}{\text{rate of reaction of A with a fresh catalyst}} = \frac{r_A}{r_{A_0}}$$

A is the initial reactant. The reaction rate can be written as follows:

$$r_A = k \cdot C_A^n \, a \ \text{ with } \ k = k_0 \, e^{-\frac{E}{RT}}$$

and

$$-\frac{da}{dt} = k_d \, C_i^{n'} \, a^d \ \text{ with } \ k_d = k_{d_0} \, e^{-\frac{E_d}{RT}}$$

where d is the order of deactivation, n' measures the concentration dependency and E_d is the activation energy of the deactivation. The fundamental assumption of this formalism is that deactivation and rate laws are separable. The physical meaning of that assumption is that coke affects the local properties but has no long-range effect[44]. Self-poisoning as a parallel reaction to isomerization and a series of deactivation from the isomers formed were presented in the general kinetic scheme. In both cases, according to Levenspiel, it is possible to write the two above equations for r_A and $-\frac{da}{dt}$. Fuentes et al. [44] reported that the reaction order relative to cyclo-pentane (13.3 kPa cyclo-pentane for 88 kPa hydrogen) on Pd/Al_2O_3 catalysts is zero at 563 K. Based on these results and taking into account that the reaction order relative to $n\text{-}C_6$ or $n\text{-}C_7$ is zero, then $r_A = ka$. Considering that a second order decay corresponds to $d = 2$, thus $-\frac{da}{dt} = k_d' \, a^2$ with $k_d' = k_d \, C_A^{n'}$. Finally the equation becomes $-\frac{da}{dt} = k_d' \, a^2$. For the second order the integration yields $\frac{1}{a} = \frac{1}{a_0} + k_d' t$.

A differential reactor, at low conversion, can be considered as a well-mixed reactor, and therefore the reaction rate is:

$$\frac{w}{F_{A_0}} = \frac{X_A}{r_A} = \frac{C_{A_0} - C_A}{C_{A_0} \cdot k} \cdot \frac{1}{a}$$

A simple calculation gives

$$\frac{w}{F_{A_0}} = \frac{C_{A_0} - C_A}{C_{A_0} \cdot k} \left[1 + k_d' t \right] \text{ where } a_0 = 1$$

115

_____

A plot of the reciprocal conversion against time gives the experimental constant of deactivation k_d defined as follows.

$$\frac{w}{F_{A_0}} = \frac{\alpha}{k}\left[1 + k_d' t\right]$$

$$\frac{1}{\alpha} = \frac{F_{A_0}}{w \cdot k} + \frac{F_{A_0}}{w} \cdot \frac{k_d'}{k} t = \frac{F_{A_0}}{w \cdot k} + k_e t \ \ \text{where} \ k_e = \frac{F_{A_0}}{w} \frac{k_d'}{k}$$

$$k_e \approx \frac{k_d'}{k} = \frac{k_d \, C_A^{n'}}{k} = \frac{k_{d_0} e^{-\frac{E_d}{RT}} C_A^{n'}}{k_0 \, e^{-\frac{E}{RT}}} \ \ \text{where} \ k^0 \approx \frac{k_{d_0} \, C_A^{n'}}{k_0}$$

It is then possible to write the experimental rate constant of deactivation $k_e \approx k^0 \, e^{-\frac{(E_d - E)}{RT}}$.

The deactivation is then determined by the curve $\dfrac{1}{\alpha} = f(t) = \dfrac{1}{\alpha_0} + k_e \, t$. The results versus the temperature for n-C_6 and n-C_7 are presented, only at 473 K, on the two figures (Figure 8 - 4 and Figure 8 - 5) below.

Figure 8 - 4: Determination of $k_e t$ (amount of isomers formed following the scheme described in Figure 5-1) for the different catalysts SZ, MnSZ, RuSZ and RuMnSZ at 473 K with n-hexane.
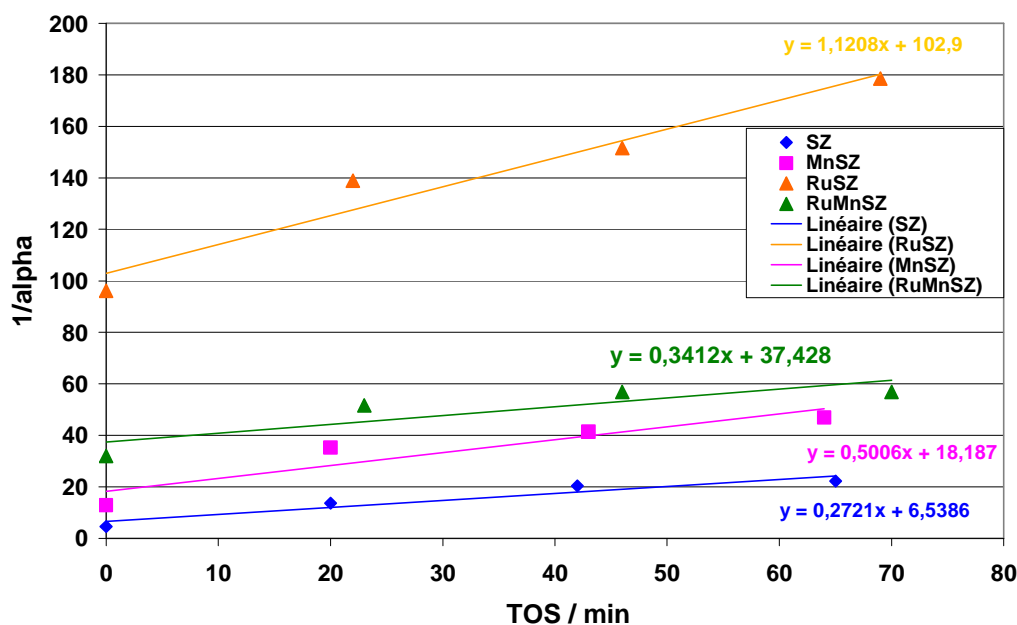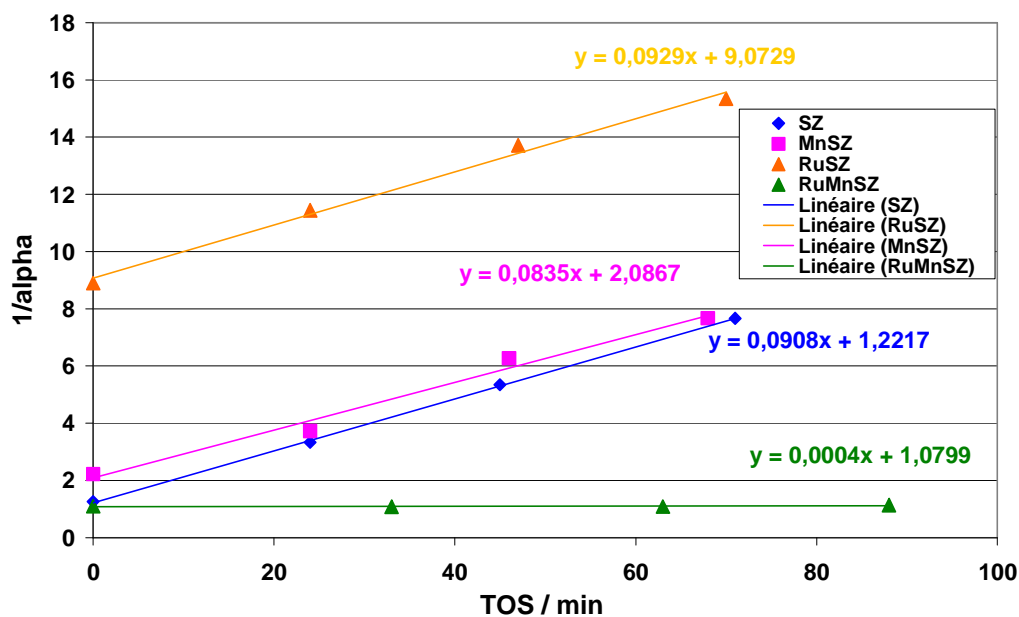
_____

Figure 8 - 5: Determination of $k_e t$ (amount of isomers formed following the scheme described in Figure 5-1) for the different catalysts SZ, MnSZ, RuSZ and RuMnSZ at 473 K with _n_-heptane.

From the curves $\dfrac{1}{\alpha} = f(t) = \dfrac{1}{\alpha_0} + k_e\, t$, the slope k_e is determined between 373 and 473 K. the

results are given in the two tables below (Table 8 - 7).

_n_-C$_6$	k_e min^{-1}			
T(K)	SZ	MnSZ	RuSZ	RuMnSZ
473	0.3	0.5	1.1	0,3
453	1.6	0.9	2.9	1.6
423	9.2	1.7	2.7	3.0
373	1.6	0.8	-	3.0

_n_-C$_7$	k_e min^{-1}			
T(K)	SZ	MnSZ	RuSZ	RuMnSZ
473	0.1	0.1	0.1	0.0
453	0.1	0.1	-0.0	0.0
423	0.2	0.2	0.1	0.0
373	0.4	0.6	5.5	11.1

Table 8 - 7: Determination of k_e for the different catalysts SZ, MnSZ, RuSZ, RuMnSZ at different temperatures (373 to 473 K).

In the case of _n_-hexane, for each catalyst, when the reaction temperature increases, the experimental value of the rate constant of deactivation, k_e, decreases. Thus, the poisoning of the catalyst slows as the carbon deposit is removed by desorption. However, with SZ and

MnSZ at 423 K, this constant, k_e, is surprisingly increased (highlighted in yellow in Table 8 - 7). In the case of *n*-heptane used as the hydrocarbon, this constant of deactivation, k_e, also decreases when the reaction temperature is increased. $\ln (k_e) = f(\dfrac{1}{T})$ was plotted in order to determine (plot not shown here) the "activation" of the process. As the slope is positive, it means that $E_{reaction} > E_d$ (deactivation). The activation of the whole reaction in that case is given ($E_{reaction} - E_d$).

8.5. *n*-Butane on PtSZ (0.5 wt% Pt)

Platinum modified sulfated zirconia in the presence of H_2 is assumed to be stable[10,28] for the *n*-butane isomerization. The performance of the catalyst of interest is investigated in the *in situ* cell and followed by UV-vis-NIR spectroscopy and GC analysis.

8.5.1. Activation

The catalyst was activated first in O_2 at 723 K for 30 minutes with a 5 K/min ramp before being cooled to 523 K. Thirty minutes of purging in He follows this oxidation treatment before reducing the catalyst for 180 min at 523 K.

8.5.2. Reaction

The reaction takes place in 40 mL min^{-1} 5 % *n*-butane diluted in 10 % H_2+ 85 % He at 523 K. This reaction was chosen to observe an activity of the catalyst (PtSZ), as at 473 K a weak activity is obtained.

8.5.3. Catalytic performance

During the first thirty minutes on stream the reaction temperature is set at 473 K and a rate of isomerization of 20 μmol g^{-1} h^{-1} was obtained. When the reaction temperature was increased to 523 K, an increase of the rate is observed; a rate similar to that obtained on the unpromoted sulfated zirconia at 373 K under 5 % *n*-butane in H_2. Besides this comparable rate, the PtSZ is stable within eighteen hours on stream (Figure 8 - 6). In parallel to the isobutane detected, methane, ethane and propane are also detected. The rate of methane is equivalent to the rate of propane. This distribution of the product implies that cracking takes place on the bifunctional catalyst in addition to the isomerization.
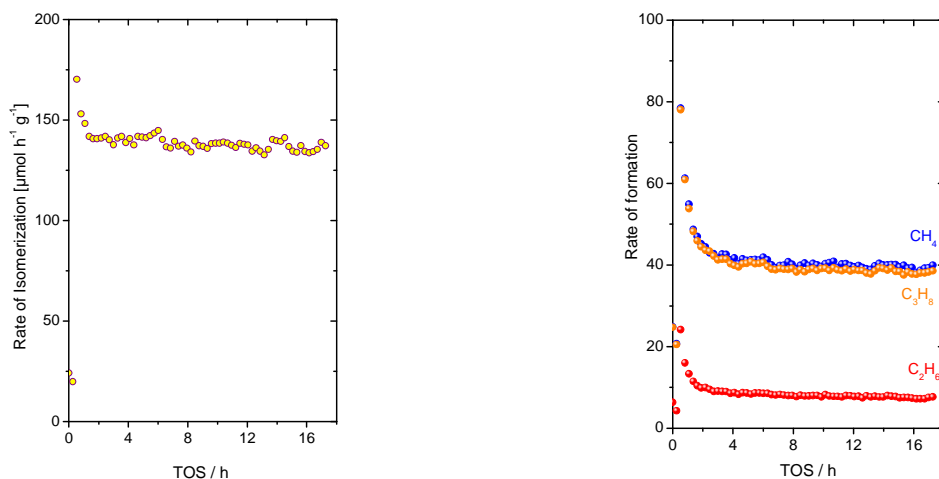
Figure 8 - 6: Rate of isomerization and rate of C_1, C_2 and C_3 formation. Activation: 30 min at 723 K, purge with He for 30 min; 180 min in reducing atmosphere at 523 K. Reaction conditions: 5% *n*-butane in 10 % H_2 and 85 % He on PtSZ (0.5 wt% Pt) at 523 K.

8.5.4. Conclusion for the PtSZ

This result shows that the activation of the Pt promoted SZ and the reaction temperature are important in the activity of the catalyst. PtSZ needed to be activated first in an oxidizing atmosphere at 723 K before being reduced for several hours at 523 K. A similar rate of isomerization to the non promoted SZ at 373 K could be obtained with a reaction temperature of 523 K. In addition, the main product of isomerization obtained with SZ (isobutane as main product; propane and pentanes as side products), products of cracking (methane, ethane and propane) are also detected with PtSZ. This difference in the products of reaction implies that in the case of PtSZ the metallic and acid characters occurred at the same time.

8.6. Conclusions

This work has shown the deactivation of the non-promoted sulfated zirconia under *n*-hexane and *n*-heptane isomerization. To postpone or reduce this deactivation process, whatever the reaction atmosphere, ruthenium and/or manganese were added to the non-promoted SZ. The platinum promoted sulfated zirconia was not completely studied because of the lack of time. Unfortunately the addition of metal, Ru, did not lead to the expected result, which was the suppression of the deactivation. However, the bifunctional character (metal and acid) of the catalysts was shown as isomers and cracked products were observed. Moreover, the acid function was proven for the isomerization process and it was clear how important the β-

_____

scission was in the reactivity of *n*-hexane and *n*-heptane. The results obtained were explained by a kinetic scheme.

[1] V. Adeeva, G.D. Lei and W.M.H. Sachtler, *Appl. Catal. A* 118, 1994, L11

[2] . Liu, G.D. Lei, W.M.H. Sachtler, *Appl. Catal. A* 146 ,1996, 165; 137, 1996, 167

[3] S.X. Song, R.A. Kydd, *Catal. Lett*. 51, 1998, 95

[4] S.X. Song, D.J. McIntosh and R.A. Kydd, *Catal. Lett*. 65, 2000, 5-7

[5] F. Schmidt, *Appl. Catal. A: General* 221, 2001, 15-21

[6] P.J. Kuchar, R.D. Gillepsie, C.D. Gosling, W.C. Martin, M.J. Cleaveland, P.J. Bullen, *Hydrocarbon Engineering*, 1999, 50-57

[7] F.C. Lange, T.-K. Cheung and B.C. Gates, *Catal. Lett*. 1996, 41, 95-99

[8] E. Iglesia, D.G. Barton, J.A. Biscardi, M.G.L. Gines, S.L. Soled, *Catal. Today* 38 (1997) 339

[9] H. Liu, G.D. Lei, V. Adeeva, W.M.H. Sachtler, *J. Molec. Catal*. 100 (1997) 38, 339

[10] F. Garin, D. Andriamasinoro, A. Abdusamad and J. Sommer, *J. Catal*. 131 (1991) 199

[11] F. Babou, G. Coudurier and J. C. Vedrine, *J. Catal*. 152 (1995) 341

[12] X. Song and A. Sayari, *Catal. Rev. Sci. Eng*. 38 (1996) 329

[13] B.H. Davis, R. A. Keogh and R. Srinivasan, *Catal. Today* 20 (1994) 219

[14] L.M. Kustov, V.B. Kazansky, F. Figuéras and D. Tichit, *J. Catal*. 150 (1994) 143

[15] F.R. Chen, G. Coudurier, J-F. Joly, J.C. Vedrine, *J. Catal*., 143, 1993, 616-626

[16] F.G. Gault, V. Amir-Ebrahimi, F. Garin, P. Parayre and F. Weisang, Bull. Soc. Chim. Belg. 88 (1979) 475

[17] F.G. Gault, Adv. Catal. 30 (1981) 1

[18] Iglesia Enrique, Soled Stuart L. and Fiato Rocco A., *United States Patent 4822824*

[19] Shikada Tsutomu, Asanuma Minoru and Ikariya Takao, *United States Patent 5055282*

[20] M. Hino and K. Arata, *React. Kinet. Catal. Lett*. 66 (1999) 2, 331-336

[21] M. Hino and K. Arata, *React. Kinet. Catal. Lett*. 71 (2000) 1, 71-76

[22] K. Arata, *Adv. Catal*. 37 (1990) 165

[23] J. Sommer, R. Jost and M. Hachoumy, *Catal. Today* 38 (1997) 309

[24] H. Liu, G.D. Lei, W.M.H. Sachtler, *Appl. Catal. A* 146 (1996) 165; 137 (1996) 167

[25] F. Garin, L. Seyfried, P. Girard, G. Maire, A. Abdusamad and J. Sommer, J. Catal. 151 (1995) 26

[26] M. Hino, S. Kobayashi and J. Arata, *J. Am. Chem. Soc*. 101 (1979) 6439

[27] M. Hino and J. Arata, *Chem. Commun*. (1980) 851

[28] V. Adeeva, G.D. Lei, , W.M.H. Sachtler, *Catal. Lett*. 33, 1995, 135

[29] K. Tomishige, A. Okabe and K. Fujimoto, *Appl. Catal. A* 194 (2000) 383

[30] E. Iglesia, S.L. Soled and G. M. Kramer, *J. Catal*. 144 (1993) 258

[31] T.J. McCarthy, G.D. Lei and W.M.H. Sachtler, *J. Catal*. 159 1996) 90

[32] T. Løften and E.A. Blekkan, *Appl. Catal. A*, 299 (2006) 250-257

[33] K. Föttinger, G. Kinger, H. Vinek, *Appl. Catal. A*: General 266, 2004, 195-202

[34] U.B. Demirci and F. Garin, *Catal. Lett*. 76 (2001) 1-2

[35] K. Föttinger, E. Halwax, H. Vinek, *Appl. Catal. A*, 301, 2006, 115-122

[36] *Industrial and Engineering Chemistry,* 39, 4, 1947, 517-550

[37] T. Loften, PhD dissertation, 2004

[38] R. Blume, H. Niehus, H. Conrad, A. Böttcher, L. Aballe, L. Gregoratti, A. Barinov, M. Kiskinova, *J. Phys. Chem. B*, 109, 2005, 14052-14058

[39] R. Blume, M. Hävecker, S. Zafeiratos, D. Teschner, E. Vass, P. Schnörch, A. Knop-Gericke, R. Schlögl, S. Lizzit, P. Dudin, A. Barinov, M. Kiskinova, *Phys. Chem. Chem. Phys*.9, 2007, 3648-3657

[40] F.G. Gault, F. Garin, G. Maire, Growth and Properties of Metal clusters, J. Bourdon (1980) 451-466

[41] F. Garin and G. Maire, *Accounts. Of Chemical. Research* (1989) 22, 100-106

[42] V. Amir-Ebrahimi, F. Garin, F. Weisang, F.G. Gault, *Nouv. J. Chimie*. 3 (1979) 529-532

[43] Chemical reaction engineering, 2nd edition, 1976, *John Willey and sons*.

[44] S. Fuentes, F. Figueras, *J. Catal*., 54 (1978) 397-404

Curriculum Vitae

Personal Data

Name:	Carine Edith CHAN THAW
Date of birth:	December 26, 1978
Place of birth:	Tamatave, Madagascar
Nationalities:	French and Malagasy
Languages:	French and Malagasy (mother tongues), German and English (fluent)

Scientific Career

Since 2004	Dissertation at the Fritz Haber Institut der Max Planck Gesellschaft (FHI-MPG)-Berlin (Germany) and LMSPC[1], CNRS-Strasbourg (France) *Title of thesis*: "Sulfated zirconia deactivation during n-butane isomerization: an in situ UV-vis-NIR spectroscopic study" in inorganic chemistry under supervision of Prof. Robert Schlögl, Dr. Friederike Jentoft and Dr. François Garin
2004	Master internship at LMSPC Strasbourg *Title:* "Ethanol reforming under pressure: designing experimental procedures for the study of peroskovite catalysts (La-Co-Fe)"
2002	Master Internship – Daimler Chrysler (EADS[2] Dornier) – Friedrichshafen (Germany) *Title:* "Long-term stability of proton exchange membrane fuel cell (PEMFC)"
2001:	Internship – Daimler Chrysler (EADS Dornier) – Friedrichshafen (Germany) *Title:* "Separation and analysis of diesel using zeolite membranes"

---

[1] LMSPC: **L**aboratoire des **M**atériaux, **S**urface et **P**rocédés pour la **C**atalyse UMR 7515 du CNRS
[2] EADS : **E**uropean **A**eronautic **D**efence and **S**pace **C**ompany (www.eads.com)

_____

Education

10/06	Joined the European Doctoral College of Strasbourg (France)
Since 2004 and the	PhD in Chemistry at the University Louis Pasteur (Strasbourg-France) Technical University of Berlin – TUB (Germany)
2004	DEA (Master degree to initiate a PhD) de Chimie Analytique et Matériaux de l´Université Louis Pasteur (Strasbourg-France)
2002	DESS (Professional Master degree) Matériaux de l´Université Lille 1, France
2001	Maîtrise de Chimie, 4-year university degree in Chemistry, University of Orleans (45), France
2000	Licence de Chimie, 3-year university degree in Chemistry, University of Orleans (45), France

Publications

Oral Conference Contributions (speaker underlined)

In Situ UV–vis–NIR Spectroscopic Investigation of Highly Reactive Surface Species Formed during Alkane Skeletal Isomerization

C. Chan Thaw, G. Tzolova-Müller, F. Garin, R. Schlögl, <u>F.C. Jentoft,</u> 20th North American Meeting, June 17 – 22, **2007**, Houston, Texas, USA

UV-vis spectroscopic studies of catalytic system

<u>C. Chan Thaw</u>, F.C. Jentoft; F. Garin, R. Schlögl, Second Max Planck Society PhD net Workshop, July 26 – 28, **2007**, Frankfurt am Main, Germany

In Situ UV–vis–NIR Spectroscopic Study of Catalyst Deactivation during Alkane Isomerization

<u>G. Tzolova-Müller</u>, C. Chan Thaw, F.C. Jentoft; R. Schlögl, Colloquium Optical Spectrometry, November 12 – 13, **2007**, Berlin, Germany

In Situ Spectroscopic Investigation of the Deactivation of H-Mordenite and Sulfated Zirconia Catalysts during Alkane Isomerization

<u>F. C. Jentoft</u>, G. Tzolova-Müller, C. Chan Thaw, K. Chakarova, J. Kröhnert, F. Garin, J. I. Villegas, D. Y. Murzin, 14th International Congress on Catalysis, July 13 – 17, **2008**, Seoul, South Korea

Poster

Initiation of Alkane Isomerization on Sulfated Zirconia Catalysts suited by In Situ X-Ray Absorption, UV-vis and IR Spectroscopy:

F.C. Jentoft, B.S. Klose, R.E. Jentoft, T. Ressler, P. Joshi, C. Chan Thaw, A. Trunschke, R. Schlögl, 19th North American Catalysis Society Meeting, May 22 – 27, **2005**, Philadelphia, USA

Catalyst deactivation during n-alkane isomerization studied by in situ UV-vis-NIR spectroscopy

G. Tzolova-Müller, C. Chan Thaw, F. Garin, F. C. Jentoft, R. Schlögl, 10th International Symposium on Catalyst Deactivation, February 5 – 8, **2006**, Berlin, Germany, LMP42

In Situ UV-vis-NIR Spectroscopy as a Tool to Understand Catalyst Deactivation

C. Chan Thaw, F. Garin, G. Tzolova-Müller, F. C. Jentoft, R. Schlögl, XXXIX. Jahrestreffen Deutscher Katalytiker, March 15 – 17, **2006**, Weimar, Germany, P130

Effect of activation and reaction atmosphere on sulfated zirconia and Mn-promoted sulfated zirconia isomerization catalysts

C. Chan Thaw, G. Tzolova-Müller, F. Garin, F.C. Jentoft, R.Schlögl1, XXXX. Jahrestreffen Deutscher Katalytiker, March 14 – 16, **2007**, Weimar, Germany, P158

Investigation of surface species during alkane isomerization on sulfated zirconia catalysts: An in situ UV-vis-NIR spectroscopic study

C. Chan Thaw,G. Tzolova-Müller, F. Garin, F. C. Jentoft, R. Schlögl, EuropaCat, August 26 – 31, **2007**, Turku, Finnland

An in situ UV-vis-NIR spectroscopic study on sulfated zirconia during n-butane isomerization
C. Chan Thaw, F. Garin, F. C. Jentoft, R. Schlögl, Paul Sabatier, September 12 – 16, **2007**, Ottrott, France

UV-vis-Spectroscopy of precursor compounds for Cu/ZnO catalysts and of the mineral reference compounds malachite and aurochalcite
M. Behrens, N. Hensel, C. Chan Thaw, G. Tzolova-Müller, A. Trunschke, R. Schlögl, S. Klokichner, O. Reu, XXXXI Jahrestreffen Deutscher Katalytiker, February 27 – 29, **2008**, Weimar, Germany